

Electronic Supplementary Information

A Redox-Active Diborane Platform Performs C(sp³)–H Activation and Nucleophilic Substitution Reactions

Thomas Kaese, Timo Trageser, Hendrik Budy, Michael Bolte, Hans-Wolfram Lerner and
Matthias Wagner*

Content:

- | | | |
|----|--|-------------|
| 1. | Experimental details and characterization data | ESI2-ESI22 |
| 2. | Plots of NMR spectra | ESI23-ESI46 |
| 3. | X-ray | ESI47-ESI59 |
| 4. | Computational details | ESI60-ESI69 |
| 5. | References | ESI70 |

1. Experimental details and characterization data

General considerations. All reactions and manipulations were carried out in an argon-filled glovebox or by applying standard Schlenk techniques under an argon atmosphere. Hexane was dried over Na, THF and Et₂O were dried over Na/benzophenone, THF-*d*₈ was dried over Na-K alloy. Prior to use, the solvents were distilled from the drying agent, degassed by applying three freeze-pump-thaw cycles, and stored over activated molecular sieves (3 Å). Compounds **1H**₂, ⁵¹Li[**1H**]⁵² and Li₂[**1**]⁵³ were synthesized according to literature procedures. The Et₂O solution of the D₃CLi·Lil complex (Sigma Aldrich) is commercially available with 99 atom-% deuterium and was used as received. Commercial Et₃SiD (Santa Cruz Biotechnology) contained 98 atom-% deuterium. Prior to use, the liquid haloalkanes were degassed by applying three freeze-pump-thaw cycles. NMR: Bruker DPX 250, Avance 300, Avance III 500 HD. Chemical shifts are referenced to (residual) solvent signals (¹H/¹³C{¹H}; THF-*d*₈: δ = 3.58/67.21 ppm),⁵⁴ external LiCl in D₂O (⁷Li), or external BF₃·Et₂O (¹¹B; ¹¹B{¹H}). Abbreviations: s = singlet, d = doublet, t = triplet, q = quartet, m = multiplet, br = broad, n.r. = multiplet expected in the NMR spectrum but not resolved, n.o. = not observed, vq = virtual quartet, vquint = virtual quintet.

Reaction of **1H₂ with 1 equiv. of H₃CLI.** An Et₂O solution of H₃CLI (0.5 M, 0.05 mL, 25 µmol) was evaporated to dryness in an NMR tube and the colorless solid residue was dissolved in THF-d₈ (0.6 mL) at room temperature. The solution was frozen at –196 °C and colorless **1H₂** (14 mg, 25 µmol) was added. The NMR tube was evacuated, flame sealed, and warmed to room temperature. The ¹H NMR spectroscopic investigation of the orange reaction solution revealed Li[**1H**]^{S2} Li[**2**], and Li[**7**] as the major products (each ca. 20-40%; the product distribution varied to some extent between repeated experiments).

In a glovebox, a representative NMR sample was transferred to an uncapped glass vial, and the vial was placed in a larger glass vessel containing hexane (2 mL). The outer vessel was covered with a lid to allow for gas-phase diffusion of the solvents in a closed environment. After 2-3 d, three types of single crystals (1 x yellow, 2 x colorless) had grown. According to X-ray crystallography, the yellow crystals consisted of the known salt [Li(thf)₃][**1H**]^{S2}. Of the colorless specimen, the first kind were too poorly diffracting to perform a full refinement, but, according to ¹H NMR spectroscopy, they consisted of Li[**7**] (cf. the reaction of **1H₂** with Li[HBET₃] for a targeted synthesis and the characterization of Li[**7**]). The second kind of colorless crystals turned out to be [Li(thf)₄][**2**] (for the X-ray crystal structure of the differently solvated analog [Li(thf)₃][**2**], see the reaction of Li₂[**1**] with methyl triflate).

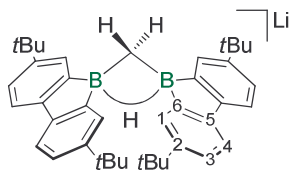


Figure S1. NMR numbering scheme for Li[**2**].

Li[2]

¹H NMR (500.2 MHz, THF-d₈): δ = 7.99 (d, ⁴J(H,H) = 1.9 Hz, 4H; H-1), 7.41 (d, ³J(H,H) = 7.9 Hz, 4H; H-4), 7.06 (dd, ³J(H,H) = 7.9 Hz, ⁴J(H,H) = 1.9 Hz, 4H; H-3), 1.94 (br, 1H; μ-H), 1.42 (s, 36H; CH₃), 0.49 (d, ³J(H,H) = 4.8 Hz, 2H; CH₂).

⁷Li NMR (194.4 MHz, THF-d₈): δ = –0.3.

¹¹B NMR (160.5 MHz, THF-d₈): δ = –14.0 (br).

¹³C{¹H} NMR (125.8 MHz, THF-d₈): δ = 159.1 (C-6), 147.8 (C-5), 146.3 (C-2), 127.9 (C-1), 121.8 (C-3), 117.7 (C-4), 35.2 (CCH₃), 32.6 (CH₃), 5.1 (CH₂).

Reaction of Li[2] with H₃C—I. An NMR tube was charged at room temperature with [Li(thf)₄][2] (5.0 mg, 5.8 μmol), THF-*d*₈ (0.5 mL), and H₃C—I (1.0 μL, 2.3 mg, 16 μmol). According to ¹H, ¹¹B, and ¹³C NMR spectroscopic investigations, Li[2] had vanished after 3 d and **14^{C1}** formed as the major product besides trace amounts of **13**.

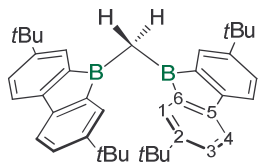


Figure S2. NMR numbering scheme for **14^{C1}**.

14^{C1}

¹H NMR (500.2 MHz, THF-*d*₈): δ = 7.41 (d, ⁴J(H,H) = 1.9 Hz, 4H; H-1), 7.13 (d, ³J(H,H) = 7.8 Hz, 4H; H-4), 7.07 (dd, ³J(H,H) = 7.8 Hz, ⁴J(H,H) = 1.9 Hz, 4H; H-3), 1.93 (s, 2H; CH₂), 1.18 (s, 36H; CH₃).

¹¹B NMR (160.5 MHz, THF-*d*₈): δ = 45 (vbr).

¹³C{¹H} NMR (125.8 MHz, THF-*d*₈): δ = 149.3 (C-5), 149.2 (C-2), 147.8 (C-6), 129.7 (C-1), 127.2 (C-3), 118.4 (C-4), 34.9 (CCH₃), 31.7 (CH₃), 14.8 (CH₂).

HRMS: Calculated for C₄₁H₅₀B₂: 564.40931, found: 564.41115.

Reaction of **1H₂** with 1 equiv. Li[HB*Et*₃].

At -30 °C

In an NMR tube, a THF solution of Li[HB*Et*₃] (1 M, 38 µL, 38 µmol) was evaporated to dryness at room temperature in a dynamic vacuum. During the addition of a THF-*d*₈ solution of **1H₂** (0.5 mL, 21 mg, 38 µmmol) and the subsequent flame-sealing of the NMR tube, the lower part of the tube was cooled to -196 °C. The sample was stored at -70 °C for 3 h prior to its NMR spectroscopic investigation at -30 °C, which showed a selective transformation to the primary hydride trapping product Li[**10**].

At room temperature

When carried out in neat THF (6 mL) at room temperature, the reaction between **1H₂** (79 mg, 143 µmol) and Li[HB*Et*₃] (0.05 M in THF, 2.7 mL, 135 µmol) furnished a clear, pale yellow solution. A ¹H NMR spectroscopic investigation (THF-*d*₈) showed the quantitative consumption of **1H₂** and the formation of two new major compounds (*i.e.*, the primary hydride trapping product Li[**10**] and its isomer Li[**7**]). After heating the sample at 50 °C for 1 h, Li[**7**] became by far the major constituent of the product mixture (>70%).

To obtain crystals, a solution of Li[HB*Et*₃] (0.2 M, 0.36 mL, 72 µmol) in THF/Et₂O (1:4) was added at room temperature to a colorless suspension of **1H₂** (40 mg, 72 µmol) in Et₂O (3 mL). After stirring for 10 min, the reaction mixture was filtered through a PTFE syringe filter (0.2 µm). Colorless thin needles of [Li(thf)₃(Et₂O)][**7**] grew from the filtrate at room temperature within 1 d.

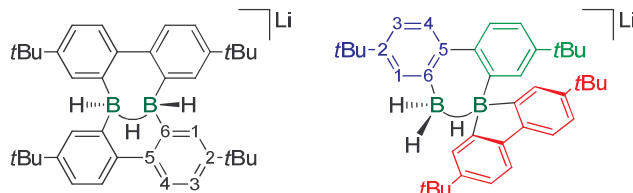


Figure S3. NMR numbering scheme for the primary hydride trapping product Li[**10**] (left) and its isomer Li[**7**] (right).

Li[10]

¹H NMR (500.2 MHz, THF-*d*₈): δ = 7.61 (d, ⁴J(H,H) = 1.9 Hz, 2H; H-1), 7.27 (d, ³J(H,H) = 8.0 Hz, 2H; H-4), 7.11 (dd, ³J(H,H) = 8.0 Hz, ⁴J(H,H) = 1.9 Hz, 2H; H-3), 6.94 (d, ³J(H,H) = 8.0 Hz, 2H; H-4), 6.78 (d, ⁴J(H,H) = 1.9 Hz, 2H; H-1), 6.59 (dd, ³J(H,H) = 8.0 Hz, ⁴J(H,H) = 1.9 Hz, 2H; H-3), 1.38 (s, 18H; CH₃), 0.94 (s, 18H; CH₃).

⁷Li NMR (194.4 MHz, THF-*d*₈): δ = -0.6.

¹¹B NMR (96.3 MHz, THF-*d*₈): δ = 33.5 (br), 8.2 (br).

¹³C{¹H} NMR (125.8 MHz, THF-*d*₈): δ = 149.6 (C-6), 149.2 (C-6), 145.4 (C-2), 144.8 (C-5), 144.5 (C-2), 141.5 (C-5), 134.4 (C-1), 129.6 (C-1), 125.7 (C-4), 125.4 (C-4), 122.1 (C-3), 119.9 (C-3), 34.6 (CCH₃), 34.2 (CCH₃), 32.1 (CH₃), 31.6 (CH₃).

Resonances of the same color belong to the same phenyl ring (as confirmed by 2D NMR experiments).

Li[7]

¹H NMR (500.2 MHz, THF-*d*₈): δ = 7.48 (d, ⁴J(H,H) = 2.3 Hz, 1H; H-1), 7.39 (d, ⁴J(H,H) = 2.3 Hz, 1H; H-1), 7.38 (d, ³J(H,H) = 8.0 Hz, 1H; H-4), 7.31 (d, ³J(H,H) = 7.9 Hz, 2H; H-4), 7.29 (d, ³J(H,H) = 8.0 Hz, 1H; H-4), 7.23 (dd, ³J(H,H) = 8.0 Hz, ⁴J(H,H) = 2.3 Hz, 1H; H-3), 7.05 (dd, ³J(H,H) = 8.0 Hz, ⁴J(H,H) = 2.3 Hz, 1H; H-3), 6.97 (n.r., 2H; H-3), 2.6 (vbr, 1H; BH), 1.34 (s, 9H; CH₃), 1.18 (s, 9H; CH₃), 1.18 (br, 18H; CH₃), n.o. (H-1 (2H), BH (2H)).

⁷Li NMR (194.4 MHz, THF-*d*₈): δ = -0.7.

¹¹B NMR (96.3 MHz, THF-*d*₈): δ = -3.6 (br), -10.1 (br).

¹³C{¹H} NMR (125.8 MHz, THF-*d*₈): δ = 147.4 (br), 147.0, 146.5, 145.9, 145.6, 145.5, 133.9 (C-1), 130.2 (C-1), 129.6 (C-1), 126.4 (C-4), 125.9 (C-4), 122.9 (C-3), 122.3 (C-3), 121.8 (C-3), 117.5 (C-4), 34.9 (CCH₃), 34.8 (CCH₃), 34.6 (CCH₃), 32.2 (CH₃), 32.1 (CH₃), 32.0 (CH₃), n.o. (3 x C^{Ar}).

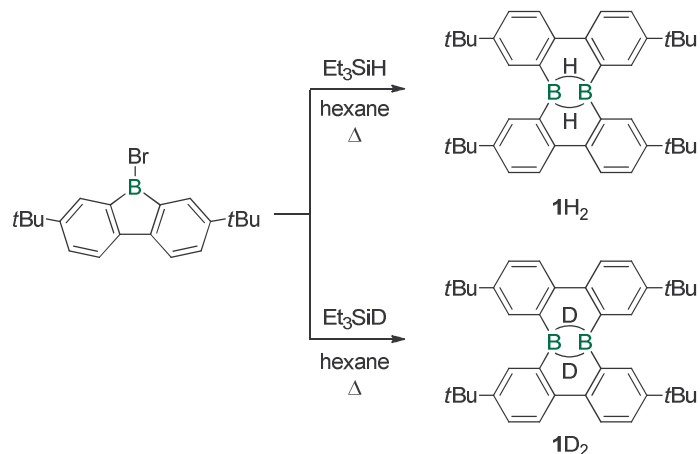
Resonances of the same color belong to the same phenyl ring (as confirmed by 2D NMR experiments). Signals marked in red could be unequivocally assigned, because they possess double intensity; the blue/green resonances were tentatively assigned by comparison of their chemical shift values with those of a related compound featuring a B–B bond instead of the bridging H atom.⁵⁵

Reaction of **1H₂ with exc. LiH.** In an NMR tube, THF-*d*₈ (0.6 mL) was added at room temperature to a solid mixture of **1H₂** (7 mg, 13 µmol) and LiH (15 mg, 1.9 mmol). ¹H and ¹¹B NMR spectra recorded on this mixture after 10 h showed no reaction. However, upon heating (60 °C, 1 d) the lithium dihydrido-2,7-di(*t*Bu)-9-boratafluorene⁵³ evolved as the major product (ca. 80%); further heating at 100 °C for 1d resulted in the quantitative conversion of **1H₂** to the lithium dihydrido-2,7-di(*t*Bu)-9-boratafluorene.

Deuterium-labeling experiments

(A) Synthesis of **1D₂**

Compound **1D₂** was obtained according to the published synthesis of **1H₂^{S1}** but by using Et₃SiD instead of Et₃SiH (Scheme S1).



Scheme S1. Reaction of 2,7-di(*t*Bu)-9-Br-9-borafluorene with Et₃SiH or Et₃SiD to afford **1H₂** or **1D₂**, respectively.

1D₂

The ¹H, ¹¹B{¹H}, and ¹³C{¹H} NMR spectra (C₆D₆) of **1H₂^{S1}** and **1D₂** are identical with the exception of a broad proton resonance at 3.5 ppm, which has been assigned to the bridging H-atoms in **1H₂^{S1}** and which is missing in **1D₂**. Instead, **1D₂** shows a signal at 3.4 ppm in the ²H NMR spectrum.

(B) Reaction of $\mathbf{1H}_2$ with $D_3\text{CLI}$

A solution of $D_3\text{CLI}\cdot\text{LiI}$ in Et_2O (0.5 M, 0.05 mL, 25 μmol) was evaporated to dryness in an NMR tube. The resulting colorless residue was dissolved in $\text{THF}-d_8$ and the solution was frozen at $-196\text{ }^\circ\text{C}$. Colorless $\mathbf{1H}_2$ (14 mg, 25 μmol) was added, the NMR tube was vacuum sealed, and warmed to room temperature. The orange reaction mixture was analyzed by NMR spectroscopy (see section D).

(C) Reaction Of $\mathbf{1D}_2$ with $H_3\text{CLI}$

A solution of $H_3\text{CLI}$ in Et_2O (0.25 M, 0.14 mL, 35 μmol) was evaporated to dryness in an NMR tube. The resulting colorless residue was dissolved in $\text{THF}-d_8$ and the solution was frozen at $-196\text{ }^\circ\text{C}$. Colorless $\mathbf{1D}_2$ (20 mg, 36 μmol) was added, the NMR tube was vacuum sealed, and warmed to room temperature. The orange reaction mixture was analyzed by NMR spectroscopy (see section D).

(D) Results of the deuterium-labeling experiments

The reactions $D_3\text{CLI}/\mathbf{1H}_2$ and $H_3\text{CLI}/\mathbf{1D}_2$ in $\text{THF}-d_8$ give complex product mixtures in which $\text{Li}[\mathbf{1H}]$ / $\text{Li}[\mathbf{1D}]$ and $\text{Li}[\mathbf{2}]/\text{Li}[\mathbf{2-d}_3]$ are present as major constituents (Figure S4). The additional, poorly resolved signals in the range 7.7 ppm to 6.5 ppm are due to hydride-trapping products. The product distributions critically depend on the exact stoichiometries employed.

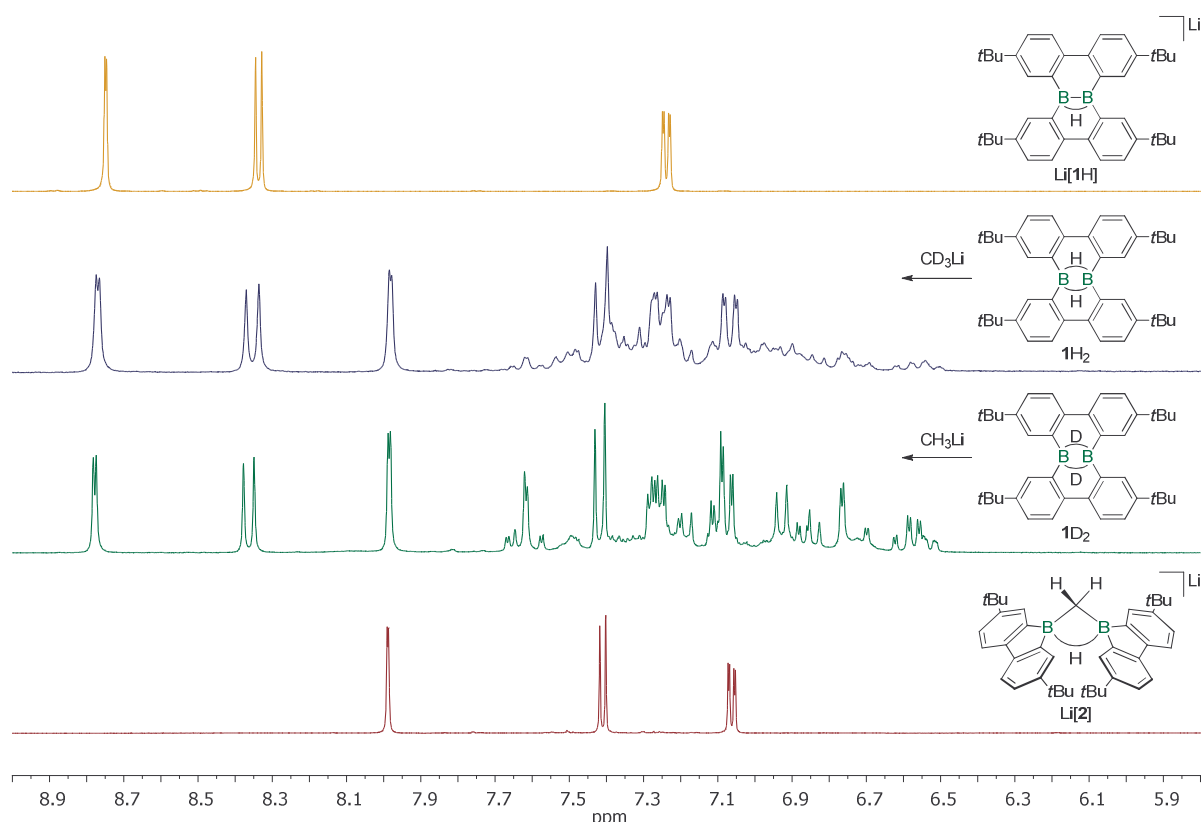


Figure S4. Aromatic regions of ^1H NMR spectra ($\text{THF}-d_8$) recorded on the reaction mixtures of $D_3\text{CLI}/\mathbf{1H}_2$ (blue; 250.1 MHz) and $H_3\text{CLI}/\mathbf{1D}_2$ (green; 300.0 MHz). Matching spectra of $\text{Li}[\mathbf{1H}]$ (orange; 500.2 MHz) and $\text{Li}[\mathbf{2}]$ (red; 500.2 MHz) are shown for comparison. Note: The spectra have been recorded at different spectrometer frequencies, which leads to slight differences in the line shapes of corresponding signals.

Li[2] shows two characteristic ^1H NMR signals, which are particularly relevant for the mechanistic considerations: a broad resonance at 1.94 ppm ($\mu\text{-H}$) and a doublet at 0.49 ppm (CH_2). Both signals are observed in the ^1H NMR spectra of $\text{H}_3\text{CLi}/\mathbf{1H}_2$, but absent in $\text{D}_3\text{CLi}/\mathbf{1H}_2$ (Figure S5). Thus, the $\mu\text{-H}$ atom of **Li[2]** does not originate from the boron-bonded H atoms of the diborane(6) starting material ($\mathbf{1H}_2$). Rather, all the CH_2 and $\mu\text{-H}$ atoms originate from the methylolithium reagent.

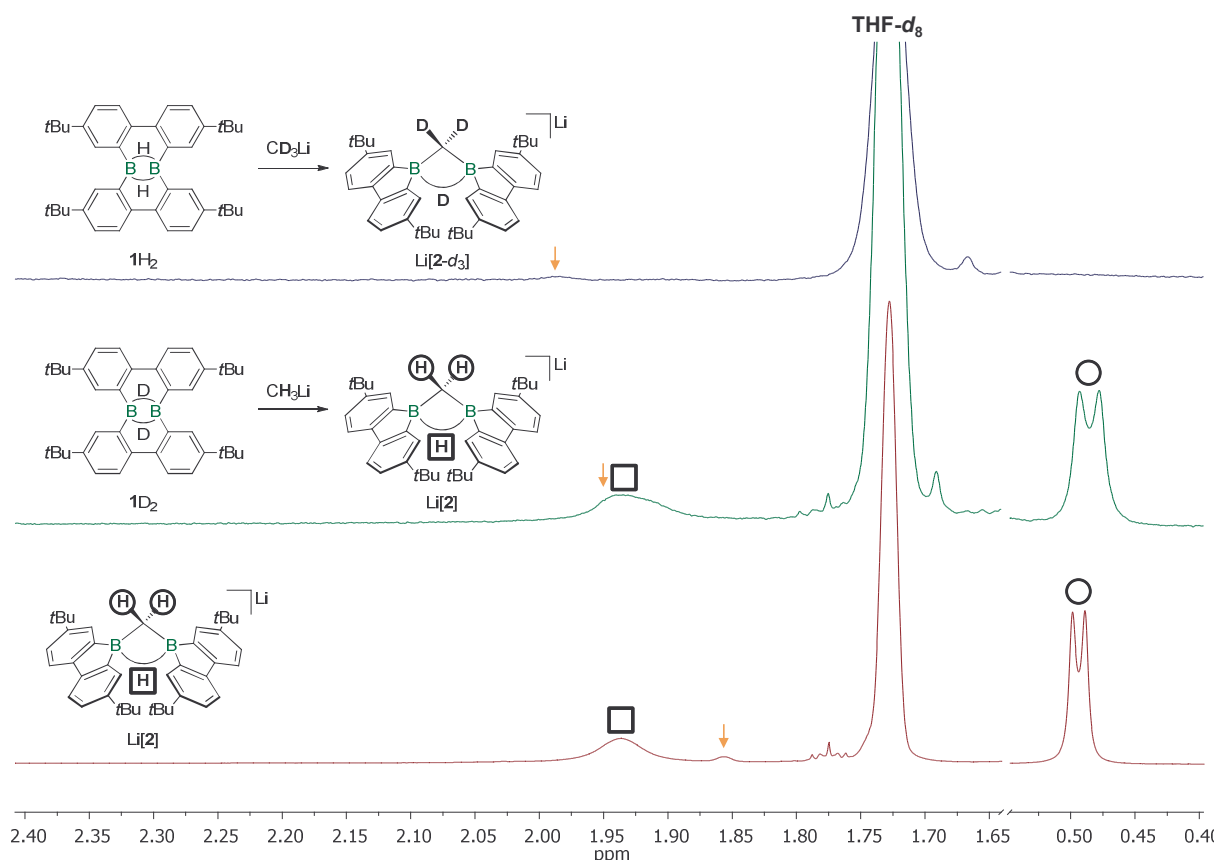


Figure S5. ^1H NMR spectra ($\text{THF}-d_8$) recorded on the reaction solutions of $\text{D}_3\text{CLi}/\mathbf{1H}_2$ (blue; 250.1 MHz) and $\text{H}_3\text{CLi}/\mathbf{1D}_2$ (green; 300.0 MHz). A spectrum of $\text{Li}[2]$ (red; 500.2 MHz) is shown for comparison. Note: The orange-colored arrows mark the ^{13}C satellites of the solvent. The spectra have been recorded at different spectrometer frequencies, which leads to slight differences in the line shapes of corresponding signals and in the positions of the satellites. The integral values of the satellite signals are negligible compared to those of the other resonances. Both in the green and in the red spectrum, the integral ratio of the $\mu\text{-H}$ signal relative to the CH_2 signal is 1:2.

The reactions $\text{D}_3\text{CLi}/\mathbf{1H}_2$ and $\text{H}_3\text{CLi}/\mathbf{1D}_2$ afford D_3CH [$\delta(^1\text{H}) = 0.14$, sept, $^2J(\text{H,D}) = 1.9$ Hz; $\delta(^2\text{H}) = 0.14$, d, $^2J(\text{H,D}) = 1.9$ Hz] and CH_3D [$\delta(^1\text{H}) = 0.18$, t, $^2J(\text{H,D}) = 1.9$ Hz; $\delta(^2\text{H}) = 0.18$, q, $^2J(\text{H,D}) = 1.9$ Hz], respectively, as byproducts (Figure S6). The presence of small amounts of CH_4 are attributable to the fact that the Et_3SiD employed contained only 98 atom-% deuterium and to minor hydrolysis during sample preparation.

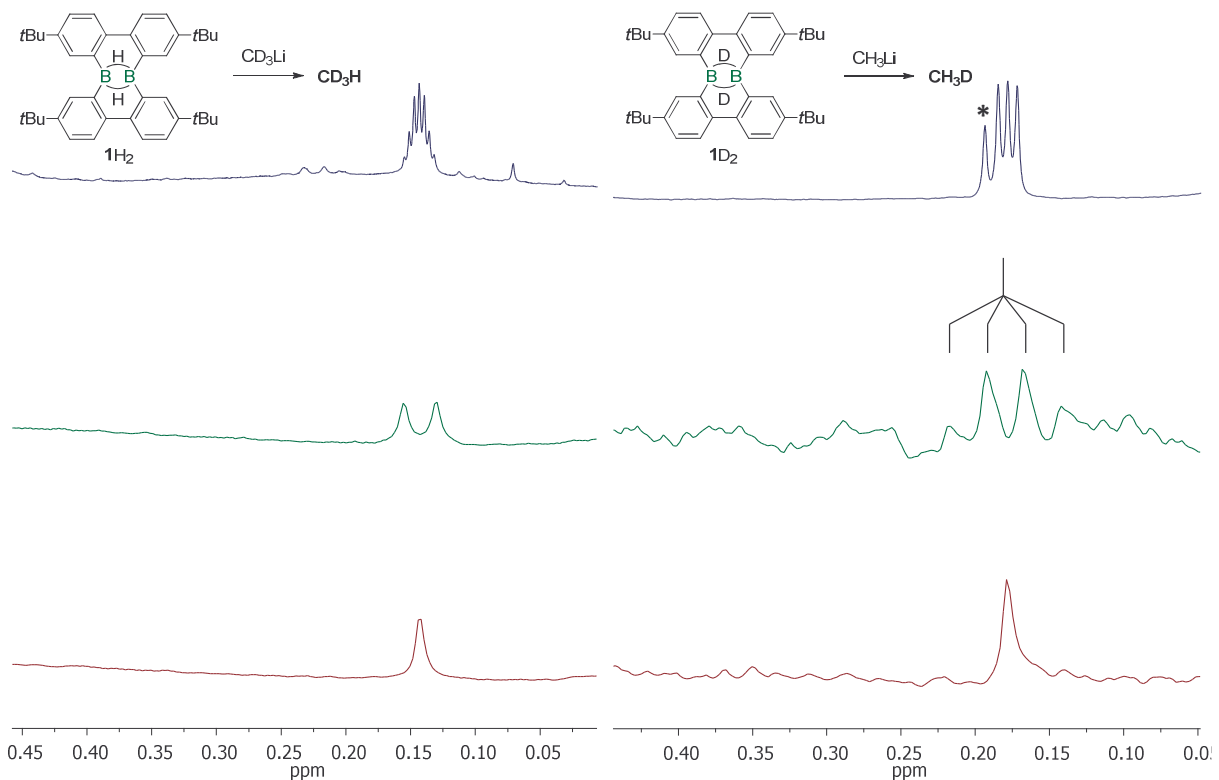


Figure S6. Stacked ^1H (blue; 500.2 MHz), ^2H (green; 76.8 MHz) and $^2\text{H}\{^1\text{H}\}$ (red) NMR spectra, recorded on the mixtures $\text{D}_3\text{CLi}/\mathbf{1H}_2$ (left) and $\text{H}_3\text{CLi}/\mathbf{1D}_2$ (right). The reactions were carried out in sealed NMR tubes ($\text{THF}-d_8$) and the spectra confirm the presence of D_3CH (left) and CH_3D (right). The signal marked with an asterisk corresponds to CH_4 (approximately 10% relative to CH_3D according to the integral values).

Reaction of Li[1H] with H₃CLI to furnish Li₂[4] and follow-up reaction with 1H₂. A solution of H₃CLI in Et₂O (1.4 M, 15 µL, 21 µmol) was evaporated to dryness in an NMR tube. The addition of yellow [Li(thf)₃][1H] (16 mg, 21 µmol) in THF-*d*₈ (0.6 mL) at room temperature furnished an orange-colored solution. The NMR tube was vacuum sealed and ¹H and ¹¹B NMR spectra were recorded. The spectra did not show the resonances of Li[2], but rather signal patterns assignable to Li₂[4] (Figures S8 and Figures S26). The sample was transferred to a new NMR tube, which had already been charged with 1H₂ (11 mg, 20 µmol). ¹H NMR spectroscopy confirmed an approximate 45% conversion to Li[2] and revealed the presence of a primary hydride trapping product Li[10], together with its rearranged isomer Li[7] (Figure S8).

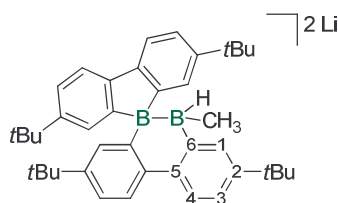


Figure S7. NMR numbering scheme for Li₂[4].

Li₂[4]

¹H NMR (300.0 MHz, THF-*d*₈): δ = 8.1 (vbr, 1H), 7.64 (d, ³J(H,H) = 8.0 Hz, 1H; H-4), 7.53 (n.r., 1H), 7.2 (vbr, 2H), 7.19 (d, ³J(H,H) = 7.9 Hz, 1H; H-4), 6.9 (vbr, 1H), 6.88 (dd, ³J(H,H) = 7.9 Hz, ⁴J(H,H) = 2.4 Hz, 1H; H-3), 6.76 (vbr, 2H), 1.35 (vbr, 9H; CCH₃), 1.26 (s, 9H; CCH₃), 1.20 (br, 9H; CCH₃), 1.08 (vbr, 9H; CCH₃), -0.1 (vbr, 3H; BCH₃). Note: An aryl resonance contributing the missing 2H is likely present at approximately 7.3 ppm, however, due to the broad line shapes and signal overlaps it cannot be unequivocally detected. Integration of the entire aryl region gives a sufficiently high integral value to match the required overall 12 aryl protons.

¹¹B NMR (96.3 MHz, THF-*d*₈): δ = -10.3 ($h_{1/2}$ = 80 Hz), -12.8 ($h_{1/2}$ = 200 Hz, B(H)CH₃). Note: Only the signal at -12.8 ppm becomes significantly sharper upon proton decoupling.

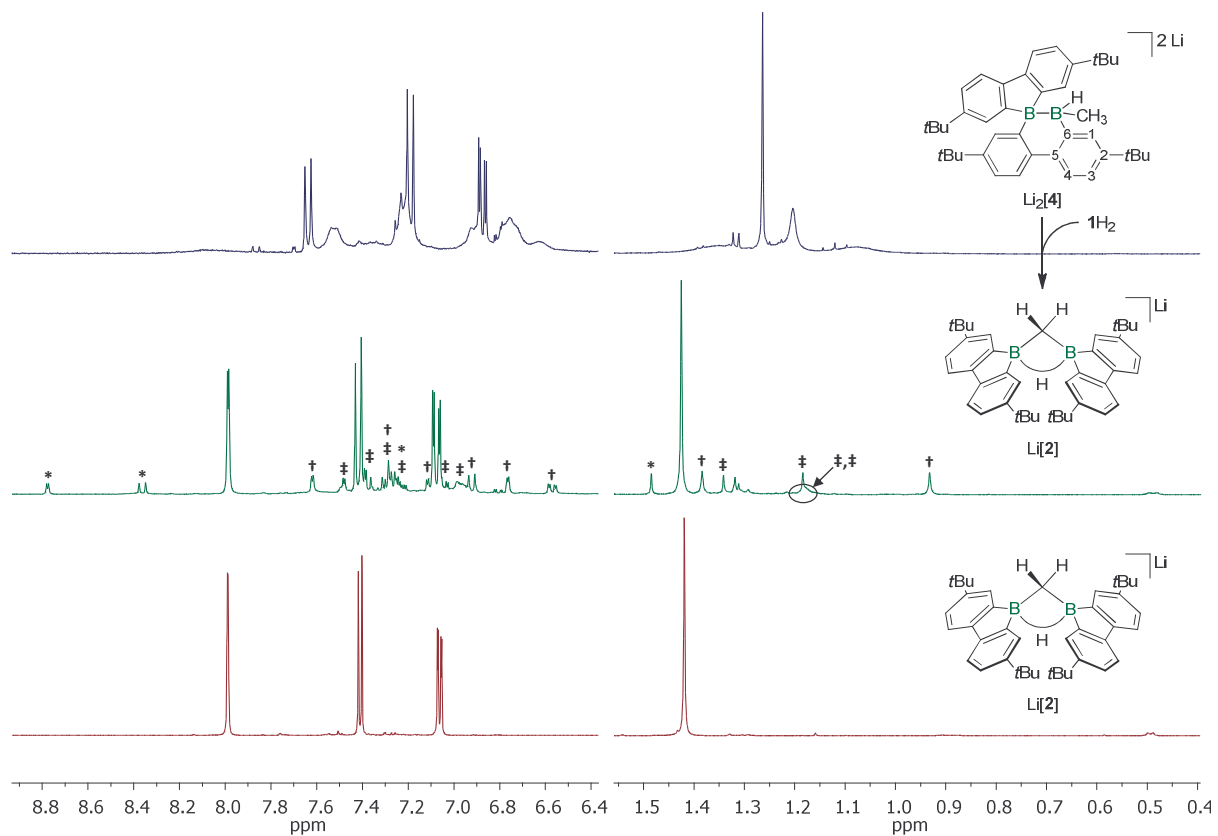


Figure S8. ^1H NMR spectrum of $\text{Li}_2[\mathbf{4}]$, obtained from the reaction $\text{H}_3\text{ClLi}/\text{Li}[\mathbf{1H}]$ (top; 300.0 MHz). Middle: ^1H NMR spectrum showing the formation of $\text{Li}[\mathbf{2}]$ as major product of the reaction $\text{H}_3\text{ClLi}/\text{Li}[\mathbf{1H}]$, after the addition of 1 equiv. $\mathbf{1H}_2$ (middle; 300.0 MHz). The marked minor signals belong to $\text{Li}[\mathbf{1H}]$ (*) and the primary hydride trapping product $\text{Li}[\mathbf{10}]$ (†), which isomerizes over time to give $\text{Li}[\mathbf{7}]$ (‡). ^1H NMR spectrum of an authentic sample of $\text{Li}[\mathbf{2}]$ (bottom; 500.2 MHz). All NMR spectra were recorded in $\text{THF}-d_8$; aromatic and alkyl regions are scaled differently.

Formation of Li₂[11]

Method A: Reaction of Li[1H] with tBuCCLi. Yellow [Li(thf)₃]**[1H]** (20 mg, 26 µmol) in THF-d₈ (0.5 mL) was added at room temperature to an NMR tube charged with solid colorless tBuCCLi (2.3 mg, 26 µmol). A ¹H NMR spectroscopic investigation of the orange-colored solution revealed an almost quantitative consumption of the starting material and the concomitant formation of Li₂[11]. The reaction mixture was layered with hexane/12-crown-4 and stored at room temperature, whereupon orange single crystals of [Li(thf)(12-crown-4)][Li(thf)₂]**[11]** formed.

Method B: Reaction of Li₂[1] with HCCtBu. A twofold excess of neat tBuCCH (4 µL, 2.7 mg, 33 µmol) was added at room temperature to a solution of [Li(thf)₃]₂**[1]** (15 mg, 15 µmol) in THF-d₈ (0.5 mL). The progress of the slow reaction was monitored by ¹H NMR spectroscopy (Figure S10). After 1 month, the signal pattern of Li₂[11] had developed to a significant extent.

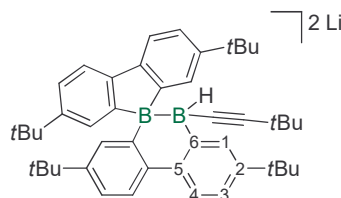


Figure S9. Schematic representation of Li₂[11].

Li₂[11]

¹H NMR (300.0 MHz, THF-d₈): δ = 8.2 (vbr, 1H), 7.61 (d, ³J(H,H) = 8.0 Hz, 1H; H-4), 7.50 (n.r., 1H), 7.32 (n.r., 2H), 7.23 (d, ³J(H,H) = 7.9 Hz, 1H; H-4), 7.12-6.95 (m, 2H), 6.82 (dd, ³J(H,H) = 7.8 Hz, ⁴J(H,H) = 2.1 Hz, 2H; H-3), 1.36 (vbr, 9H; C(CH₃)₃), 1.30 ppm (s, 9H; C(CH₃)₃), 1.19 (s, 9H; C(CH₃)₃), 1.09 (vbr, 9H; C(CH₃)₃), 0.97 (br, 9H; C≡CC(CH₃)₃). Note: An aryl resonance contributing the missing 2H cannot be unequivocally detected. Integration of the entire aryl region gives a sufficiently high integral value to match the required overall 12 aryl protons.

¹¹B NMR (96.3 MHz, THF-d₈): δ = -11.8 (*h*_{1/2} = 60 Hz), -23.3 (*h*_{1/2} = 190 Hz; B(H)CCtBu). Note: Only the signal at -23.3 ppm becomes significantly sharper upon proton decoupling.

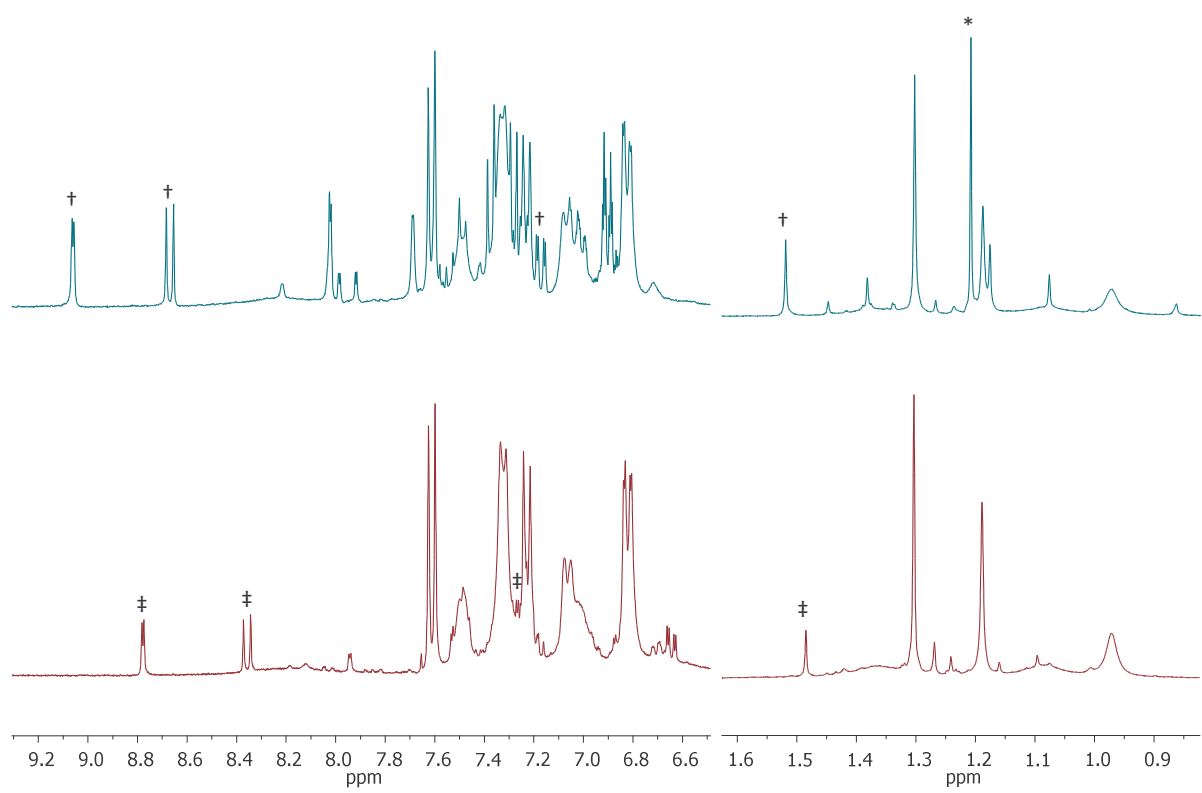


Figure S10: ¹H NMR spectra (300.0 MHz; THF-*d*₈) of the reaction mixtures 2 *t*BuCCH/Li₂[1] after 30 d (top) and *t*BuCCLi/Li[1H] after 1 d (bottom). Additional signals belong to residual Li₂[1] (†), Li[1H] (‡), and *t*BuCCH (*).

Reaction of Li₂[1] with 1 equiv. of H₃C—I. Neat H₃C—I (0.9 µL, 2.1 mg, 15 µmol) was added at room temperature with stirring to a dark red solution of [Li(thf)₃]₂[1] (15 mg, 15 µmol) in THF-*d*₈ (0.6 mL). A ¹H, ¹¹B, and ¹³C{¹H} NMR spectroscopic investigation of the resulting pale yellow solution revealed the conversion of Li₂[1] to Li[2] (major product) and **13** (minor product).

For the NMR data of Li[2] see the reaction H₃CLi/**1H₂**.

Reaction of Li₂[1] with excess H₃CCl. Neat dark red [Li(thf)₃]₂[1] (25 mg, 25 µmol) was placed in a J. Young flask (30 mL) and dissolved in THF (2 mL). The solution was frozen at –196 °C. The flask was evacuated, closed, allowed to warm to room temperature, and filled with H₃CCl gas (1 atm), whereupon the stirred solution instantaneously changed its color from red to orange. All volatiles were removed in a dynamic vacuum and the orange solid residue was dissolved in THF-*d*₈. A ¹H and ¹¹B NMR spectroscopic investigation revealed the quantitative conversion of Li₂[1] to Li[2]. The entire sample was transferred to a small vial, which was placed in a larger vessel containing hexane (2 mL). The outer vessel was covered with a lid to allow for gas-phase diffusion of the solvents in a closed environment. Colorless crystalline material of [Li(thf)₄][2] (17 mg, 20 µmol, 80%) was obtained. For the NMR data of Li[2], see the reaction H₃CLi/**1H₂**.

Reaction of Li₂[1] with 3 equiv. of H₃C—I. Neat H₃C—I (2.8 µL, 6.4 mg, 45 µmol) was added at room temperature with stirring to a dark red solution of [Li(thf)₃]₂[1] (15 mg, 15 µmol) in THF-*d*₈ (0.6 mL). A ¹H, ¹¹B, and ¹³C{¹H} NMR spectroscopic investigation of the resulting pale yellow solution revealed the quantitative conversion of Li₂[1] to **13**.

Reaction of Li₂[1] with 2 equiv. of methyl triflate. Neat methyl triflate (2.8 µL, 4.0 mg, 25 µmol) was added at room temperature with stirring to a dark red solution of [Li(thf)₃]₂[1] (12 mg, 12 µmol) in C₆H₆ (0.5 mL). All volatiles were removed in a dynamic vacuum and the residue was dissolved in THF-*d*₈. A ¹H, ¹¹B, and ¹³C{¹H} NMR spectroscopic investigation of the yellow solution confirmed the quantitative conversion of Li₂[1] to **13**. The addition of only 1.1 equiv. of methyl triflate to [Li(thf)₃]₂[1] in C₆H₆ furnished Li[2] as the major product, which crystallizes as at room temperature from the reaction solution in the form of [Li(thf)₃][2]. For the NMR data of Li[2], see the reaction H₃CLi/**1H₂**.

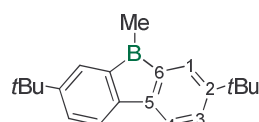


Figure S11. NMR numbering scheme for **13**.

13

¹H NMR (500.2 MHz, THF-*d*₈): δ = 7.50 (dd, ⁴J(H,H) = 2.0 Hz, ⁵J(H,H) = 0.6 Hz, 2H; H-1), 7.38 (dd, ³J(H,H) = 7.9 Hz, ⁵J(H,H) = 0.6 Hz, 2H; H-4), 7.16 (dd, ³J(H,H) = 7.9 Hz, ⁴J(H,H) = 2.0 Hz, 2H; H-3), 1.33 (s, 18H; CCH₃), 0.31 (s, 3H; BCH₃).

¹¹B NMR (160.5 MHz, THF-*d*₈): δ = 13.7.

¹³C{¹H} NMR (125.8 MHz, THF-*d*₈): δ = 152.6 (br, C-6), 148.6 (C-2), 147.3 (C-5), 127.3 (C-1), 124.5 (C-3), 118.5 (C-4), 34.9 (CCH₃), 31.9 (CH₃), 3.2 (BCH₃).

Note: An authentic sample of **13**, prepared from 2,7-di(*t*Bu)-9-Br-9-borafluorene and H₃CMgI in Et₂O/toluene, gave identical NMR shift values.

Reaction of $\text{Li}_2[\mathbf{1}]$ with 1 equiv. ethyl bromide. Neat ethyl bromide (1.3 μL , 1.9 mg, 17 μmol) was added at room temperature with stirring to a dark red solution of $[\text{Li}(\text{thf})_3]_2[\mathbf{1}]$ (15 mg, 15 μmol) in $\text{THF}-d_8$ (0.5 mL). A ^1H , ^{11}B , and $^{13}\text{C}\{^1\text{H}\}$ NMR spectroscopic investigation of the resulting yellow solution revealed the quantitative conversion of $\text{Li}_2[\mathbf{1}]$ to $\text{Li}[\mathbf{19}]$.

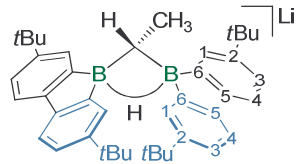


Figure S12. NMR numbering scheme for $\text{Li}[\mathbf{19}]$.

Li[19]

^1H NMR (500.2 MHz, $\text{THF}-d_8$): $\delta = 8.14$ (d, $^4J(\text{H},\text{H}) = 1.6$ Hz, 2H; H-1), **7.99** (d, $^4J(\text{H},\text{H}) = 1.6$ Hz, 2H; H-1), 7.45 (d, $^3J(\text{H},\text{H}) = 7.8$ Hz, 2H; H-4), **7.42** (d, $^3J(\text{H},\text{H}) = 7.8$ Hz, 2H; H-4), 7.09 (dd, $^3J(\text{H},\text{H}) = 7.8$ Hz, $^4J(\text{H},\text{H}) = 1.6$ Hz, 2H; H-3), **7.06** (dd, $^3J(\text{H},\text{H}) = 7.8$ Hz, $^4J(\text{H},\text{H}) = 1.6$ Hz, 2H; H-3), 2.02 (br, 1H; $\mu\text{-H}$), 1.47 (d, $^3J(\text{H},\text{H}) = 7.0$ Hz, 3H; CHCH_3), 1.44 (s, 18H, $\text{C}(\text{CH}_3)_3$), **1.43** (s, 18H, $\text{C}(\text{CH}_3)_3$), 0.95 (qd, $^3J(\text{H},\text{H}) = 7.0$ Hz, $^3J(\text{H},\text{H}) = 3.0$ Hz, 1H; CHCH_3).

^7Li NMR (116.6 MHz, $\text{THF}-d_8$): $\delta = -1.8$.

^{11}B NMR (160.5 MHz, $\text{THF}-d_8$): $\delta = -12.6$ (br).

$^{13}\text{C}\{^1\text{H}\}$ NMR (125.8 MHz, $\text{THF}-d_8$): $\delta = \text{159.6 (C-6), 156.5 (C-6), 148.3 (C-5), 147.4 (C-5), 146.3 (C-2), 146.0 (C-2), 130.1 (C-1), 127.9 (C-1), 121.7 (C-3), 121.6 (C-3), 117.7 (C-4), 117.6 (C-4), 35.2 (C(CH}_3)_3, 35.2 (\text{C(CH}_3)_3, 32.6 (\text{C(CH}_3)_3, 14.3 (\text{CHCH}_3), 11.0 (br, CHCH}_3)$.

Note: The tentative assignment of resonances to the blue vs black aromatic rings is based on 2D NMR experiments and a comparison with the NMR spectra of the corresponding compound $\text{Li}[\mathbf{2}]$ featuring a symmetrical CH_2 bridge.

Reaction of $\text{Li}_2[\mathbf{1}]$ with benzyl chloride. A dark red solution of $[\text{Li}(\text{thf})_3]_2[\mathbf{1}]$ (30 mg, 30 μmol) in $\text{THF}-d_8$ (0.3 mL) was added dropwise with stirring at room temperature to benzyl chloride (4.1 μL , 4.5 mg, 36 μmol) in $\text{THF}-d_8$ (0.2 mL). A ^1H , ^{11}B , and $^{13}\text{C}\{^1\text{H}\}$ NMR spectroscopic investigation of the resulting yellow solution revealed the selective conversion of $\text{Li}_2[\mathbf{1}]$ to $\text{Li}[\mathbf{16}]$ (> 90%). Upon addition of the reaction mixture to hexane (2 mL), a colorless precipitate formed. The mother liquor was removed, the precipitate washed with hexane (3 x 0.2 mL), and dried under vacuum to obtain pure $\text{Li}[\mathbf{16}]$ (according to NMR spectroscopy). Colorless single crystals of $[\text{Li}(\text{thf})_4][\mathbf{16}]$ were grown by gas-phase diffusion of hexane into a THF solution of $\text{Li}[\mathbf{16}]$ (3 d, room temperature). Note: $\text{Li}[\mathbf{16}]$ was also observed as the major product (> 90%) when 1 equiv. of benzyl bromide was used instead of benzyl chloride.

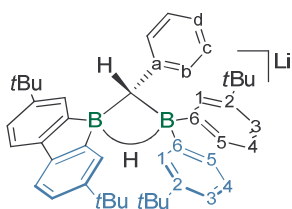


Figure S13. NMR numbering scheme for $\text{Li}[\mathbf{16}]$.

$\text{Li}[\mathbf{16}]$

^1H NMR (500.2 MHz, $\text{THF}-d_8$): $\delta = 8.09$ (n.r., 2H; H-1), 7.51 (n.r., 2H; H-1), 7.45 (d, $^3J(\text{H},\text{H}) = 7.9$ Hz, 2H; H-4), 7.43 (d, $^3J(\text{H},\text{H}) = 7.9$ Hz, 2H; H-4), 7.10 (dd, $^3J(\text{H},\text{H}) = 7.9$ Hz, $^4J(\text{H},\text{H}) = \text{n.r.}$, 2H; H-3), 7.03-7.02 (m, 4H; H-3, H-b), 6.80-6.77 (m, 2H; H-c), 6.71-6.68 (m, 1H; H-d), 2.73 (s, 1H; BCH), 2.26 (br, 1H; BHB), 1.44 (s, 18H; CH_3), 1.23 (s, 18H; CH_3).

^{11}B NMR (160.5 MHz, $\text{THF}-d_8$): $\delta = -13.1$ (br).

$^{13}\text{C}\{^1\text{H}\}$ NMR (125.8 MHz, $\text{THF}-d_8$): $\delta = 158.4$ (br; C-6), 155.5 (br; C-6), 150.7 (C-a), 148.1 (C-5), 147.8 (C-5), 146.4 (C-2), 145.8 (C-2), 134.6 (C-b), 131.5 (C-1), 127.8 (C-1), 126.4 (C-c), 122.1 (C-3), 121.8 (C-d), 121.7 (C-3), 117.7 (C-4), 117.5 (C-4), 35.2 (CCH_3), 35.0 (CCH_3), 32.6 (CH_3), 32.4 (CH_3), 27.3 (br; BCH).

Reaction of $\text{Li}_2[1]$ with the radical clock (bromomethyl)cyclopropane. A dark red solution of $[\text{Li}(\text{thf})_3]_2[1]$ (12 mg, 12 μmol) in $\text{THF}-d_8$ (0.3 mL) was added dropwise with stirring at room temperature to (bromomethyl)cyclopropane (1.4 μL , 1.9 mg, 14 μmol) in $\text{THF}-d_8$ (0.2 mL). A ^1H , ^{11}B , and $^{13}\text{C}\{^1\text{H}\}$ NMR spectroscopic investigation of the resulting yellow solution revealed the selective conversion of $\text{Li}_2[1]$ to $\text{Li}[17]$ (> 90%). No signals were observed in the allylic region of the ^1H NMR spectrum. Note: $\text{Li}[17]$ decomposes in $\text{THF}-d_8$ at room temperature within days.

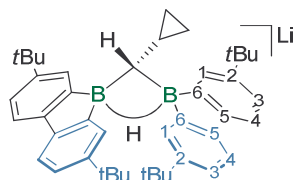


Figure S14. NMR numbering scheme for $\text{Li}[17]$.

$\text{Li}[17]$

^1H NMR (300.0 MHz, $\text{THF}-d_8$): δ = 8.27 (d, $^4J(\text{H},\text{H})$ = 1.8 Hz, 2H; H-1), 7.92 (d, $^4J(\text{H},\text{H})$ = 1.8 Hz, 2H; H-1), 7.44 (d, $^3J(\text{H},\text{H})$ = 7.9 Hz, 2H; H-4), 7.41 (d, $^3J(\text{H},\text{H})$ = 7.9 Hz, 2H; H-4), 7.08 (dd, $^3J(\text{H},\text{H})$ = 7.9 Hz, $^4J(\text{H},\text{H})$ = 1.8 Hz, 2H; H-3), 7.05 (dd, $^3J(\text{H},\text{H})$ = 7.9 Hz, $^4J(\text{H},\text{H})$ = 1.8 Hz, 2H; H-3), 2.09 (br, 1H; BHB), 1.58-1.50 (m, 1H; CH_2CH), 1.44 (s, 18H; CH_3), 1.41 (s, 18H; CH_3), 0.86 (dd, $^3J(\text{H},\text{H})$ = 6.3 Hz, $^3J(\text{H},\text{H})$ = 2.9 Hz, 1H; BCH), 0.25-0.19 (m, 2H; CH_2), -0.14-(-0.19) (m, 2H; CH_2).

^{11}B NMR (96.3 MHz, $\text{THF}-d_8$): δ = -14.9 (br).

$^{13}\text{C}\{^1\text{H}\}$ NMR (125.8 MHz, $\text{THF}-d_8$): δ = 159.4 (C-6), 156.8 (C-6), 148.2 (C-5), 147.5 (C-5), 146.4 (C-2), 145.9 (C-2), 130.6 (C-1), 127.7 (C-1), 121.8 (C-3), 121.6 (C-3), 117.7 (C-4), 117.6 (C-4), 35.2 (CCH_3), 32.6 (CH_3), 24.6 (br; BCH), 13.1 (CHCH_2), 9.5 (CH_2).

Reactions of $\text{Li}_2[\mathbf{1}]$ with α,ω -dihaloalkanes

All reactions were conducted by adding a dark red solution of $[\text{Li}(\text{thf})_3]_2[\mathbf{1}]$ in $\text{THF}-d_8$ (0.3 mL) at room temperature with stirring to a small excess of an α,ω -dihaloalkane $X(\text{CH}_2)_nX$ in $\text{THF}-d_8$ (0.2 mL). The amounts of starting materials used in each individual experiment and the products obtained are listed in Table S1.

Table S1: Starting materials and products of the reactions of α,ω -dihaloalkanes $X(\text{CH}_2)_nX$ with $[\text{Li}(\text{thf})_3]_2[\mathbf{1}]$. The percentages of conversion of the boron compound (determined through integration of the ^1H NMR spectra) are listed in parentheses.

starting materials		product(s)
1,2-dihaloethane		
Cl	1,2-dichloroethane (1.7 μL , 2.1 mg, 21 μmol), $[\text{Li}(\text{thf})_3]_2[\mathbf{1}]$ (17 mg, 17 μmol)	14^{C2} (100%)
Br	1,2-dibromoethane (1.8 μL , 3.9 mg, 21 μmol), $[\text{Li}(\text{thf})_3]_2[\mathbf{1}]$ (17 mg, 17 μmol)	14^{C2} (100%)
1,3-dihalopropane		
Cl	1,3-dichloropropane (3.2 μL , 3.8 mg, 34 μmol), $[\text{Li}(\text{thf})_3]_2[\mathbf{1}]$ (30 mg, 30 μmol)	Complex mixture of yet unidentified products
Br	1,3-dibromopropane (3.6 μL , 7.2 mg, 35 μmol), $[\text{Li}(\text{thf})_3]_2[\mathbf{1}]$ (30 mg, 30 μmol)	14^{C3} (> 90%; yield: 15 mg, 25 μmol , 83%)
1,4-dihalobutane		
Cl	1,4-dichlorobutane (3.9 μL , 4.5 mg, 36 μmol), $[\text{Li}(\text{thf})_3]_2[\mathbf{1}]$ (30 mg, 30 μmol)	$\text{Li}[\mathbf{15}^{\text{C}4,\text{Cl}}]$ (92%; yield: 17 mg, 21 μmol , 70% (calcd for $[\text{Li}(\text{thf})_{2.5}][\mathbf{15}^{\text{C}4,\text{Cl}}]$)), 14^{C4} (8%)
Br	1,4-dibromobutane (6.0 μL , 11 mg, 50 μmol), $[\text{Li}(\text{thf})_3]_2[\mathbf{1}]$ (42 mg, 42 μmol)	14^{C4} (92%), $\text{Li}[\mathbf{15}^{\text{C}4,\text{Br}}]$ (8%)
1,5-dihalopentane		
Cl	1,5-dichloropentane (4.4 μL , 4.8 mg, 34 μmol), $[\text{Li}(\text{thf})_3]_2[\mathbf{1}]$ (29 mg, 29 μmol)	$\text{Li}[\mathbf{15}^{\text{C}5,\text{Cl}}]$ (> 90%)
Br	1,5-dibromopentane (4.8 μL , 8.1 mg, 35 μmol), $[\text{Li}(\text{thf})_3]_2[\mathbf{1}]$ (30 mg, 30 μmol)	$\text{Li}[\mathbf{15}^{\text{C}5,\text{Br}}]$ (> 90%)
1,6-dihalohexane		
Cl	1,6-dichlorohexane (5.0 μL , 5.3 mg, 34 μmol), $[\text{Li}(\text{thf})_3]_2[\mathbf{1}]$ (29 mg, 29 μmol)	$\text{Li}[\mathbf{15}^{\text{C}6,\text{Cl}}]$ (> 90%)
Br	1,6-dibromohexane (5.0 μL , 7.9 mg, 33 μmol), $[\text{Li}(\text{thf})_3]_2[\mathbf{1}]$ (28 mg, 28 μmol)	$\text{Li}[\mathbf{15}^{\text{C}6,\text{Br}}]$ (> 90%)

The neutral compounds **14^{C2}**, **14^{C3}**, and **14^{C4}** were crystallized by slow evaporation of the solvent. The crystals were rinsed with small volumes of hexane (**14^{C2}**: 0 mL, **14^{C3}**: 3 \times 0.2 mL, **14^{C4}**: 3 \times 0.2 mL) and THF (**14^{C2}**: 0 mL, **14^{C3}**: 2 \times 0.1 mL, **14^{C4}**: 0 mL), and dried in a dynamic vacuum. The salts $\text{Li}[\mathbf{15}^{\text{C}4,\text{Cl}}]$, $\text{Li}[\mathbf{15}^{\text{C}4,\text{Br}}]$, $\text{Li}[\mathbf{15}^{\text{C}5,\text{Cl}}]$, $\text{Li}[\mathbf{15}^{\text{C}5,\text{Br}}]$, $\text{Li}[\mathbf{15}^{\text{C}6,\text{Cl}}]$, and $\text{Li}[\mathbf{15}^{\text{C}6,\text{Br}}]$ were precipitated from the reaction mixtures by addition of hexane (2 mL). The precipitates were washed with hexane (3 \times 0.2 mL) and dried in a dynamic vacuum. Colorless single crystals of $[\text{Li}(12\text{-crown-4})_2][\mathbf{15}^{\text{C}5,\text{Cl}}]$ were obtained by layering a solution of $\text{Li}[\mathbf{15}^{\text{C}5,\text{Cl}}]$ in THF with hexane/12-crown-4 (3 d; room temperature).

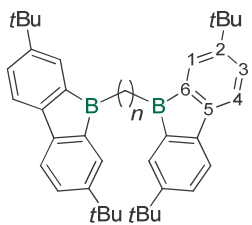


Figure S15. NMR numbering scheme for **14^{Cn}**.

14^{C2}

¹H NMR (500.2 MHz, THF-*d*₈): δ = 7.66 (d, ⁴J(H,H) = 1.9 Hz, 4H; H-1), 7.39 (d, ³J(H,H) = 7.8 Hz, 4H; H-4), 7.17 (dd, ³J(H,H) = 7.8 Hz, ⁴J(H,H) = 1.9 Hz, 4H; H-3), 1.35 (s, 36H; CH₃), 1.07 (s, 4H; C₂H₄).

¹¹B NMR (160.5 MHz, THF-*d*₈): δ = 15.9.

¹³C{¹H} NMR (125.8 MHz, THF-*d*₈): δ = 153.0 (C-6), 148.2 (C-2), 147.6 (C-5), 128.0 (C-1), 124.3 (C-3), 118.5 (C-4), 34.9 (CCH₃), 32.0 (CH₃), 16.1 (C₂H₄).

14^{C3}

¹H NMR (500.2 MHz, THF-*d*₈): δ = 7.48 (d, ⁴J(H,H) = 1.9 Hz, 4H; H-1), 7.37 (d, ³J(H,H) = 7.9 Hz, 4H; H-4), 7.13 (dd, ³J(H,H) = 7.9 Hz, ⁴J(H,H) = 1.9 Hz, 4H; H-3), 1.53-1.47 (m, 2H; CCH₂), 1.30 (s, 36H; CH₃), 0.95-0.92 (m, 4H; BCH₂).

¹¹B NMR (160.5 MHz, THF-*d*₈): δ = 15.4 (vbr).

¹³C{¹H} NMR (125.8 MHz, THF-*d*₈): δ = 152.7 (br; C-6), 148.3 (C-2), 147.6 (C-5), 128.1 (C-1), 124.2 (C-3), 118.4 (C-4), 34.9 (CCH₃), 32.0 (CH₃), 26.0 (br; BCH₂), 23.0 (CCH₂).

14^{C4}

¹H NMR (500.2 MHz, THF-*d*₈): δ = 7.51 (d, ⁴J(H,H) = 1.9 Hz, 4H; H-1), 7.37 (d, ³J(H,H) = 7.9 Hz, 4H; H-4), 7.14 (dd, ³J(H,H) = 7.9 Hz, ⁴J(H,H) = 1.9 Hz, 4H; H-3), 1.32 (s, 36H; CH₃), 1.32-1.29 (m, 4H; BCCH₂), 0.92-0.90 (m, 4H; BCH₂).

¹¹B NMR (160.5 MHz, THF-*d*₈): δ = 14.4 (vbr).

¹³C{¹H} NMR (125.8 MHz, THF-*d*₈): δ = 152.4 (br; C-6), 148.3 (C-2), 147.6 (C-5), 127.9 (C-1), 124.3 (C-3), 118.4 (C-4), 34.9 (CCH₃), 32.0 (CH₃), 30.9 (BCCH₂), 21.5 (br; BCH₂).

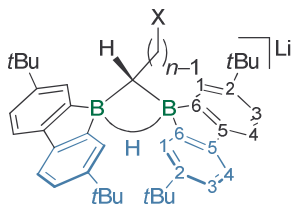


Figure S16. NMR numbering scheme for $\mathbf{15}^{Cn,X}$.

Li[$\mathbf{15}^{C4,C1}$]

^1H NMR (500.2 MHz, THF- d_8): $\delta = 8.15$ (d, $^4J(\text{H},\text{H}) = 1.9$ Hz, 2H; H-1), **8.01** (d, $^4J(\text{H},\text{H}) = 1.9$ Hz, 2H; H-1), 7.46 (d, $^3J(\text{H},\text{H}) = 7.9$ Hz, 2H; H-4), **7.43** (d, $^3J(\text{H},\text{H}) = 7.9$ Hz, 2H; H-4), 7.10 (dd, $^3J(\text{H},\text{H}) = 7.9$ Hz, $^4J(\text{H},\text{H}) = 1.9$ Hz, 2H; H-3), **7.07** (dd, $^3J(\text{H},\text{H}) = 7.9$ Hz, $^4J(\text{H},\text{H}) = 1.9$ Hz, 2H; H-3), 3.19 (t, $^3J(\text{H},\text{H}) = 7.4$ Hz, 2H; ClCH₂), 2.16 (vq, $^3J(\text{H},\text{H}) = 7.4$ Hz, 2H; BCCH₂), 2.04 (br, 1H; BHB), 1.52 (vquint, $^3J(\text{H},\text{H}) = 7.4$ Hz, 2H; ClCCH₂), 1.45 (s, 18H; CH₃), **1.43** (s, 18H; CH₃), 0.94 (dt, $^3J(\text{H},\text{H}) = 7.8$ Hz, $^3J(\text{H},\text{H}) = 2.6$ Hz, 1H; BCH).

^{11}B NMR (160.5 MHz, THF- d_8): $\delta = -13.0$ (br).

$^{13}\text{C}\{\text{H}\}$ NMR (125.8 MHz, THF- d_8): $\delta = \textcolor{blue}{159.0}$ (br; C-6), 156.4 (br; C-6), 148.3 (C-5), **147.4** (C-5), **146.5** (C-2), 146.1 (C-2), 129.8 (C-1), **127.8** (C-1), **121.8** (C-3), 121.7 (C-3), 117.8 (C-4), **117.7** (C-4), 46.8 (ClCH₂), 38.8 (ClCCH₂), **35.3** (CCH₃), 35.2 (CCH₃), 32.7 (CH₃ or CH₃), 32.6 (CH₃ or CH₃), 28.2 (BCCH₂), 19.3 (br; BCH).

Li[$\mathbf{15}^{C5,C1}$]

^1H NMR (500.2 MHz, THF- d_8): $\delta = 8.16$ (d, $^4J(\text{H},\text{H}) = 1.8$ Hz, 2H; H-1), **8.01** (d, $^4J(\text{H},\text{H}) = 1.8$ Hz, 2H; H-1), 7.46 (d, $^3J(\text{H},\text{H}) = 7.9$ Hz, 2H; H-4), **7.42** (d, $^3J(\text{H},\text{H}) = 7.9$ Hz, 2H; H-4), 7.09 (dd, $^3J(\text{H},\text{H}) = 7.9$ Hz, $^4J(\text{H},\text{H}) = 1.8$ Hz, 2H; H-3), **7.07** (dd, $^3J(\text{H},\text{H}) = 7.9$ Hz, $^4J(\text{H},\text{H}) = 1.8$ Hz, 2H; H-3), 3.14 (t, $^3J(\text{H},\text{H}) = 7.3$ Hz, 2H; ClCH₂), 2.07 (vq, $^3J(\text{H},\text{H}) = 7.5$ Hz, 2H; BCCH₂), 2.04 (br, 1H; BHB), 1.51 (vquint, $^3J(\text{H},\text{H}) = 7.3$ Hz, 2H; ClCCH₂), 1.45 (s, 18H; CH₃), **1.43** (s, 18H; CH₃), 1.14 (vquint, $^3J(\text{H},\text{H}) = 7.3$ Hz, 2H; ClCCCH₂), 0.93 (td, $^3J(\text{H},\text{H}) = 7.6$ Hz, $^3J(\text{H},\text{H}) = 2.3$ Hz, 1H; BCH).

^{11}B NMR (160.5 MHz, THF- d_8): $\delta = -13.7$ (br).

$^{13}\text{C}\{\text{H}\}$ NMR (125.8 MHz, THF- d_8): $\delta = \textcolor{blue}{159.3}$ (br; C-6), 156.6 (br; C-6), 148.3 (C-5), **147.3** (C-5), **146.4** (C-2), 146.1 (C-2), 129.8 (C-1), **127.8** (C-1), **121.7** (C-3), 121.7 (C-3), 117.8 (C-4), **117.7** (C-4), 46.0 (ClCH₂), **35.3** (CCH₃), 35.2 (CCH₃), 34.1 (ClCCH₂), 32.7 (CH₃, CH₃), 32.4 (ClCCCH₂), 29.7 (BCCH₂), 20.4 (br; BCH).

Li[$\mathbf{15}^{C5,Br}$]

^1H NMR (500.2 MHz, THF- d_8): $\delta = 8.15$ (d, $^4J(\text{H},\text{H}) = 1.8$ Hz, 2H; H-1), **8.01** (d, $^4J(\text{H},\text{H}) = 1.8$ Hz, 2H; H-1), 7.46 (d, $^3J(\text{H},\text{H}) = 7.9$ Hz, 2H; H-4), **7.43** (d, $^3J(\text{H},\text{H}) = 7.9$ Hz, 2H; H-4), 7.10 (dd, $^3J(\text{H},\text{H}) = 7.9$ Hz, $^4J(\text{H},\text{H}) = 1.8$ Hz, 2H; H-3), **7.07** (dd, $^3J(\text{H},\text{H}) = 7.9$ Hz, $^4J(\text{H},\text{H}) = 1.8$ Hz, 2H; H-3), 3.03 (t, $^3J(\text{H},\text{H}) = 7.3$ Hz, 2H; BrCH₂), 2.07 (vq, $^3J(\text{H},\text{H}) = 7.5$ Hz, 2H; BCCH₂), 2.04 (br, 1H; BHB), 1.60 (vquint, $^3J(\text{H},\text{H}) = 7.3$ Hz, 2H; BrCCH₂), 1.45 (s, 18H; CH₃), **1.43** (s, 18H; CH₃), 1.15 (vquint, $^3J(\text{H},\text{H}) = 7.3$ Hz, 2H; BrCCCH₂), 0.93 (td, $^3J(\text{H},\text{H}) = 7.6$ Hz, $^3J(\text{H},\text{H}) = 2.3$ Hz, 1H; BCH).

^{11}B NMR (160.5 MHz, THF- d_8): $\delta = -12.9$ (br).

$^{13}\text{C}\{\text{H}\}$ NMR (125.8 MHz, THF- d_8): $\delta = \textcolor{blue}{159.4}$ (br; C-6), 156.6 (br; C-6), 148.2 (C-5), **147.3** (C-5), **146.5** (C-2), 146.1 (C-2), 129.8 (C-1), **127.8** (C-1), **121.8** (C-3), 121.7 (C-3), 117.8 (C-4), **117.7** (C-4), **35.3** (CCH₃), 35.2 (BrCH₂, CCH₃), 34.3 (BrCCH₂), 33.7 (BrCCCH₂), 32.7 (CH₃), 29.5 (BCCH₂), 20.4 (br; BCH).

Li[15^{C6,C1}]

¹H NMR (500.2 MHz, THF-*d*₈): δ = 8.17 (d, ⁴J(H,H) = 1.8 Hz, 2H; H-1), 8.01 (d, ⁴J(H,H) = 1.8 Hz, 2H; H-1), 7.45 (d, ³J(H,H) = 7.9 Hz, 2H; H-4), 7.42 (d, ³J(H,H) = 7.9 Hz, 2H; H-4), 7.09 (dd, ³J(H,H) = 7.9 Hz, ⁴J(H,H) = 1.8 Hz, 2H; H-3), 7.06 (dd, ³J(H,H) = 7.9 Hz, ⁴J(H,H) = 1.8 Hz, 2H; H-3), 3.15 (t, ³J(H,H) = 7.1 Hz, 2H; ClCH₂), 2.05 (vq, ³J(H,H) = 7.5 Hz, 2H; BCCH₂), 2.04 (br, 1H; BHB), 1.45 (s, 18H; CH₃), 1.44 (vquint, ³J(H,H) = 7.2 Hz, 2H; ClCCH₂), 1.43 (s, 18H; CH₃), 1.16 (vquint, ³J(H,H) = 7.5 Hz, 2H; ClCCCH₂), 1.07 (vquint, ³J(H,H) = 7.3 Hz, 2H; BCCCH₂), 0.94 (td, ³J(H,H) = 7.6 Hz, ⁴J(H,H) = 2.6 Hz, 1H; BCH).

¹¹B NMR (160.5 MHz, THF-*d*₈): δ = -14.0 (br).

¹³C{¹H} NMR (125.8 MHz, THF-*d*₈): δ = 159.6 (br; C-6), 156.8 (br; C-6), 148.2 (C-5), 147.4 (C-5), 146.4 (C-2), 146.0 (C-2), 129.9 (C-1), 127.8 (C-1), 121.6 (C-3), 121.6 (C-3), 117.7 (C-4), 117.6 (C-4), 45.8 (ClCH₂), 35.3 (CCH₃), 35.2 (CCH₃), 34.4 (BCCCH₂), 33.8 (ClCCH₂), 32.7 (CH₃), 30.2 (BCCH₂), 27.7 (ClCCCH₂), 20.6 (br; BCH).

Li[15^{C6,Br}]

¹H NMR (500.2 MHz, THF-*d*₈): δ = 8.16 (d, ⁴J(H,H) = 1.8 Hz, 2H; H-1), 8.01 (d, ⁴J(H,H) = 1.8 Hz, 2H; H-1), 7.46 (d, ³J(H,H) = 7.9 Hz, 2H; H-4), 7.43 (d, ³J(H,H) = 7.9 Hz, 2H; H-4), 7.10 (dd, ³J(H,H) = 7.9 Hz, ⁴J(H,H) = 1.8 Hz, 2H; H-3), 7.07 (dd, ³J(H,H) = 7.9 Hz, ⁴J(H,H) = 1.8 Hz, 2H; H-3), 3.05 (t, ³J(H,H) = 7.2 Hz, 2H; BrCH₂), 2.05 (vq, ³J(H,H) = 7.5 Hz, 2H; BCCH₂), 2.03 (br, 1H; BHB), 1.54 (vquint, ³J(H,H) = 7.3 Hz, 2H; BrCCH₂), 1.45 (s, 18H; CH₃), 1.44 (s, 18H; CH₃), 1.17 (vquint, ³J(H,H) = 7.3 Hz, 2H; BrCCCH₂), 1.07 (vquint, ³J(H,H) = 7.3 Hz, 2H; BCCCH₂), 0.94 (td, ³J(H,H) = 7.5 Hz, ³J(H,H) = 2.2 Hz, 1H; BCH).

¹¹B NMR (160.5 MHz, THF-*d*₈): δ = -13.6 (br).

¹³C{¹H} NMR (125.8 MHz, THF-*d*₈): δ = 159.5 (br; C-6), 156.8 (br; C-6), 148.2 (C-5), 147.3 (C-5), 146.5 (C-2), 146.1 (C-2), 129.9 (C-1), 127.9 (C-1), 121.7 (C-3), 121.7 (C-3), 117.8 (C-4), 117.7 (C-4), 35.3 (CCH₃), 35.2 (CCH₃), 34.8 (BrCH₂), 34.2 (BCCCH₂), 34.1 (BrCCH₂), 32.7 (CH₃, CH₃), 30.2 (BCCH₂), 29.0 (BrCCCH₂), 20.7 (br; BCH).

2. Plots of NMR spectra

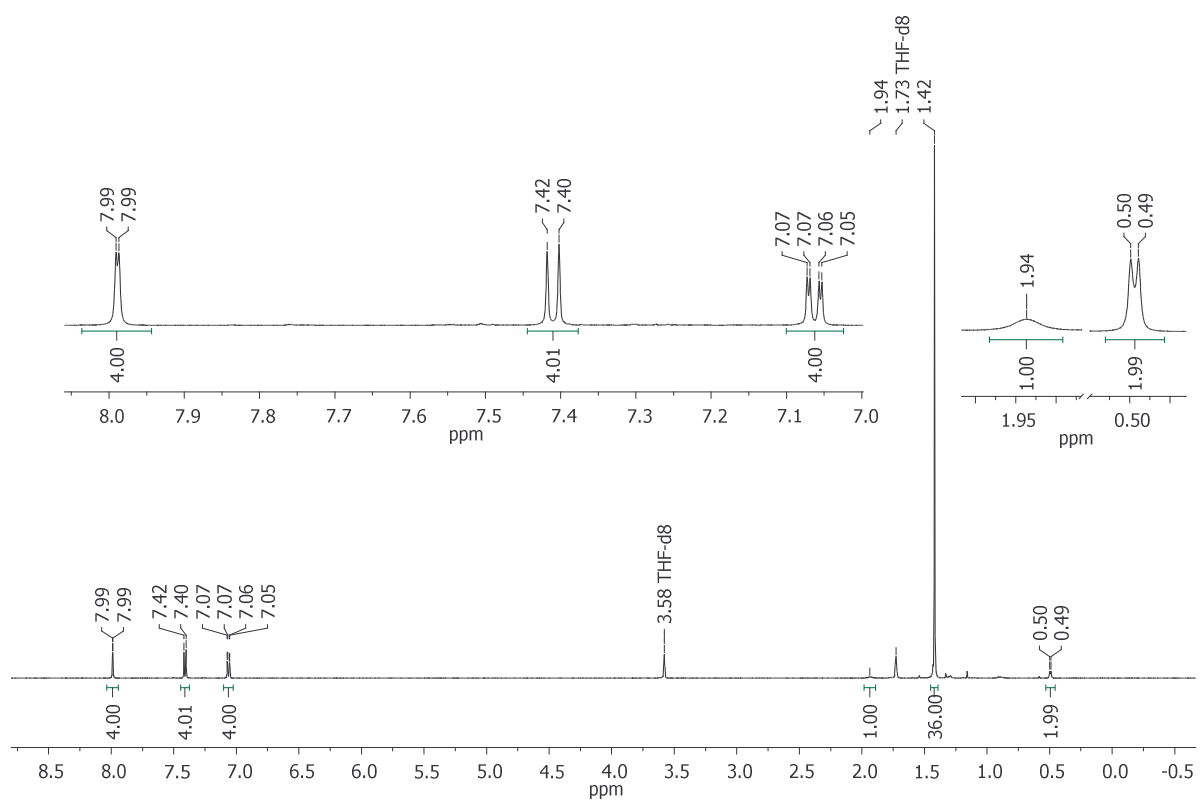


Figure S17: ^1H NMR spectrum of $\text{Li}[\mathbf{2}]$ (500.2 MHz, THF- d_8).

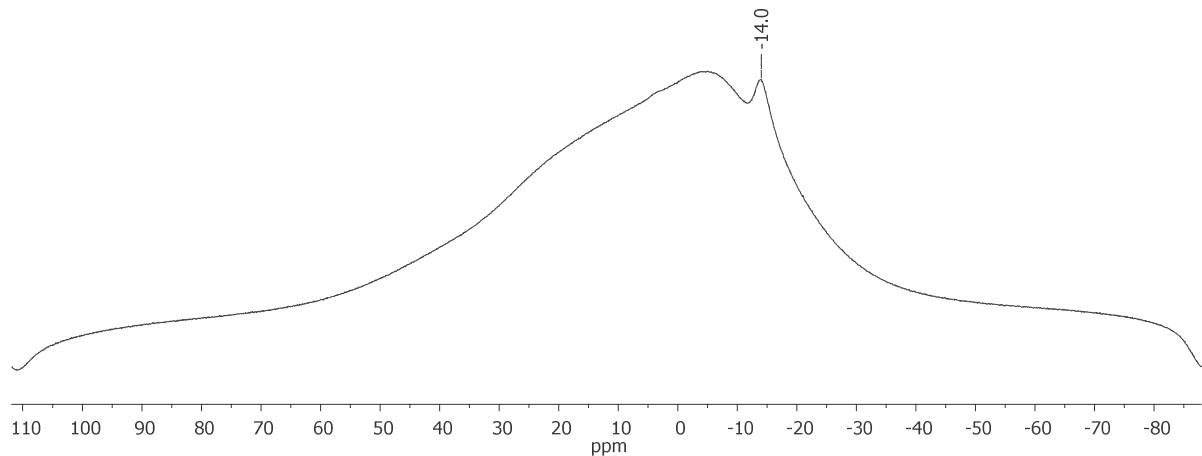


Figure S18: ^{11}B NMR spectrum of $\text{Li}[\mathbf{2}]$ (160.5 MHz, THF- d_8).

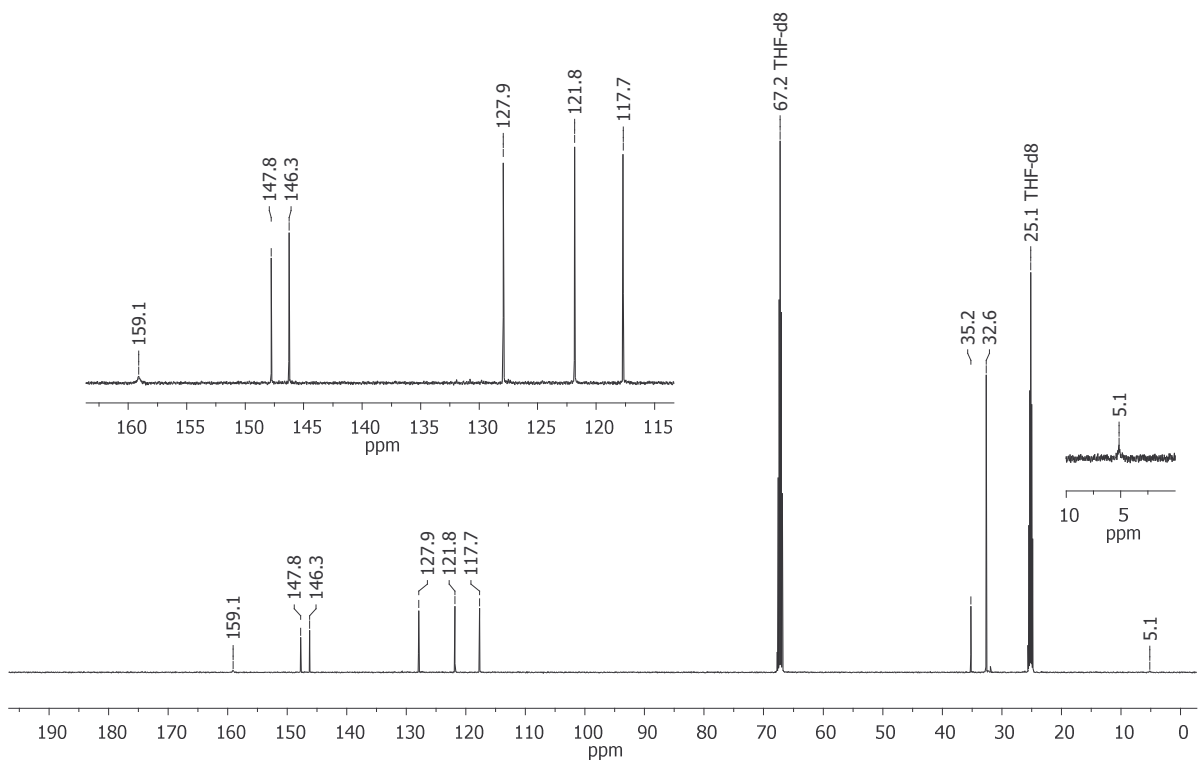


Figure S19: $^{13}\text{C}\{^1\text{H}\}$ NMR spectrum of Li[**2**] (125.8 MHz, THF-*d*₈).

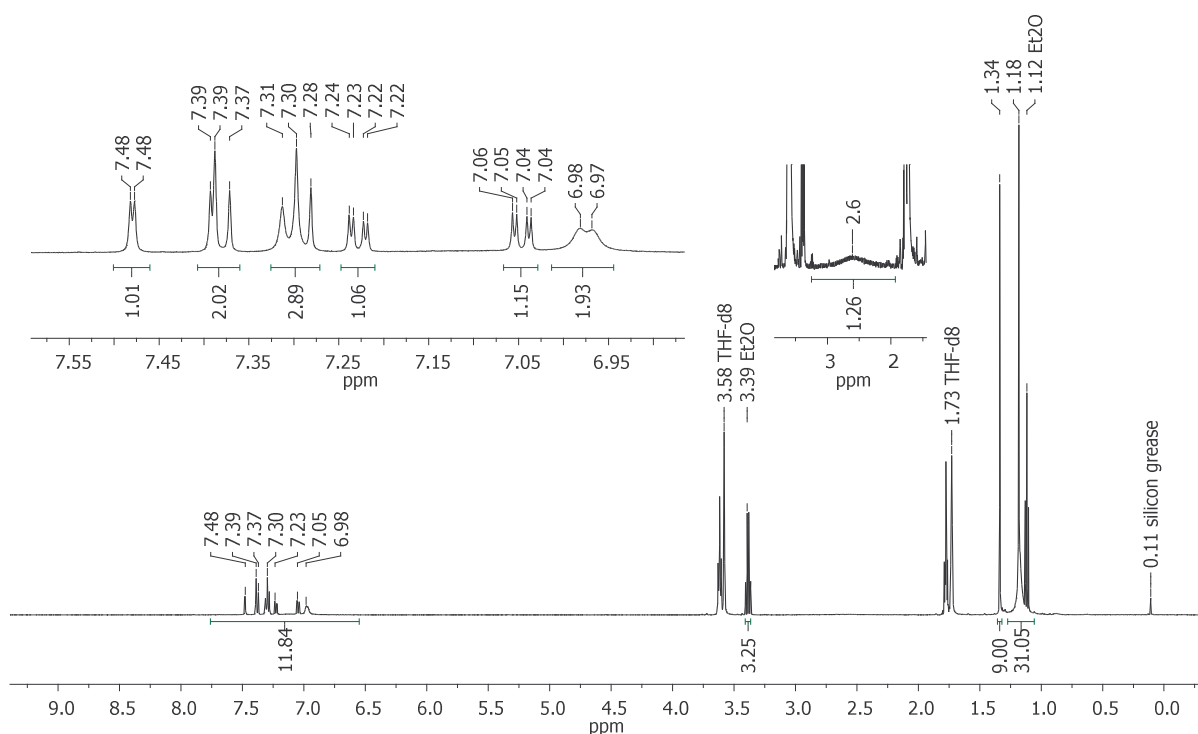


Figure S20: ^1H NMR spectrum of Li[7] (500.2 MHz, THF- d_8).

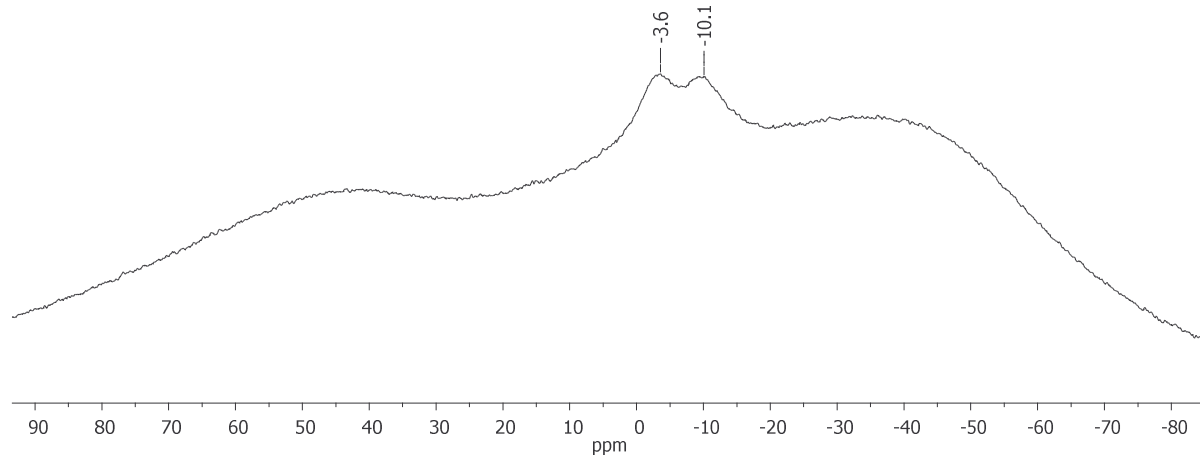
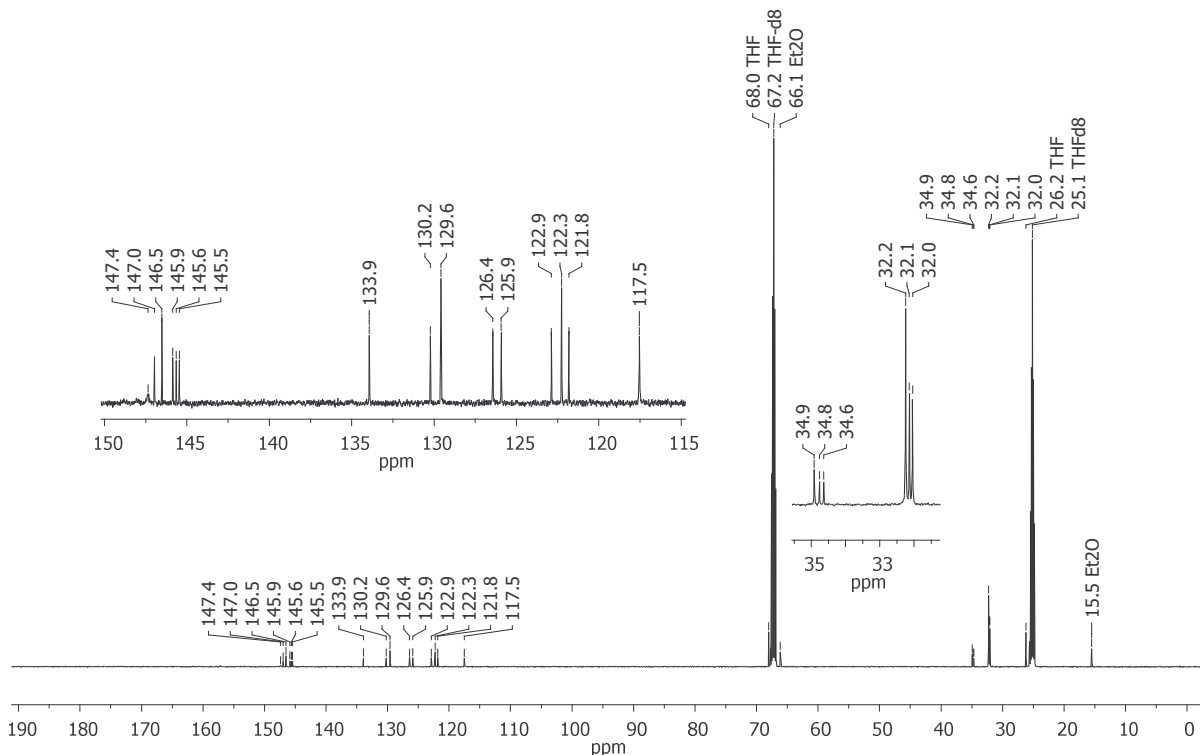


Figure S21: ^{11}B NMR spectrum of $\text{Li}[7]$ (96.3 MHz, $\text{THF}-d_8$).



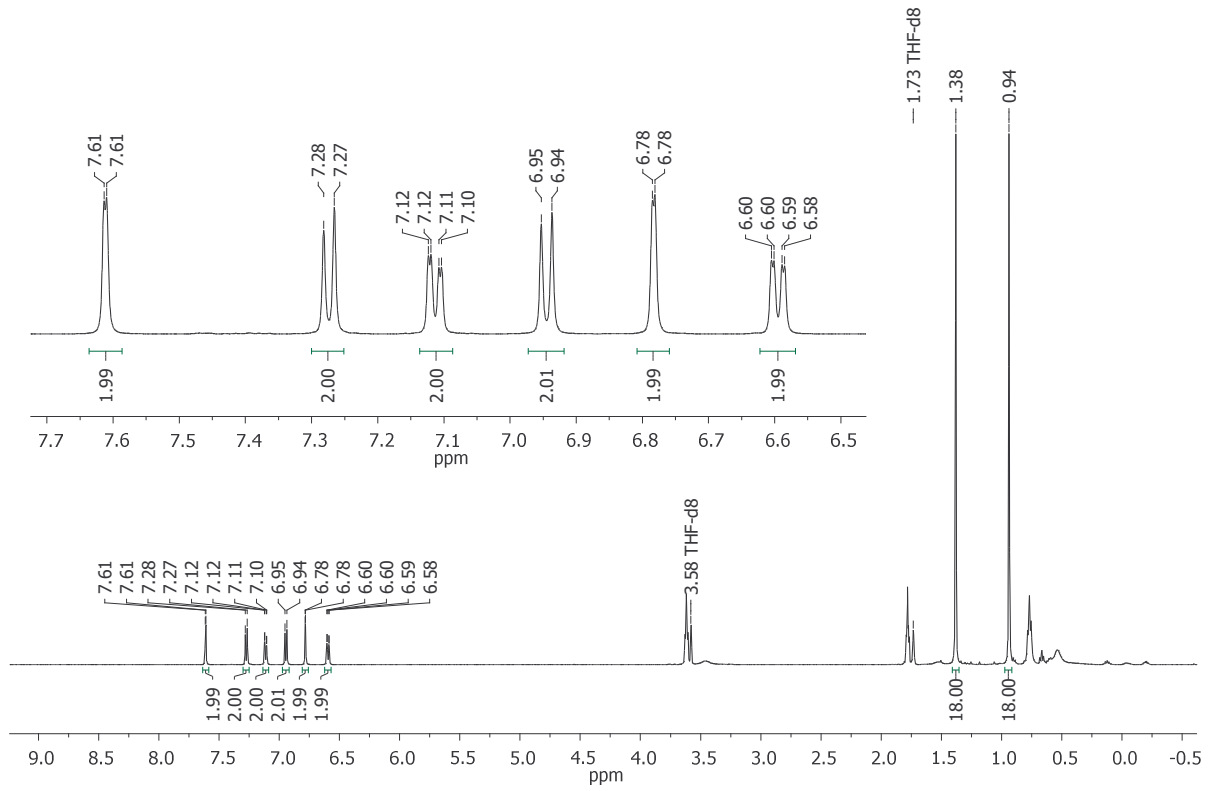


Figure S23: ^1H NMR spectrum of Li[10] (500.2 MHz, THF- d_8).

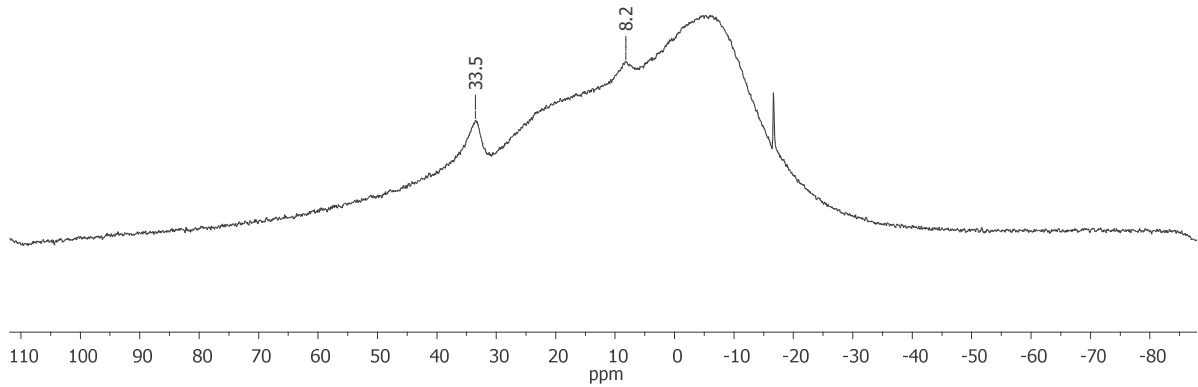


Figure S24: ^{11}B NMR spectrum of Li[10] (96.3 MHz, THF- d_8).

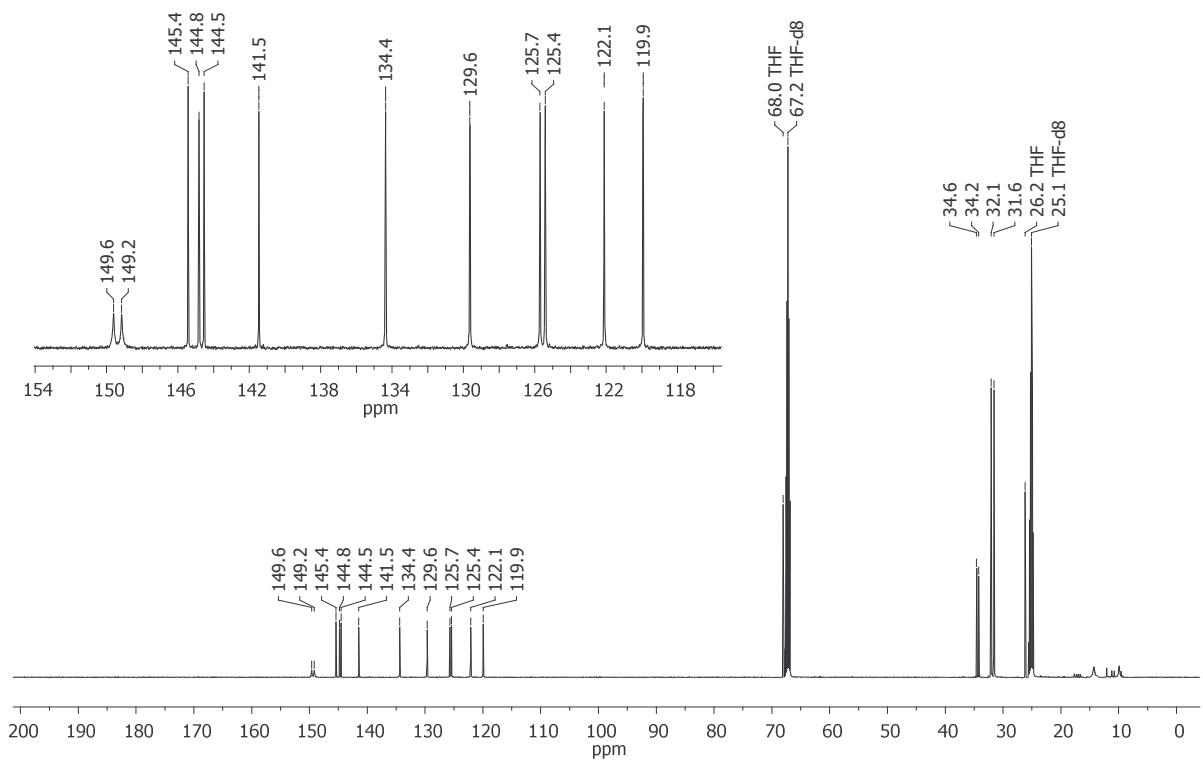


Figure S25: $^{13}\text{C}\{^1\text{H}\}$ NMR spectrum of Li[10] (125.8 MHz, THF- d_8).

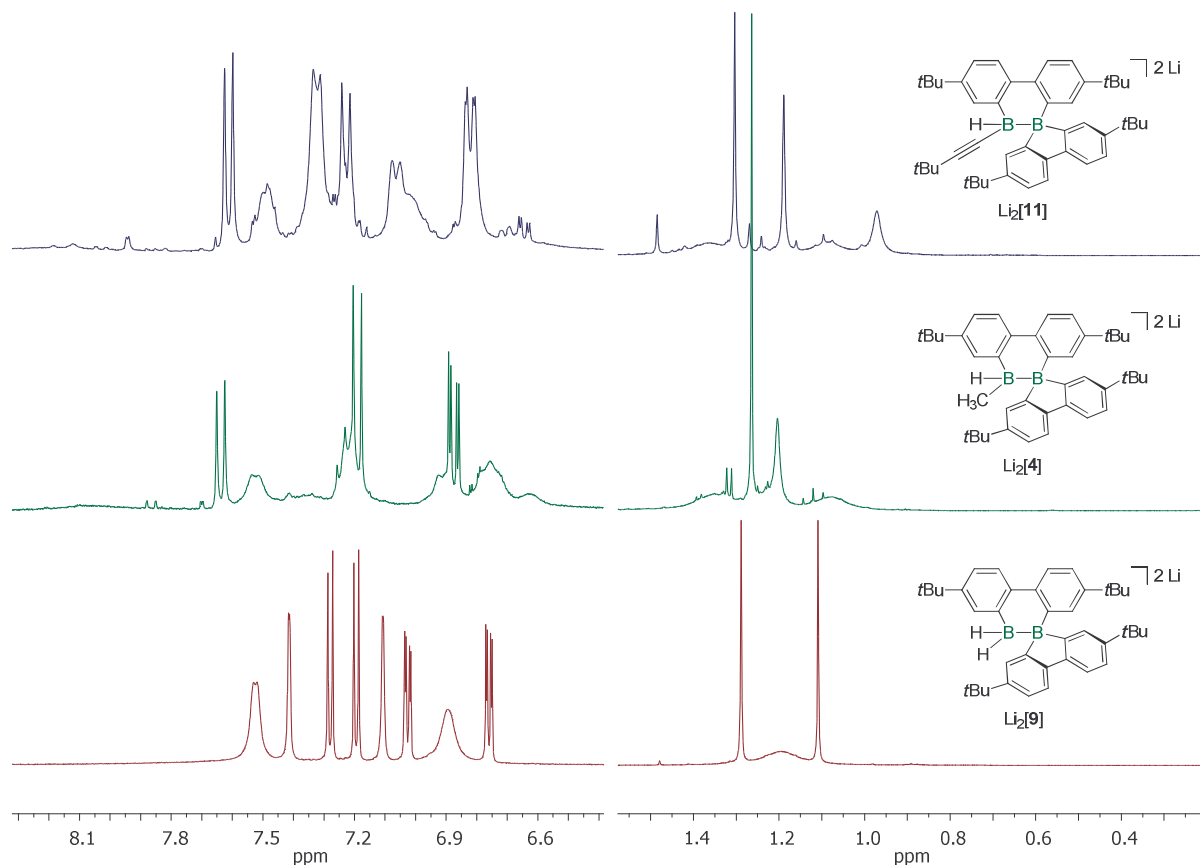


Figure S26: ^1H NMR spectra of $\text{Li}_2[\mathbf{11}]$ (top; 300.0 MHz), $\text{Li}_2[\mathbf{4}]$ (middle; 300.0 MHz), and $\text{Li}_2[\mathbf{9}]$ (bottom; 500.2 MHz) in $\text{THF}-d_8$. Aryl and alkyl regions are scaled differently. In the case of $\text{Li}_2[\mathbf{9}]$, the poor resolution of some signals in the aromatic and aliphatic spectral region originates from a dynamic behavior of the system in solution, which arises from conformational changes of the twisted B_2C_4 ring and/or from an association-dissociation equilibrium between the cations and the anions.^{S5} In the cases of $\text{Li}_2[\mathbf{4}]$ and $\text{Li}_2[\mathbf{11}]$, the phenomenon is even more pronounced due to further symmetry breaking by the boron-bonded organyl substituents.

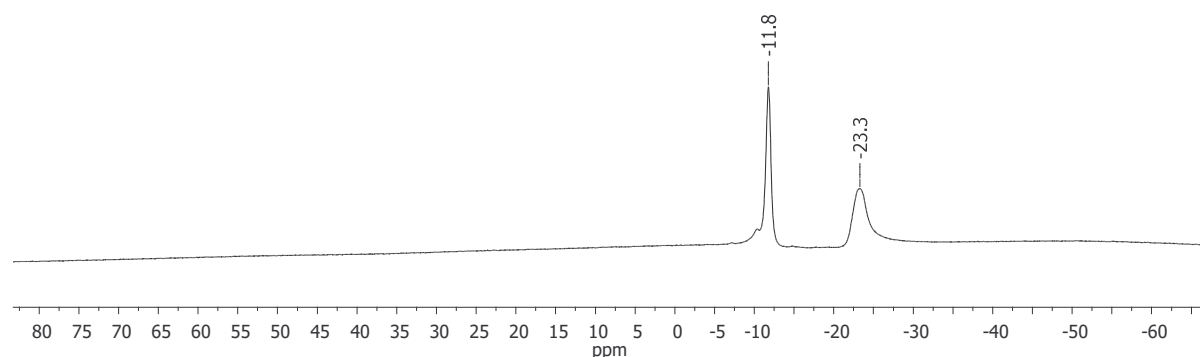


Figure S27: ^{11}B NMR spectrum of $\text{Li}_2[\mathbf{11}]$ (96.3 MHz, $\text{THF}-d_8$).

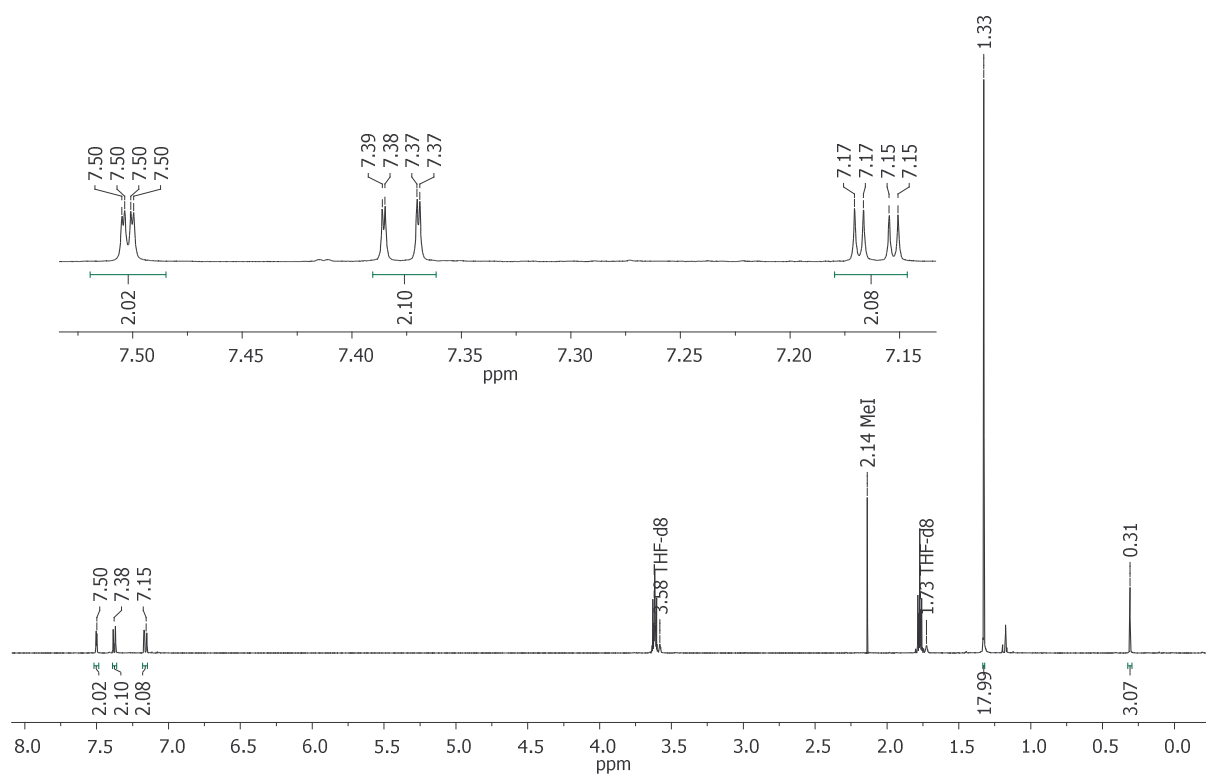


Figure S28: ^1H NMR spectrum of **13** (500.2 MHz, THF- d_8).

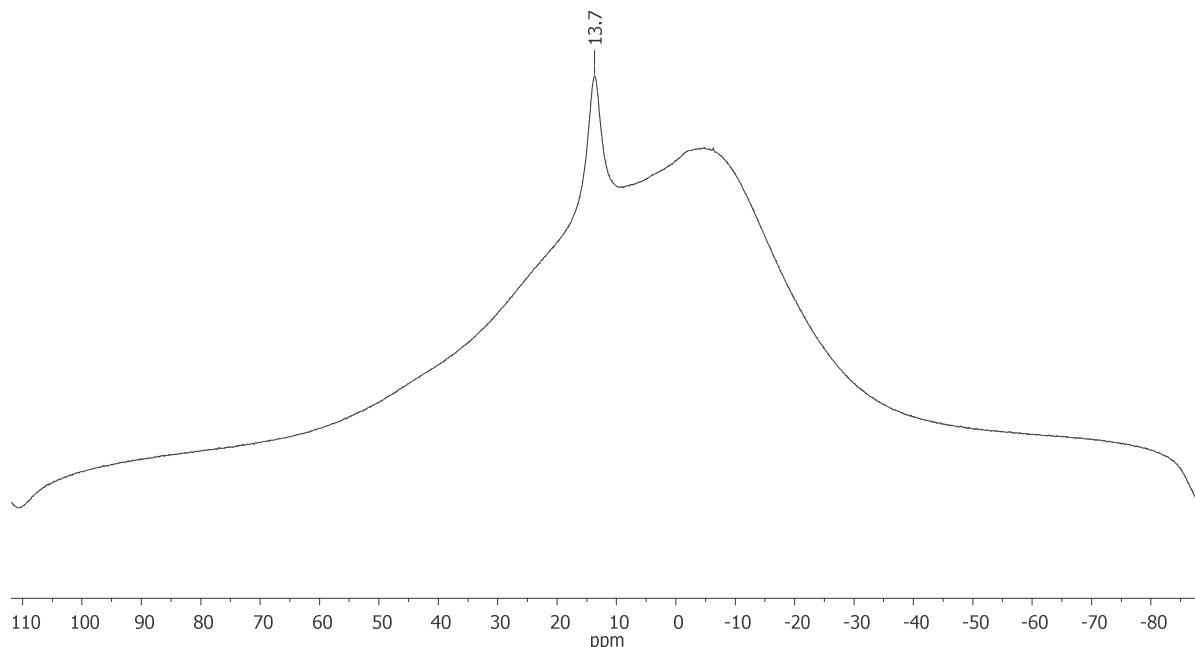


Figure S29: ^{11}B NMR spectrum of **13** (160.5 MHz, THF- d_8).

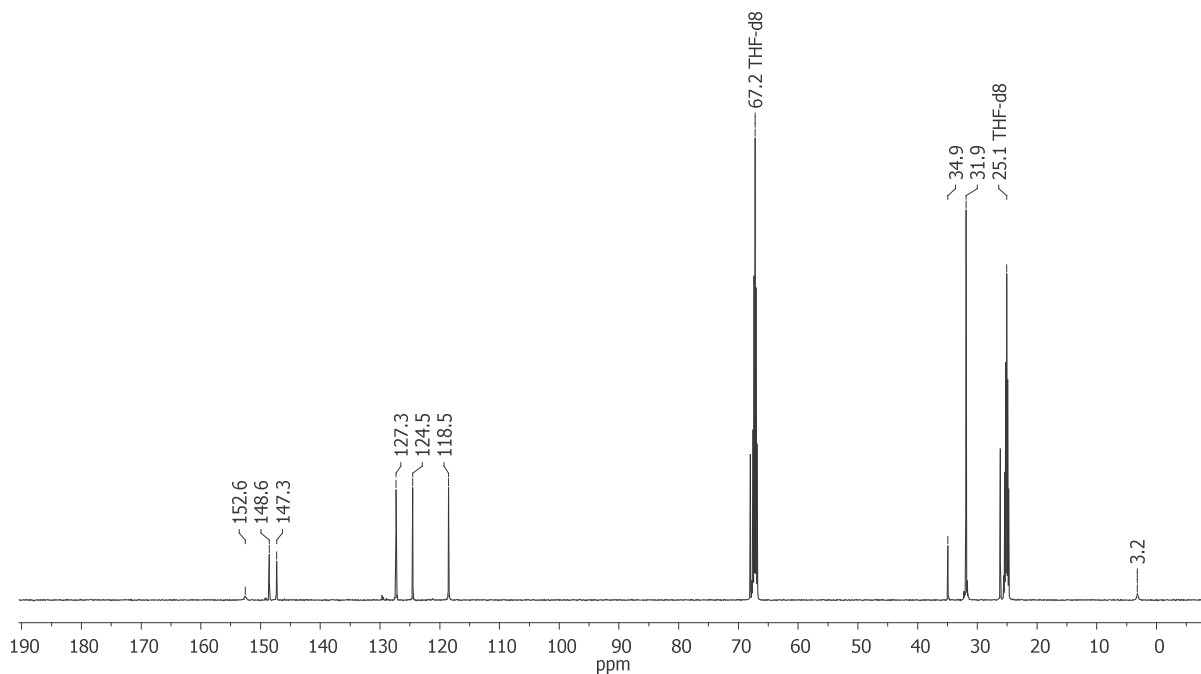


Figure S30: $^{13}\text{C}\{\text{H}\}$ NMR spectrum of **13** (125.8 MHz, THF-*d*₈).

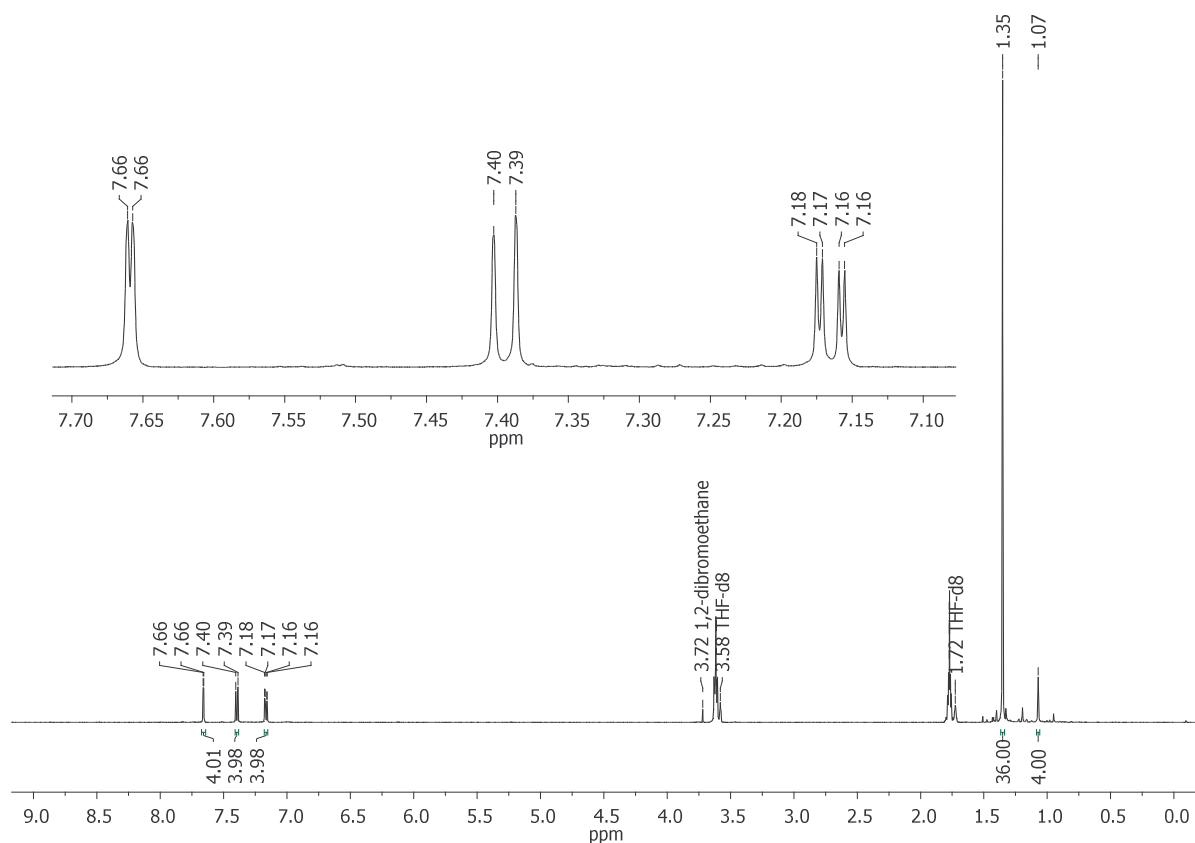


Figure S31: ^1H NMR spectrum of **14^{C2}** (500.2 MHz, THF-*d*₈).

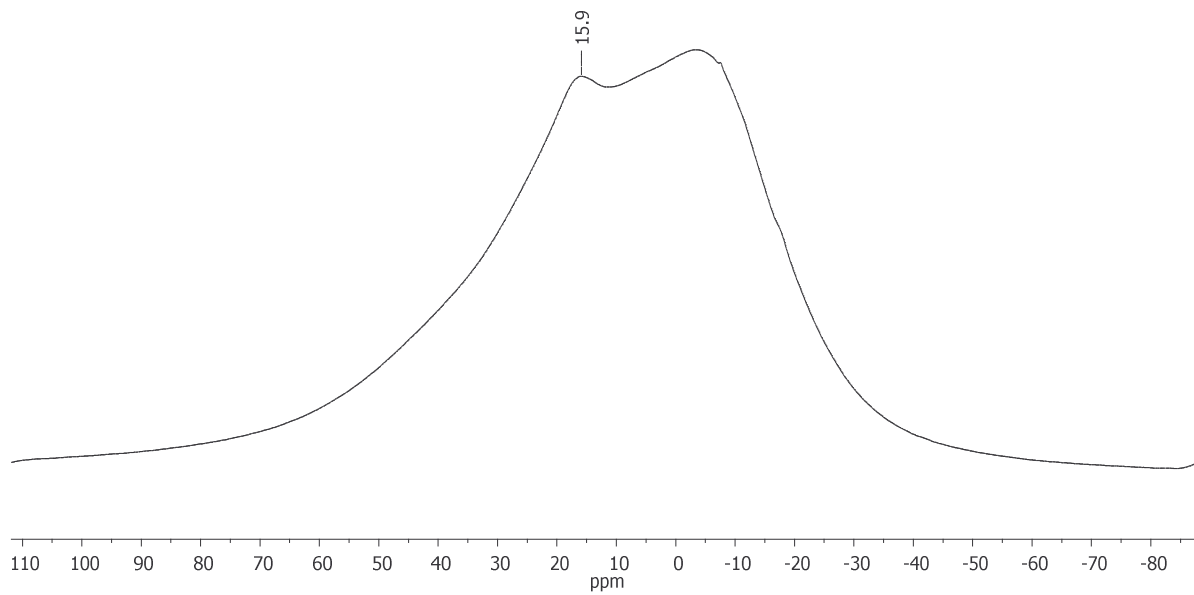


Figure S32: ^{11}B NMR spectrum of $\mathbf{14}^{\text{C}2}$ (160.5 MHz, THF- d_8).

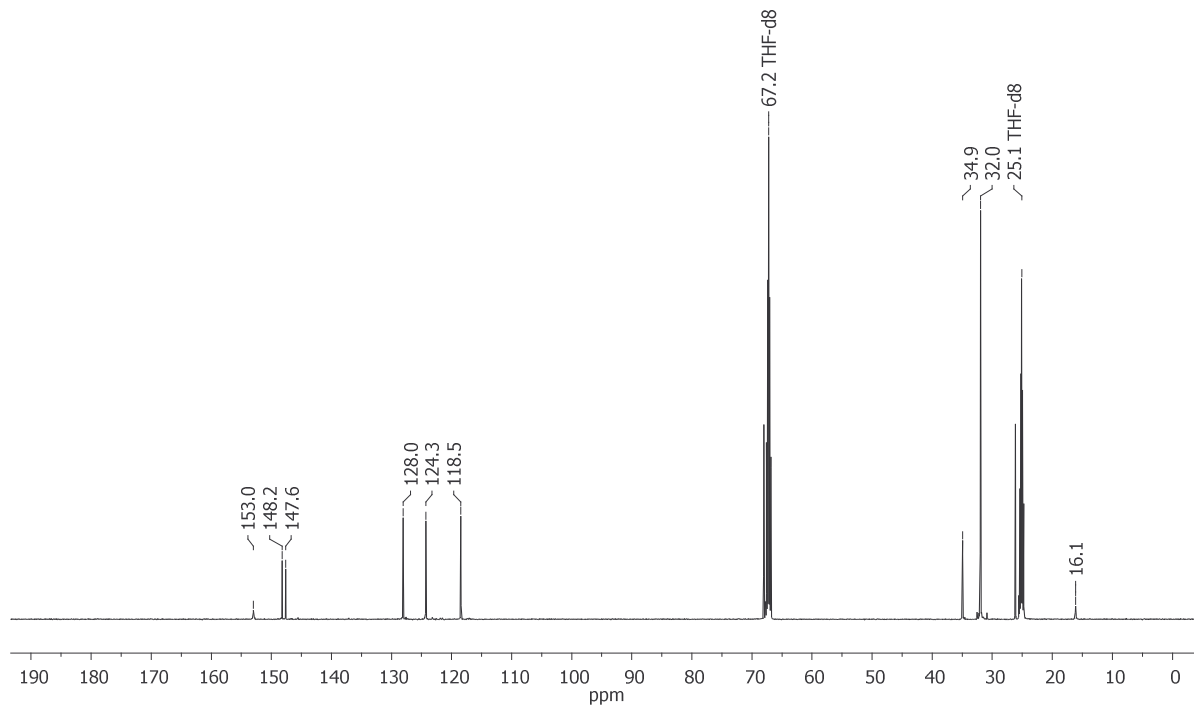


Figure S33: $^{13}\text{C}\{^1\text{H}\}$ NMR spectrum of $\mathbf{14}^{\text{C}2}$ (125.8 MHz, THF- d_8).

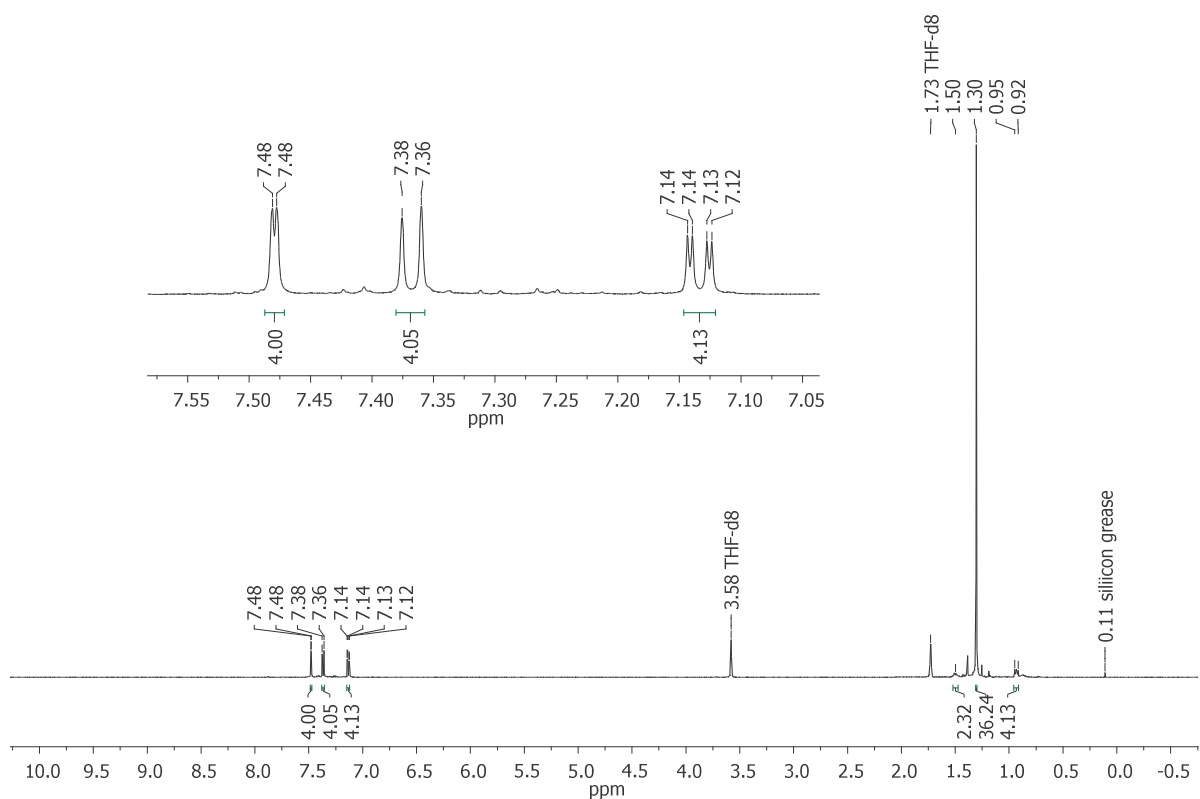


Figure S34: ^1H NMR spectrum of $\mathbf{14}^{\text{C}3}$ (500.2 MHz, THF- d_8).

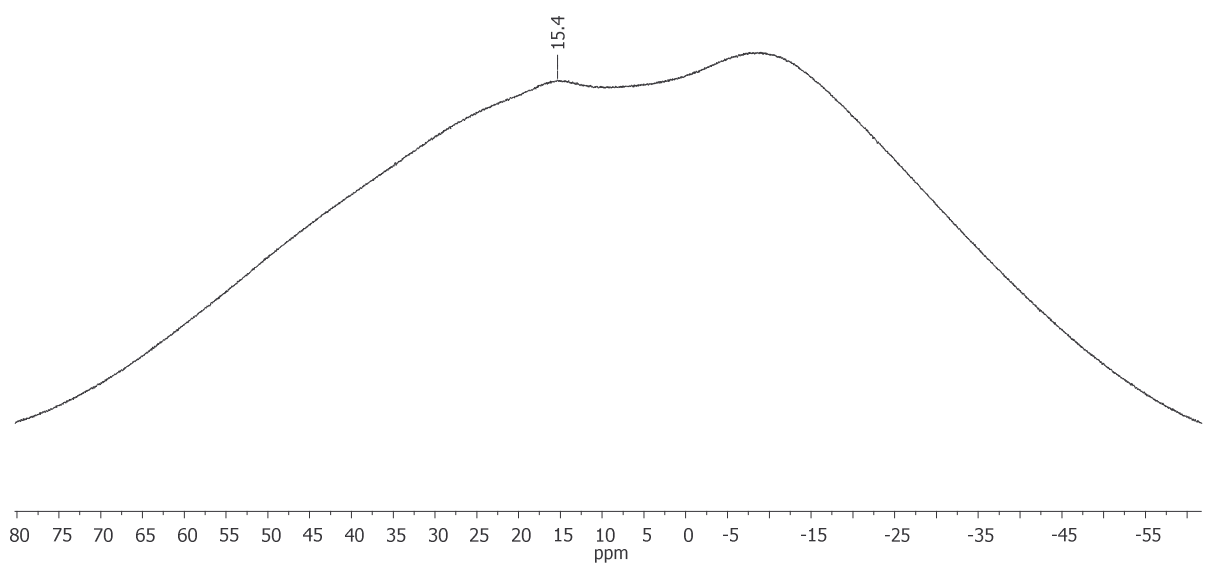


Figure S35: ^{11}B NMR spectrum of $\mathbf{14}^{\text{C}3}$ (160.5 MHz, THF- d_8).

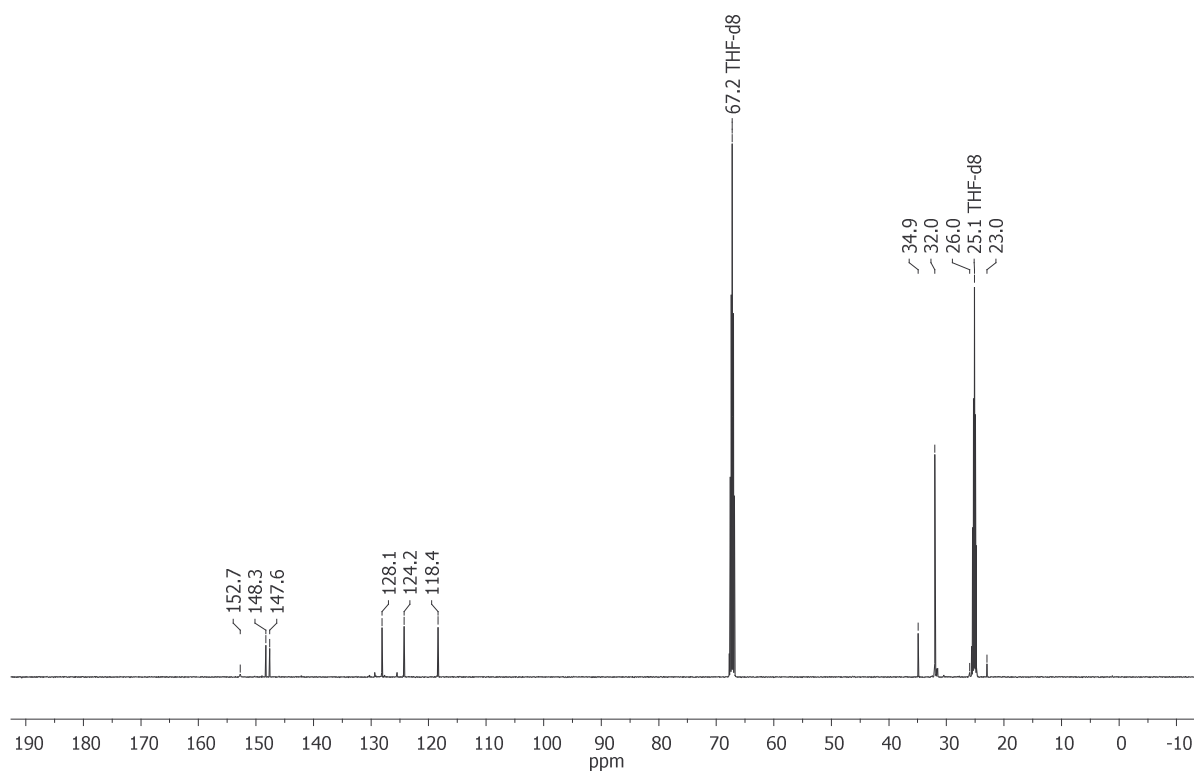


Figure S36: ¹³C{¹H} NMR spectrum of **14^{C3}** (125.8 MHz, THF-*d*₈).

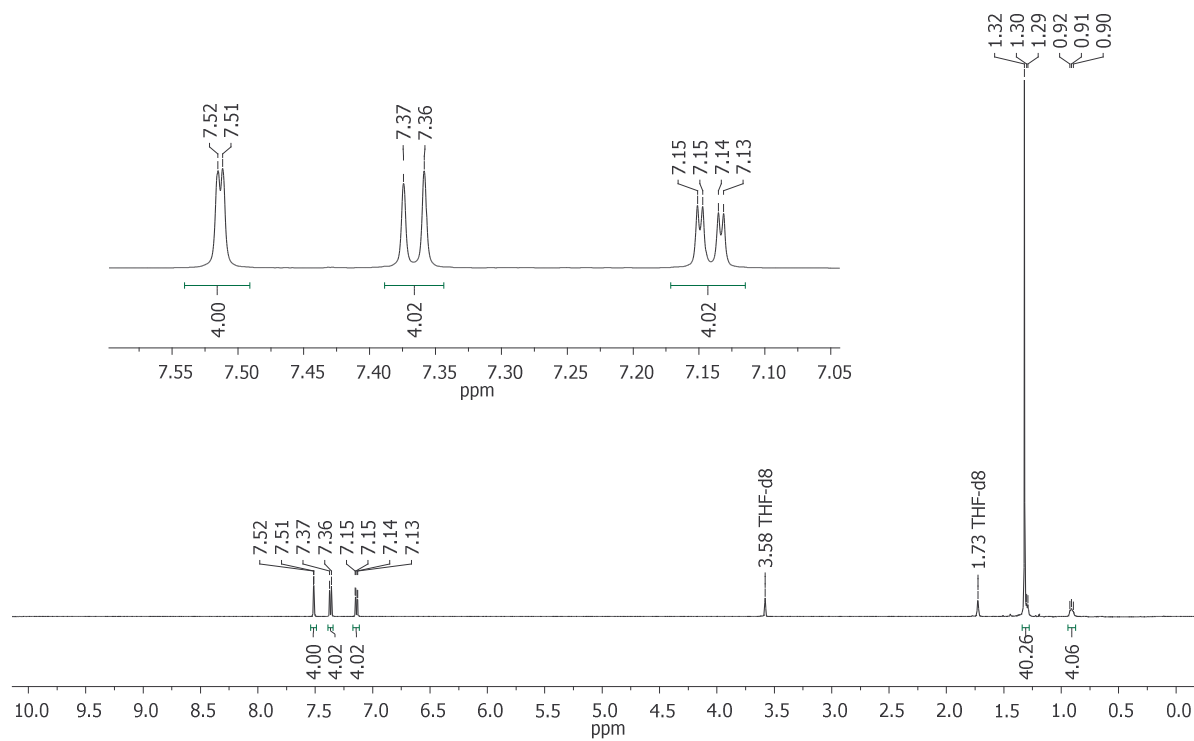


Figure S37: ¹H NMR spectrum of **14^{C4}** (500.2 MHz, THF-*d*₈).

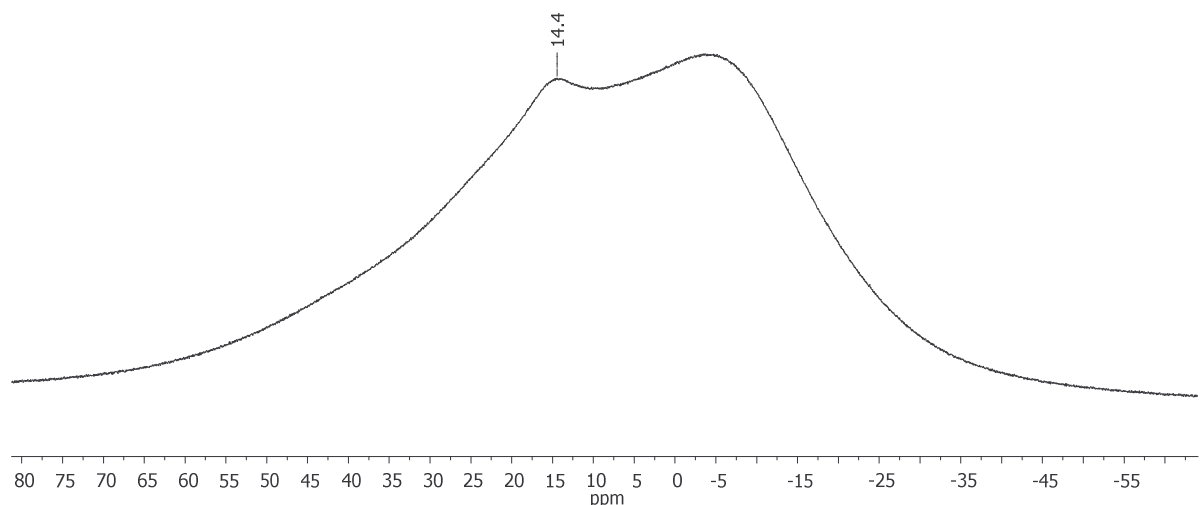


Figure S38: ^{11}B NMR spectrum of $\mathbf{14}^{\text{C}4}$ (160.5 MHz, THF- d_8).

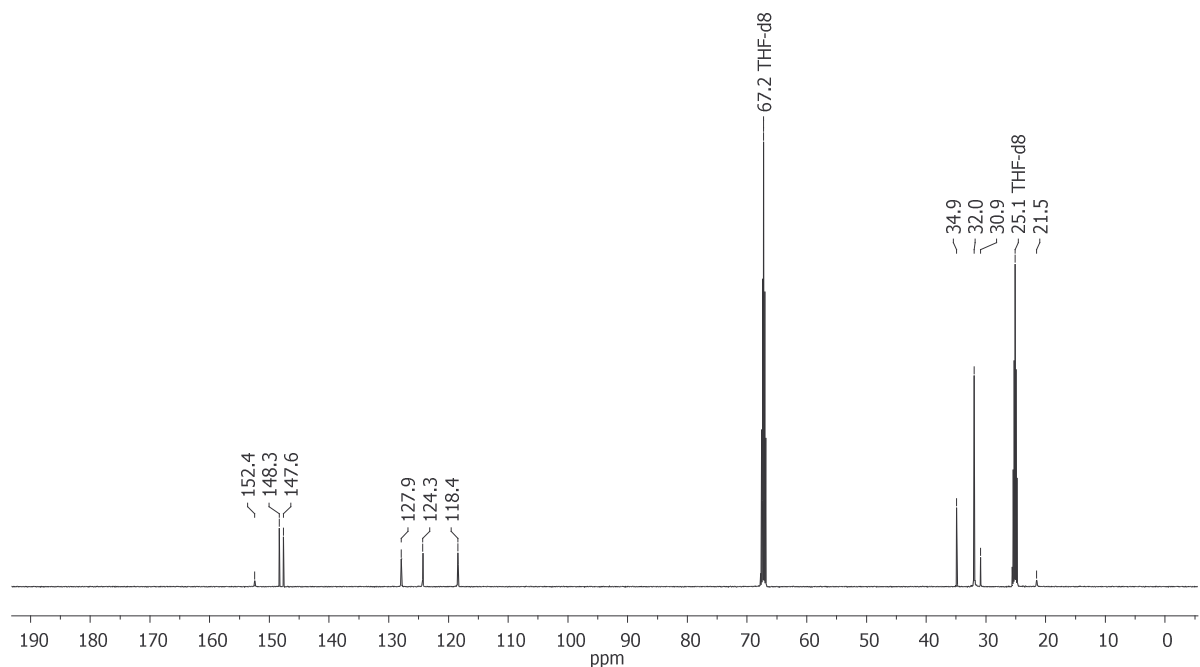


Figure S39: $^{13}\text{C}\{^1\text{H}\}$ NMR spectrum of $\mathbf{14}^{\text{C}4}$ (125.8 MHz, THF- d_8).

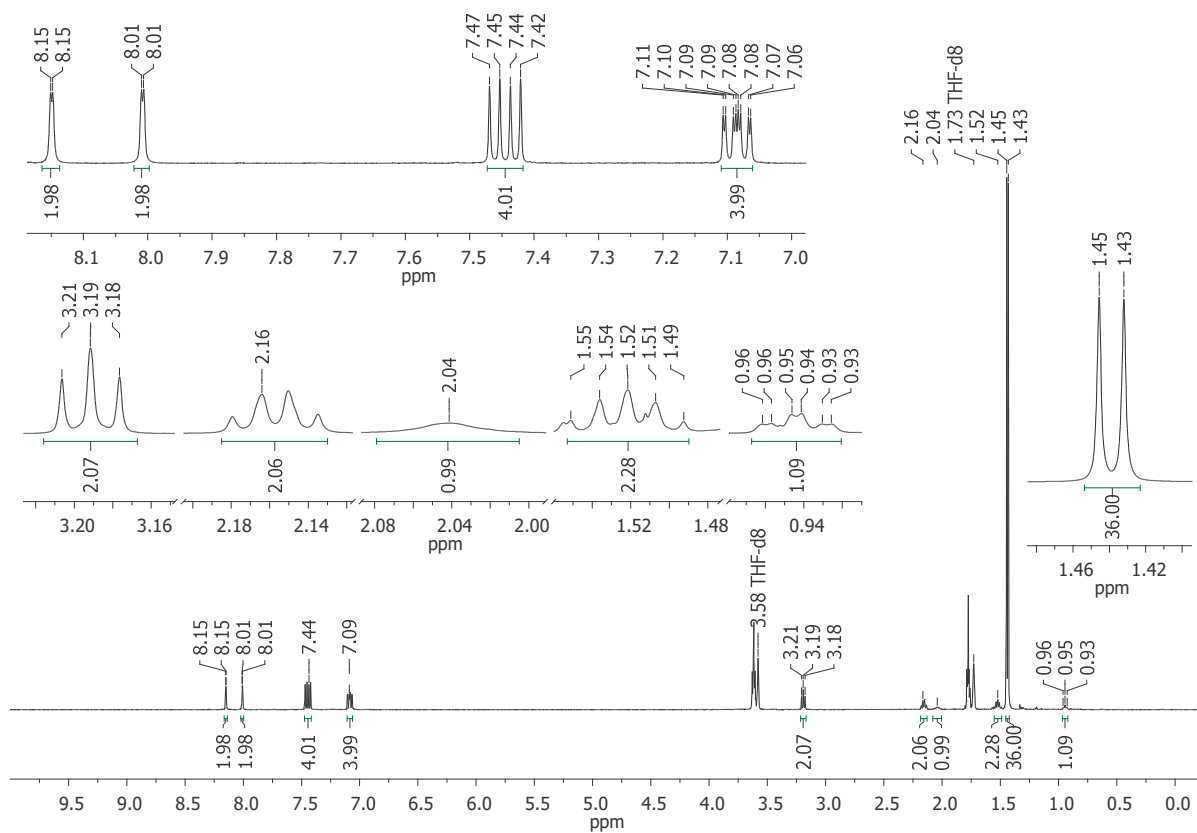


Figure S40: ^1H NMR spectrum of Li[15^{C4,Cl}] (500.2 MHz, THF-*d*₈).

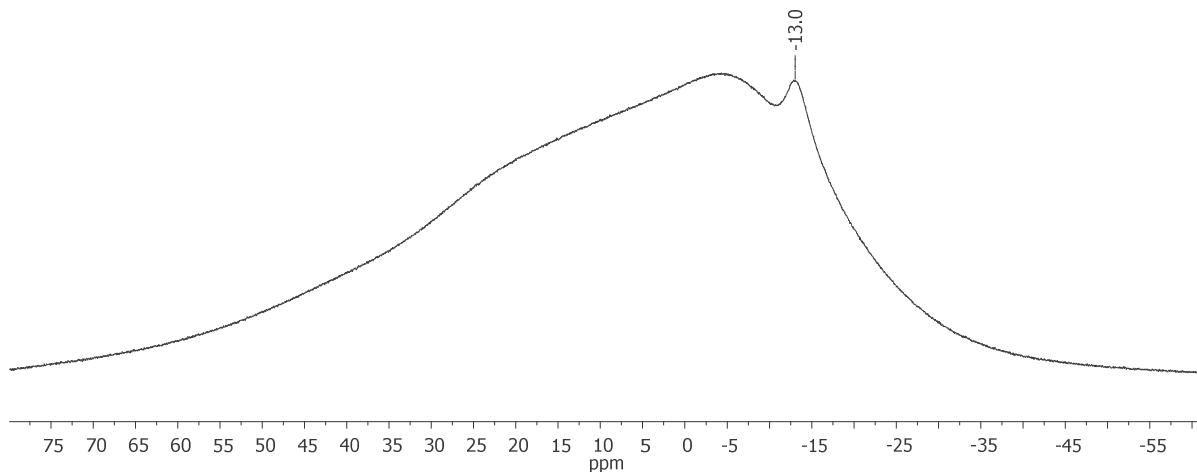


Figure S41: ^{11}B NMR spectrum of $\text{Li}[15^{\text{C}4,\text{Cl}}]$ (160.5 MHz, $\text{THF-}d_8$).

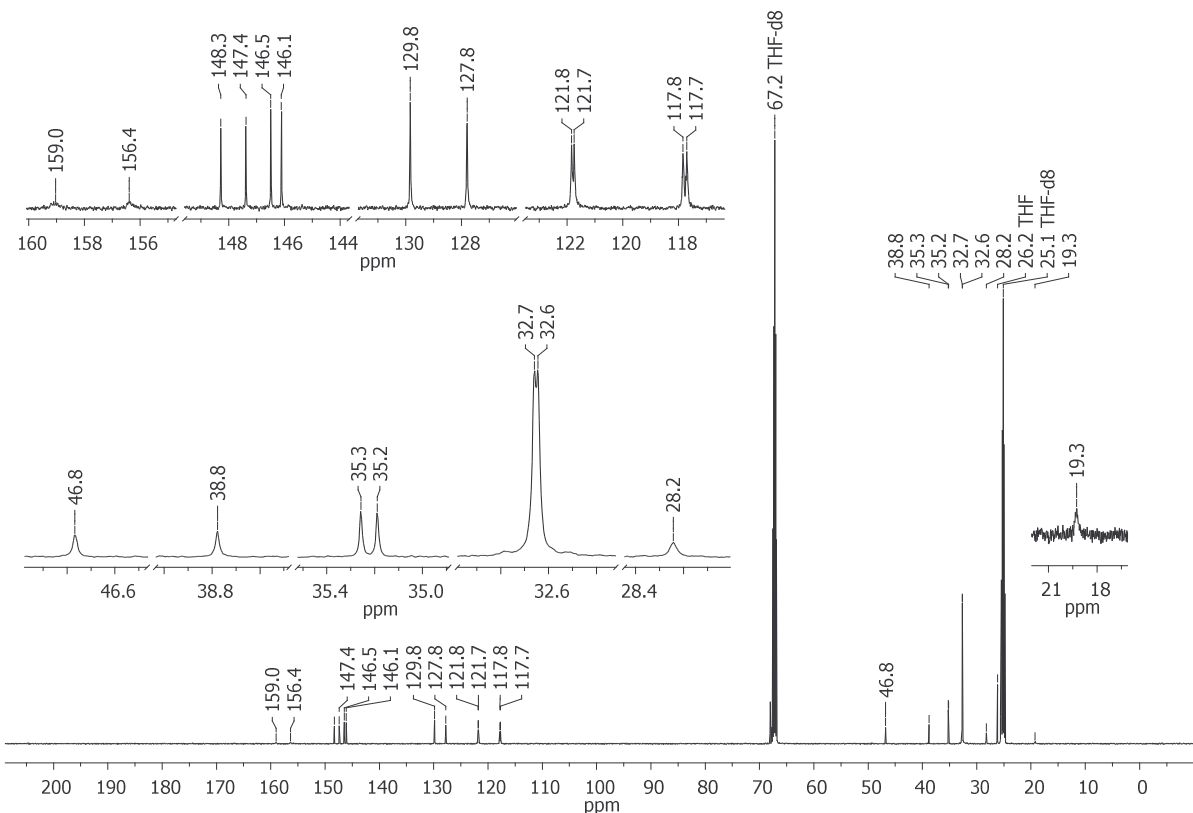


Figure S42: $^{13}\text{C}\{^1\text{H}\}$ NMR spectrum of Li[15^{C4,Cl}] (125.8 MHz, THF-*d*₈).

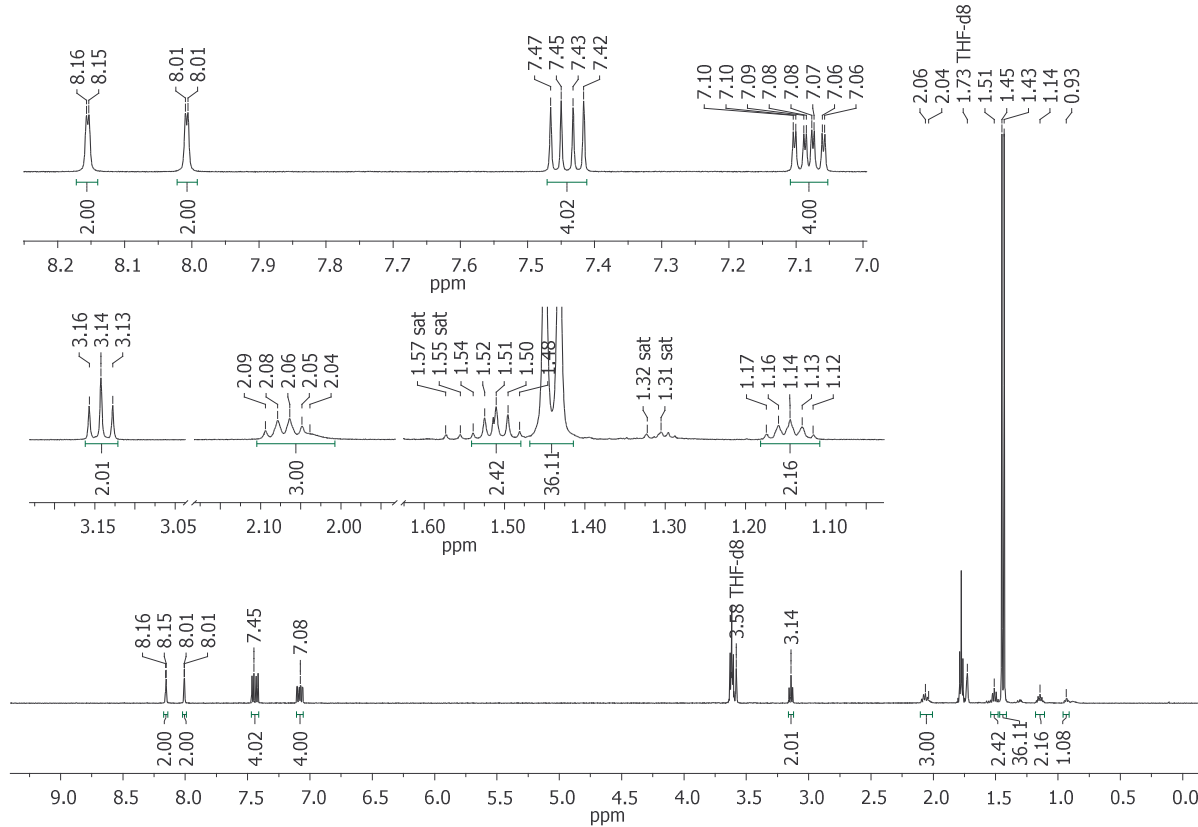


Figure S43: ^1H NMR spectrum of Li[15 ^{13}C] (500.2 MHz, THF- d_8 ; sat = ^{13}C satellite of a CH_3 signal).

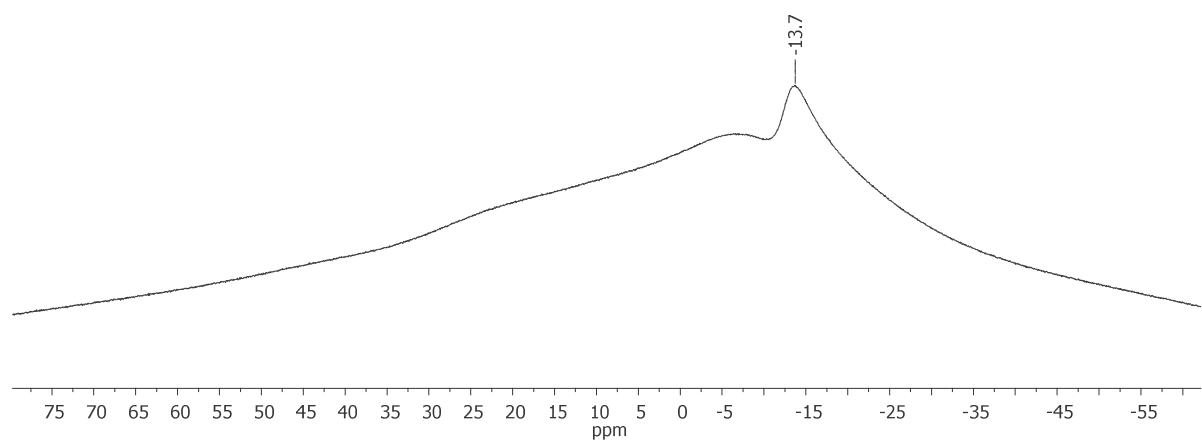


Figure S44: ^{11}B NMR spectrum of $\text{Li}[15^{\text{C}5,\text{Cl}}]$ (160.5 MHz, $\text{THF-}d_8$).

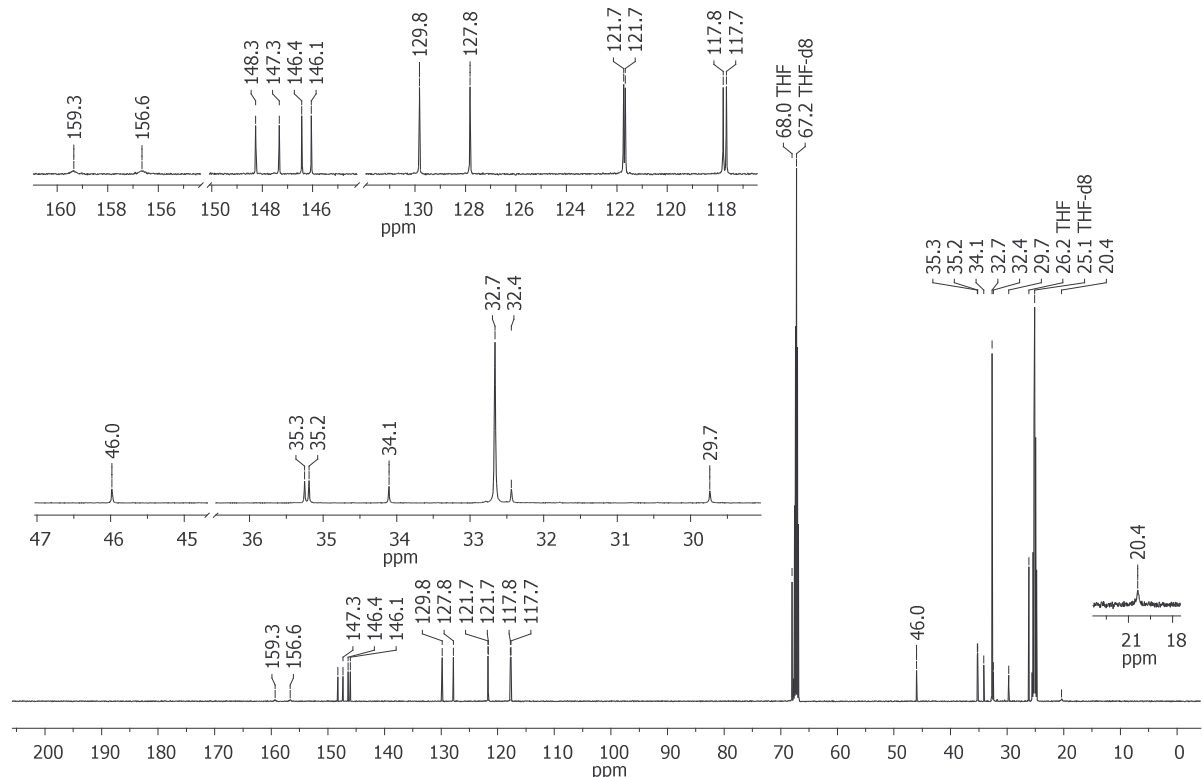


Figure S45: $^{13}\text{C}\{^1\text{H}\}$ NMR spectrum of $\text{Li}[15^{\text{C}5,\text{Cl}}]$ (125.8 MHz, $\text{THF-}d_8$).

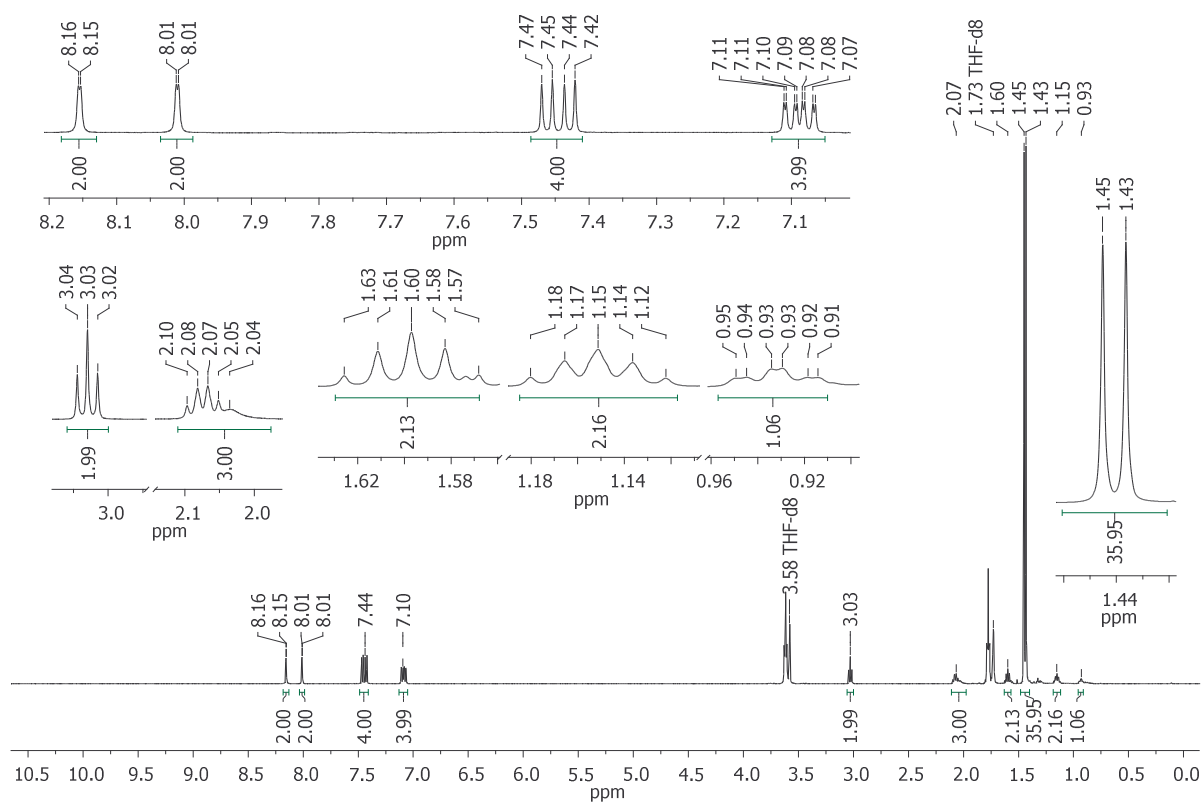


Figure S46: ^1H NMR spectrum of $\text{Li}[15^{\text{C}5,\text{Br}}]$ (500.2 MHz, $\text{THF}-d_8$).

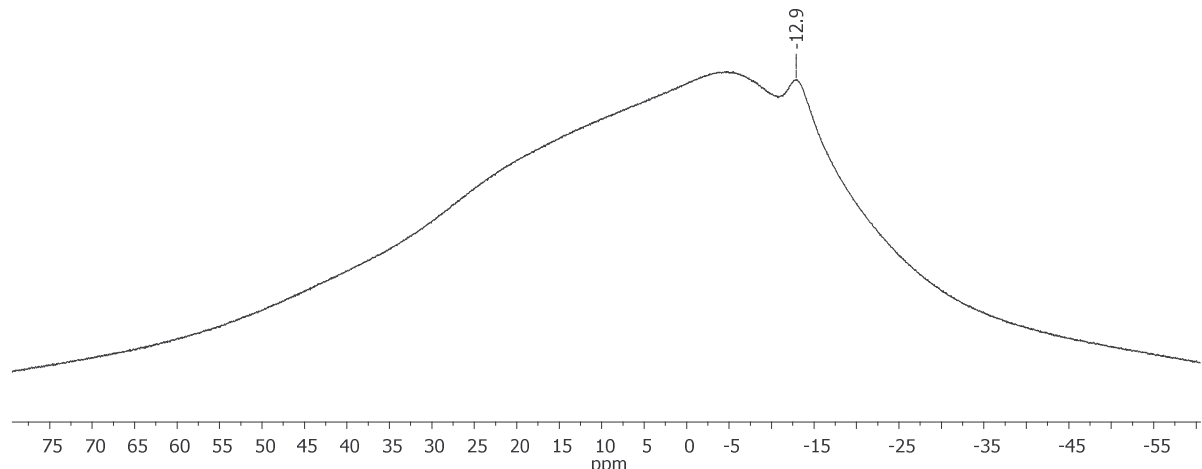


Figure S47: ^{11}B NMR spectrum of $\text{Li}[15^{\text{C}5,\text{Br}}]$ (160.5 MHz, $\text{THF}-d_8$).

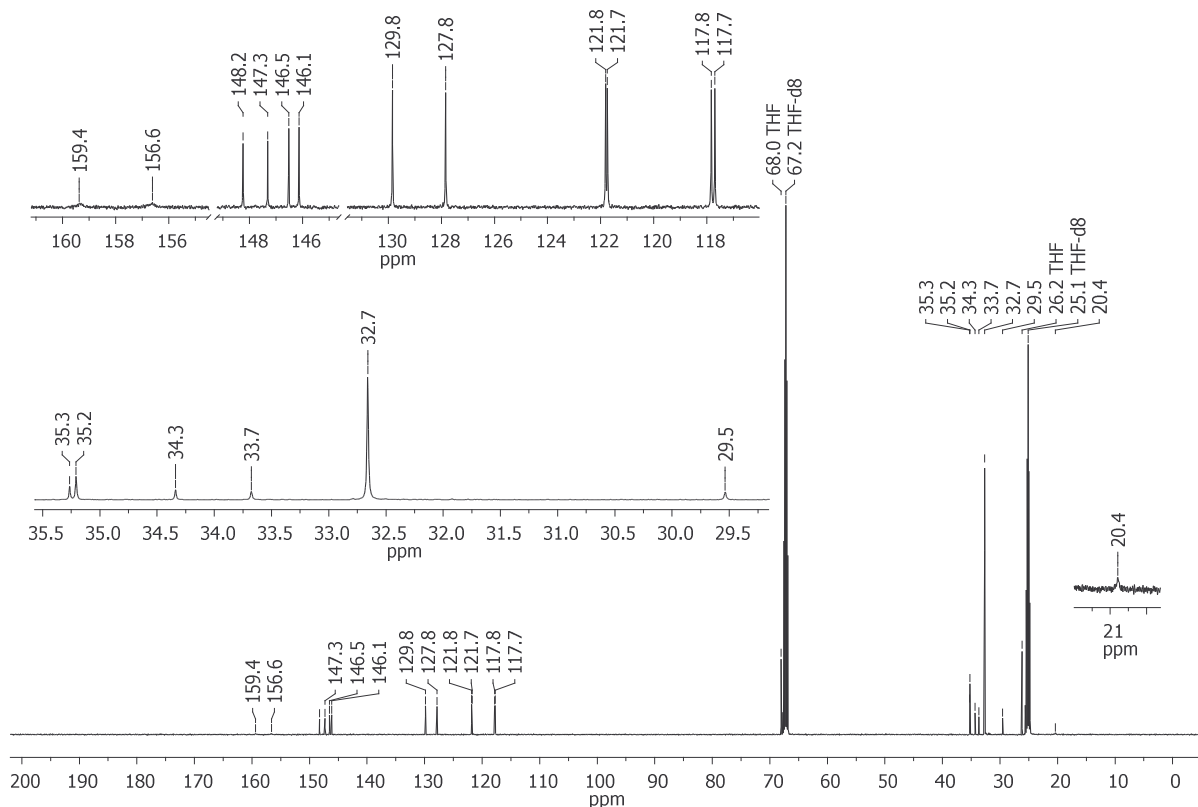


Figure S48: $^{13}\text{C}\{^1\text{H}\}$ NMR spectrum of $\text{Li}[15^{\text{C5},\text{Br}}]$ (125.8 MHz, $\text{THF}-d_8$).

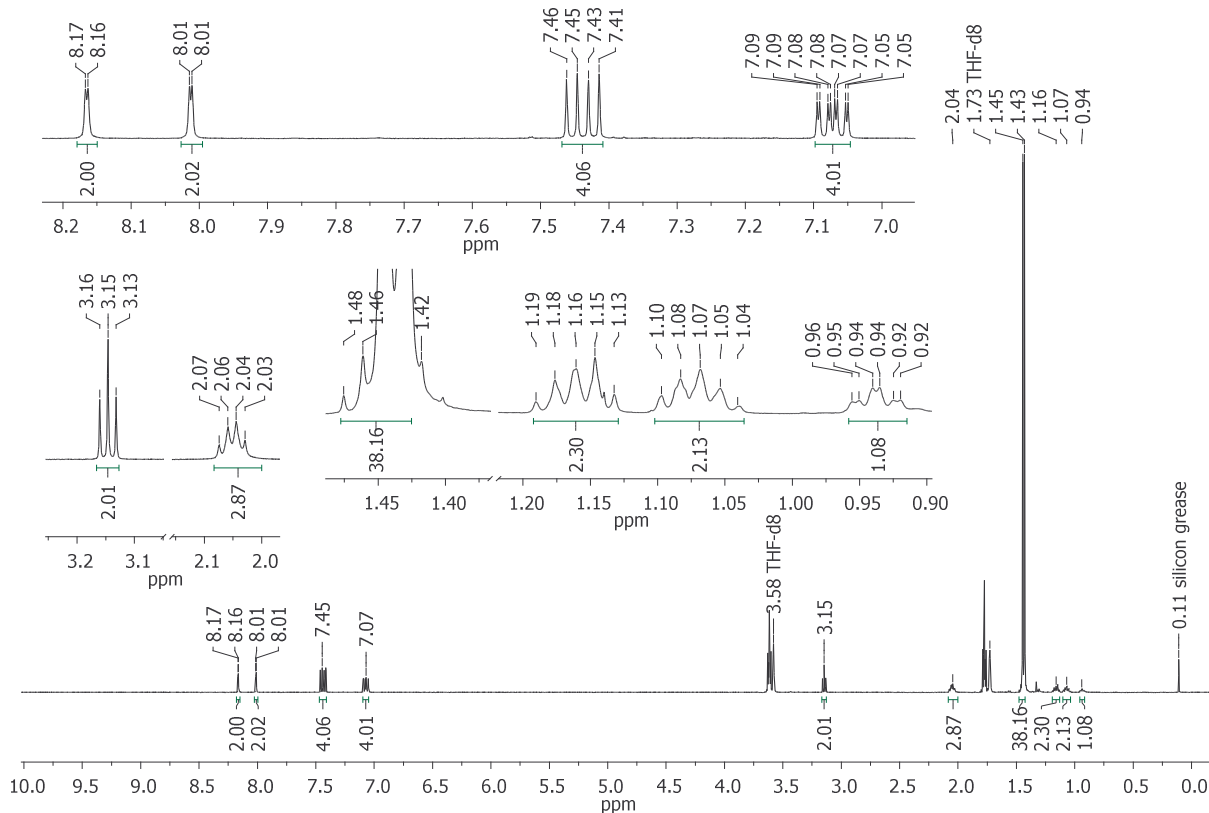


Figure S49: ^1H NMR spectrum of Li[15 $^{C6,\text{Cl}}$] (500.2 MHz, THF- d_8).

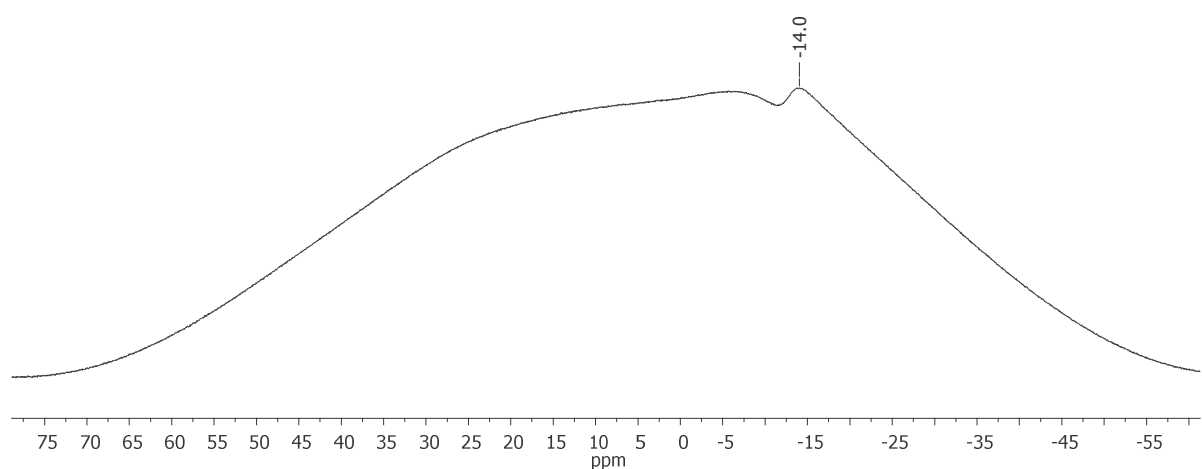


Figure S50: ^{11}B NMR spectrum of $\text{Li}[15^{\text{C}6,\text{Cl}}]$ (160.5 MHz, $\text{THF}-d_8$,).

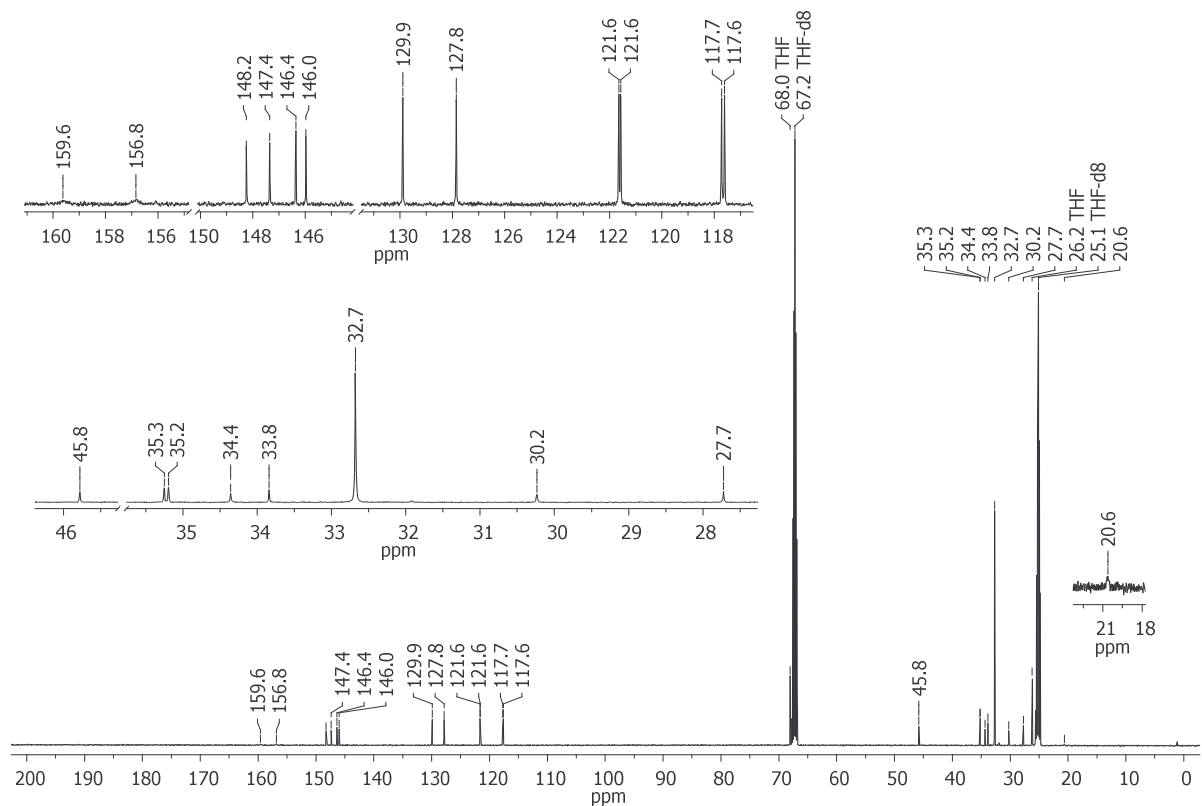


Figure S51: $^{13}\text{C}\{^1\text{H}\}$ NMR spectrum of $\text{Li}[15^{\text{C}6,\text{Cl}}]$ (125.8 MHz, $\text{THF}-d_8$,).

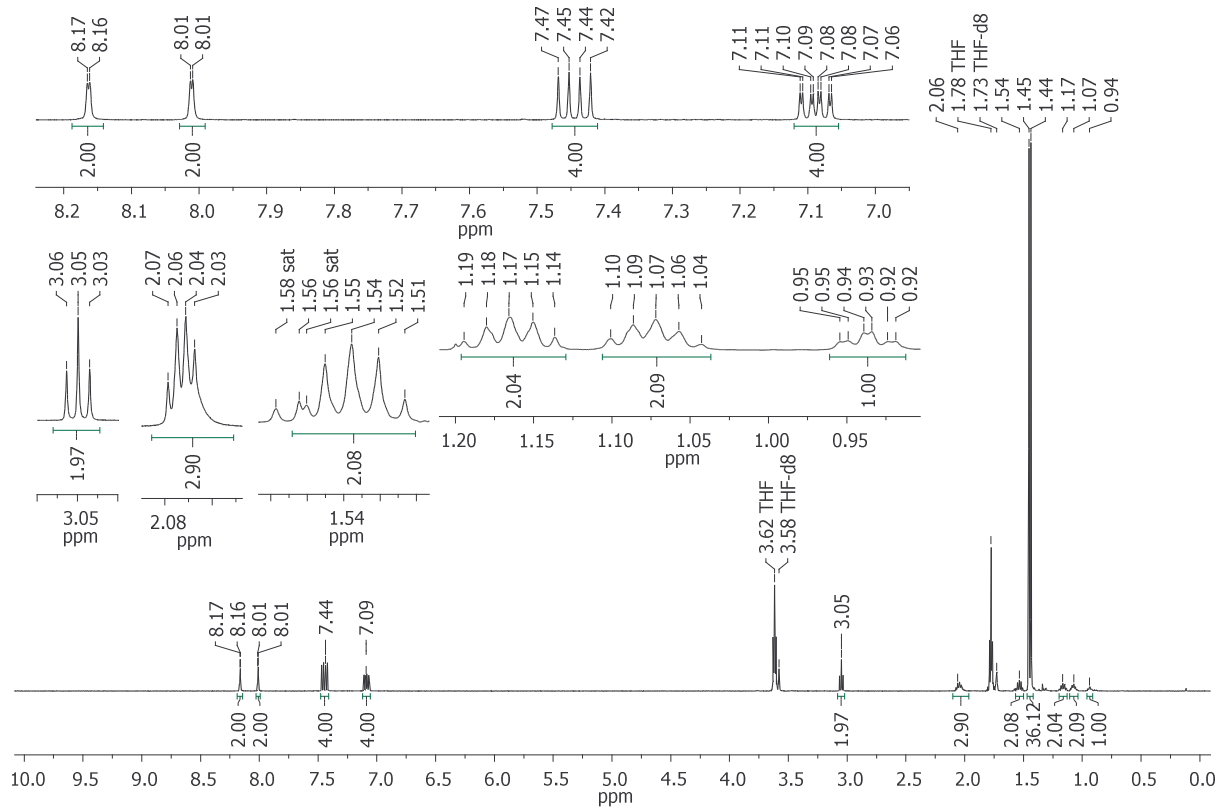


Figure S52: ^1H NMR spectrum of $\text{Li}[15^{\text{C}6,\text{Br}}]$ (500.2 MHz, $\text{THF}-d_8$; sat = ^{13}C satellite of a CH_3 signal).

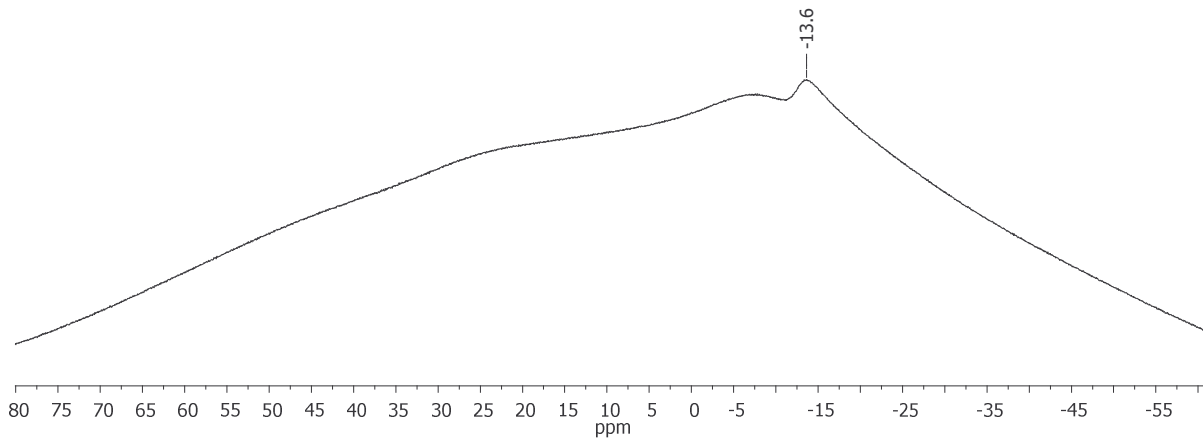


Figure S53: ^{11}B NMR spectrum of $\text{Li}[15^{\text{C}6,\text{Br}}]$ (160.5 MHz, $\text{THF}-d_8$).

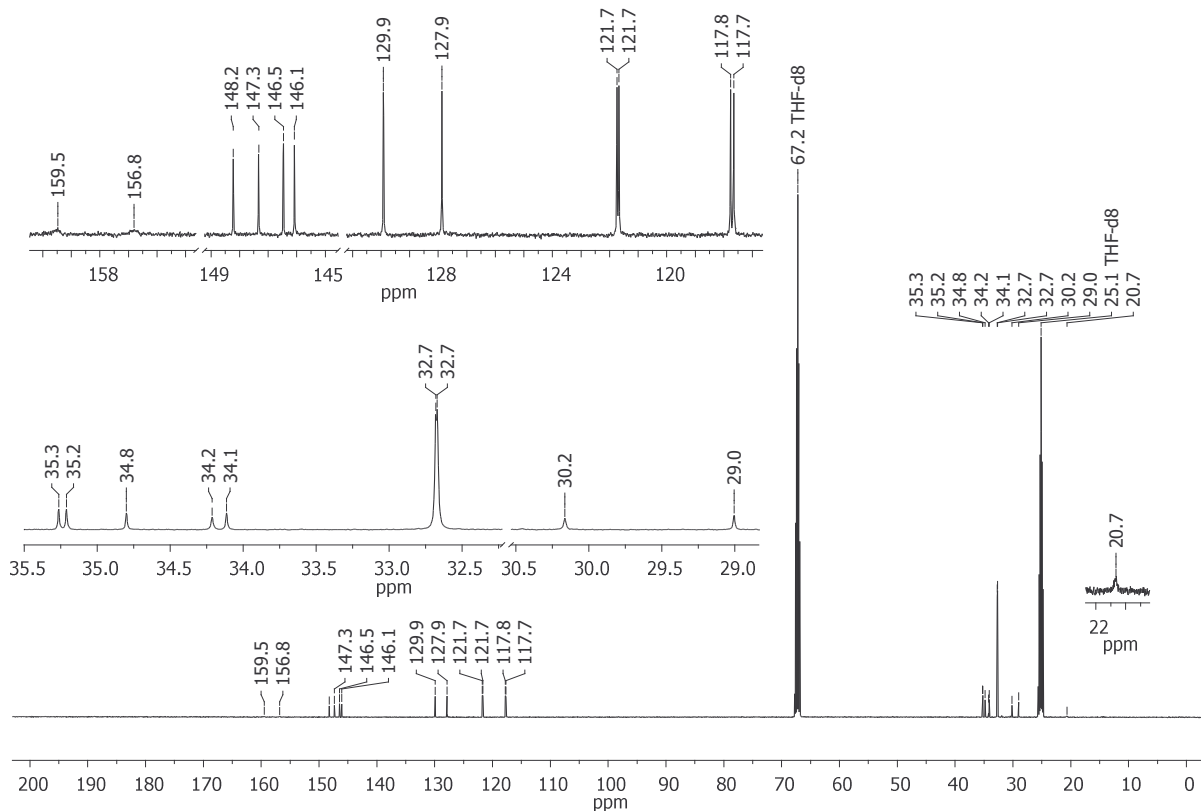


Figure S54: $^{13}\text{C}\{^1\text{H}\}$ NMR spectrum of $\text{Li}[15^{\text{C}6,\text{Br}}]$ (125.8 MHz, THF- d_8).

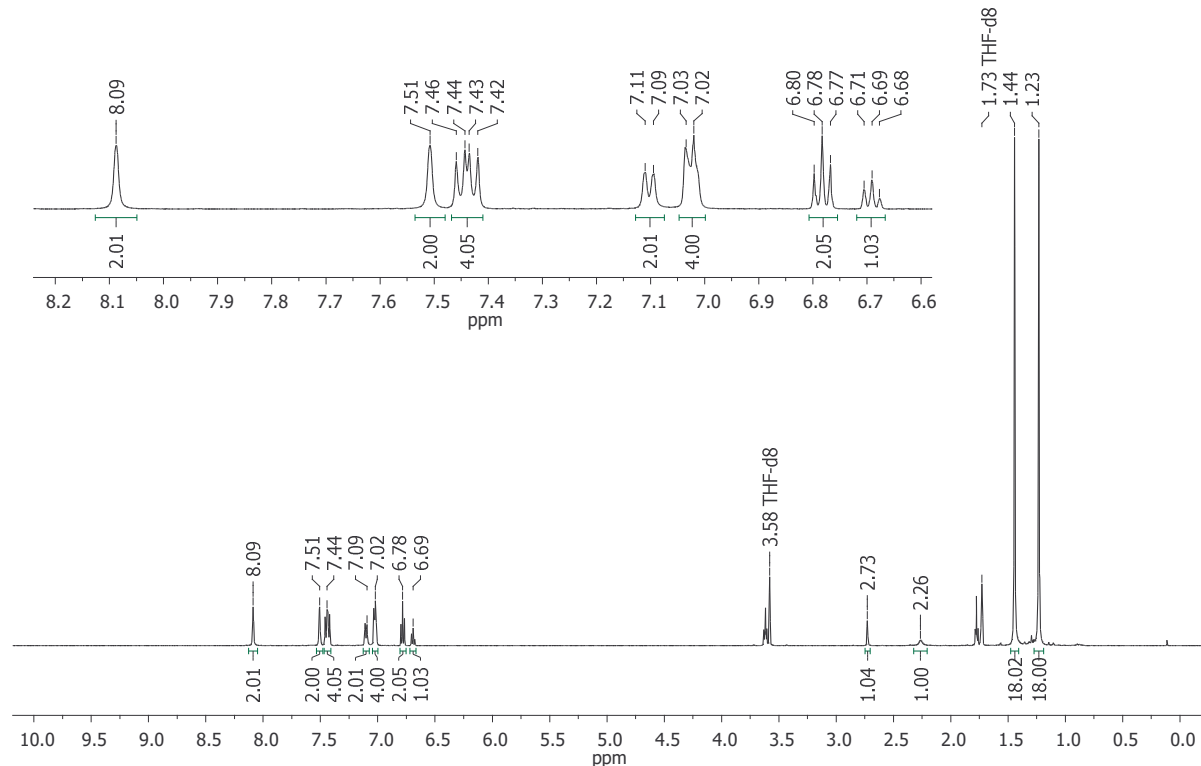


Figure S55: ^1H NMR spectrum of Li[16] (500.2 MHz, THF- d_8).

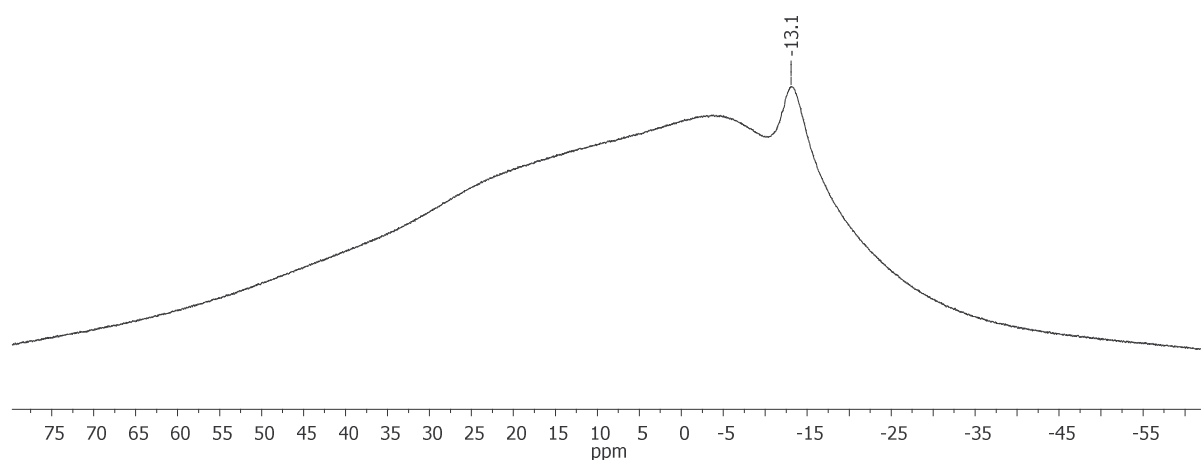


Figure S56: ^{11}B NMR spectrum of $\text{Li}[16]$ (160.5 MHz, THF-d_8).

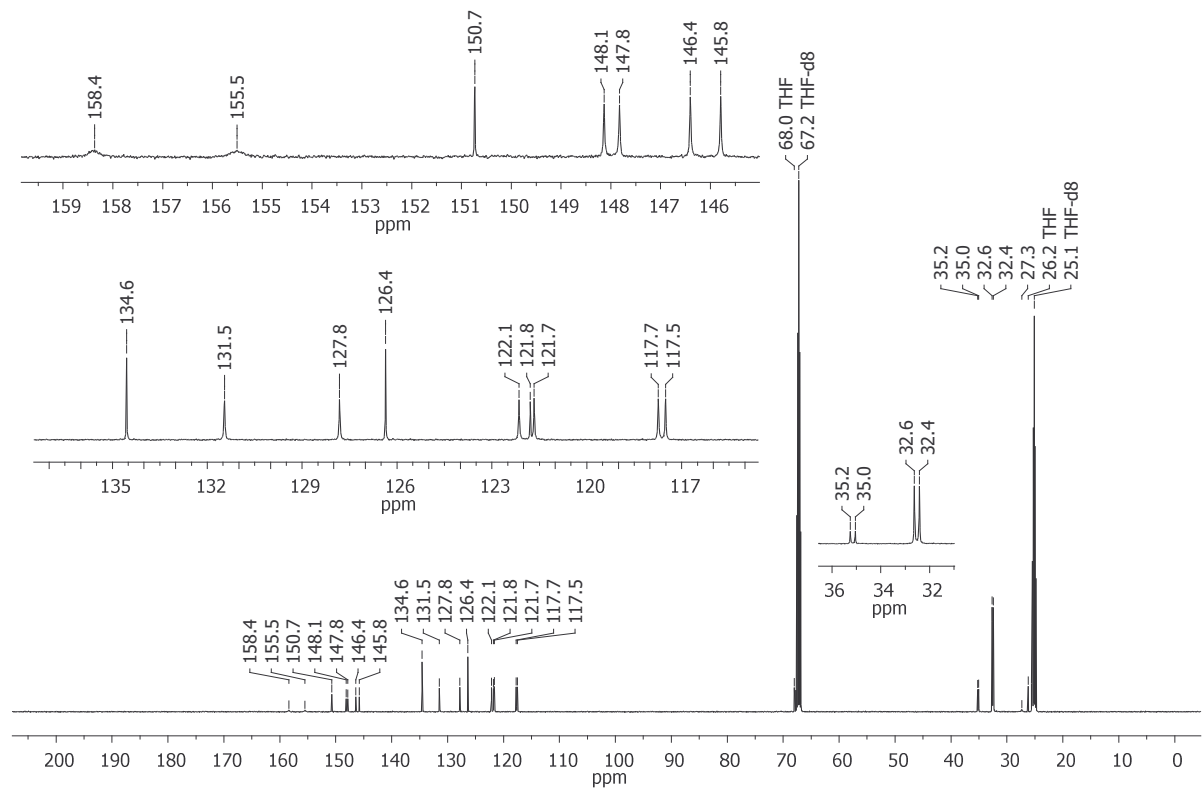


Figure S57: $^{13}\text{C}\{^1\text{H}\}$ NMR spectrum of $\text{Li}[16]$ (125.8 MHz, THF-d_8).

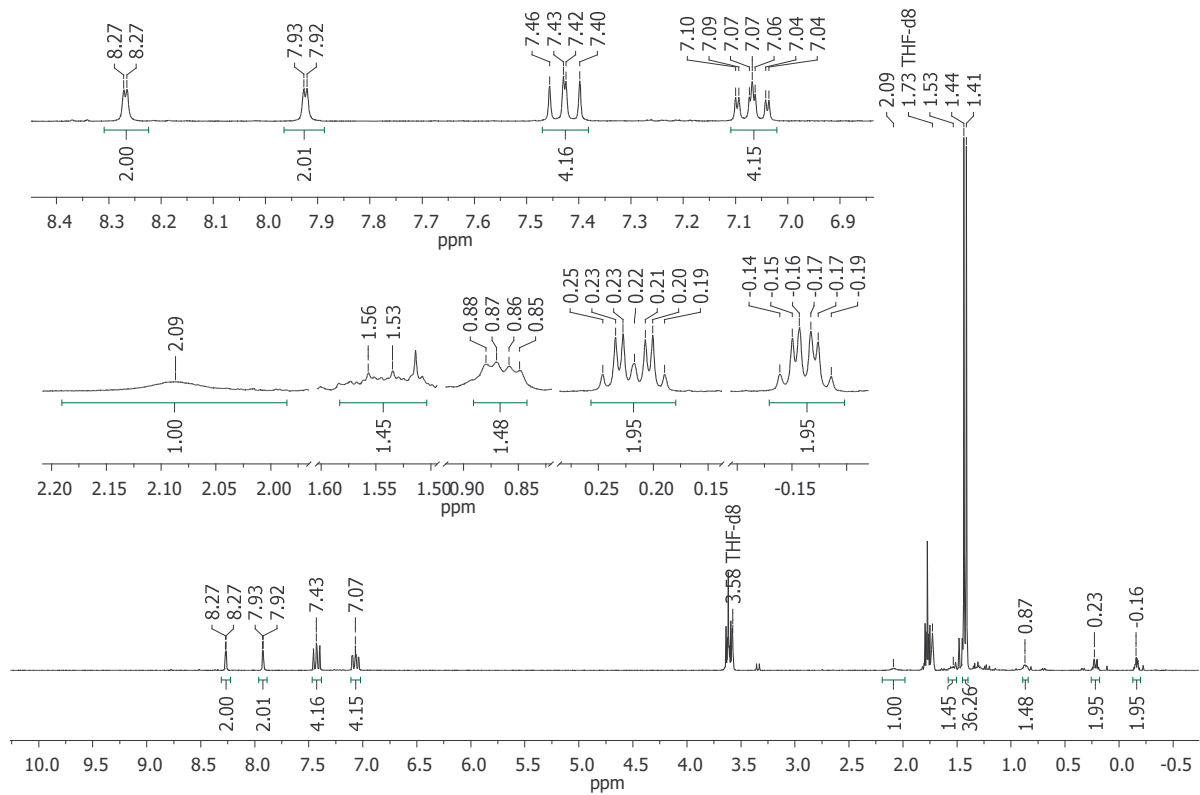


Figure S58: ^1H NMR spectrum of Li[17] (300.0 MHz, THF- d_8).

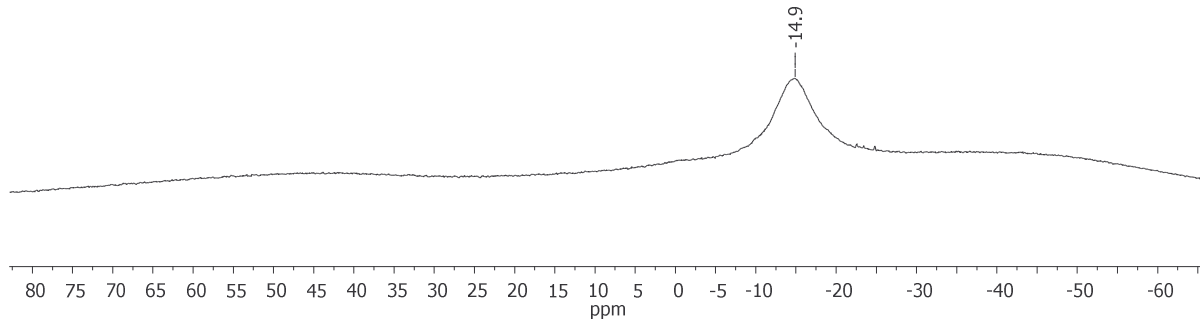


Figure S59: ^{11}B NMR spectrum of Li[17] (96.3 MHz, THF- d_8).

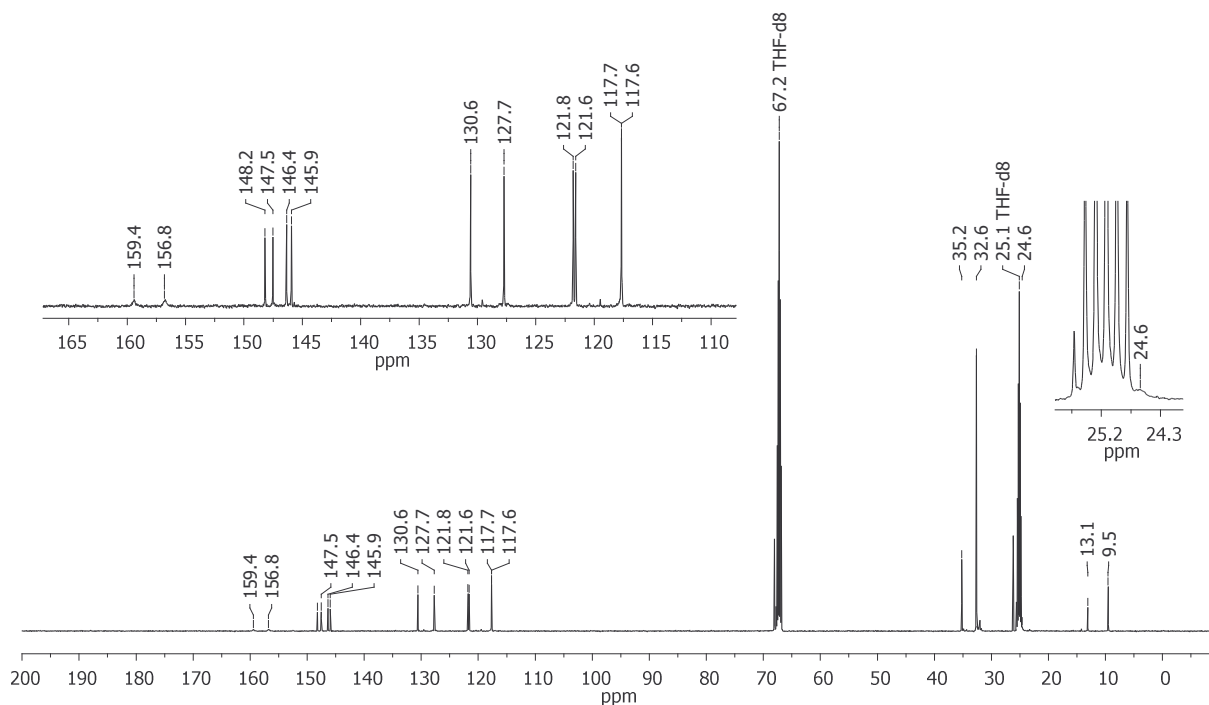


Figure S60: $^{13}\text{C}\{^1\text{H}\}$ NMR spectrum of Li[17] (125.8 MHz, THF- d_8).

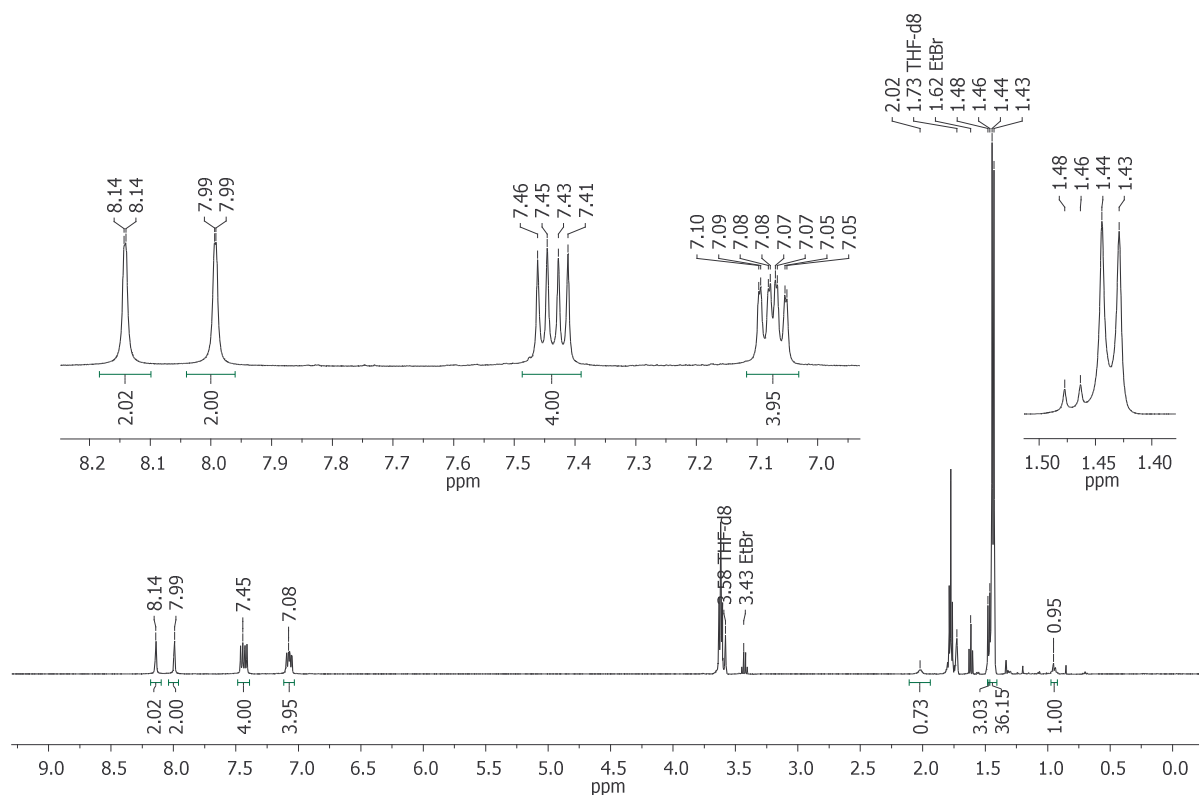


Figure S61: ^1H NMR spectrum of Li[19] (500.2 MHz, THF- d_8).

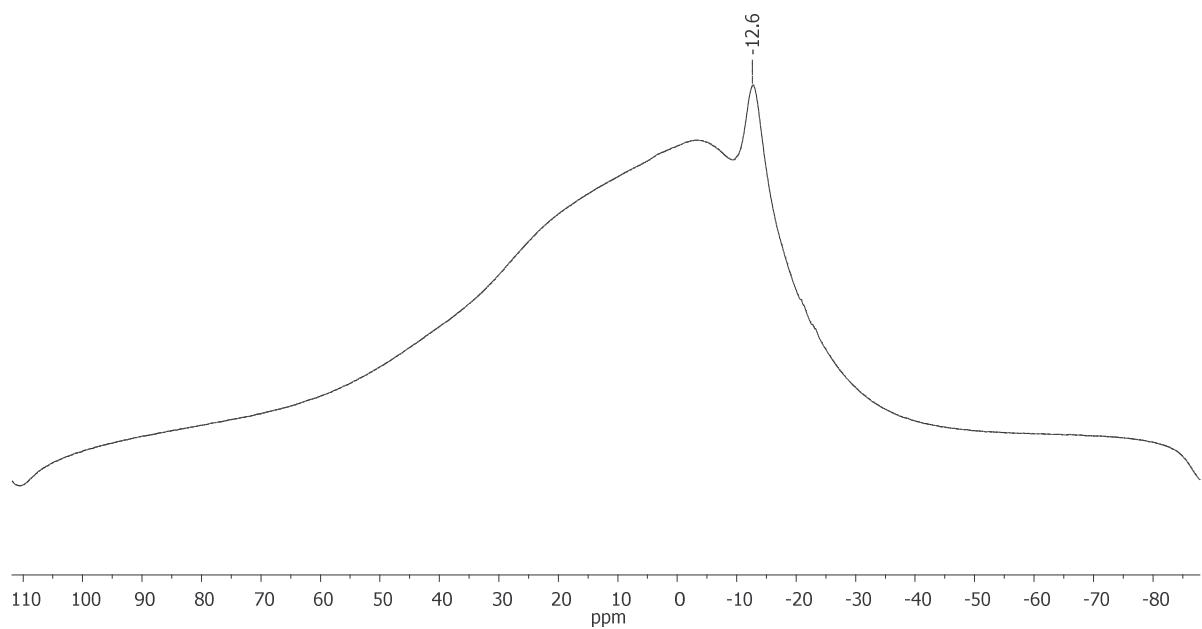


Figure S62: ^{11}B NMR spectrum of Li[19] (160.5 MHz, THF- d_8).

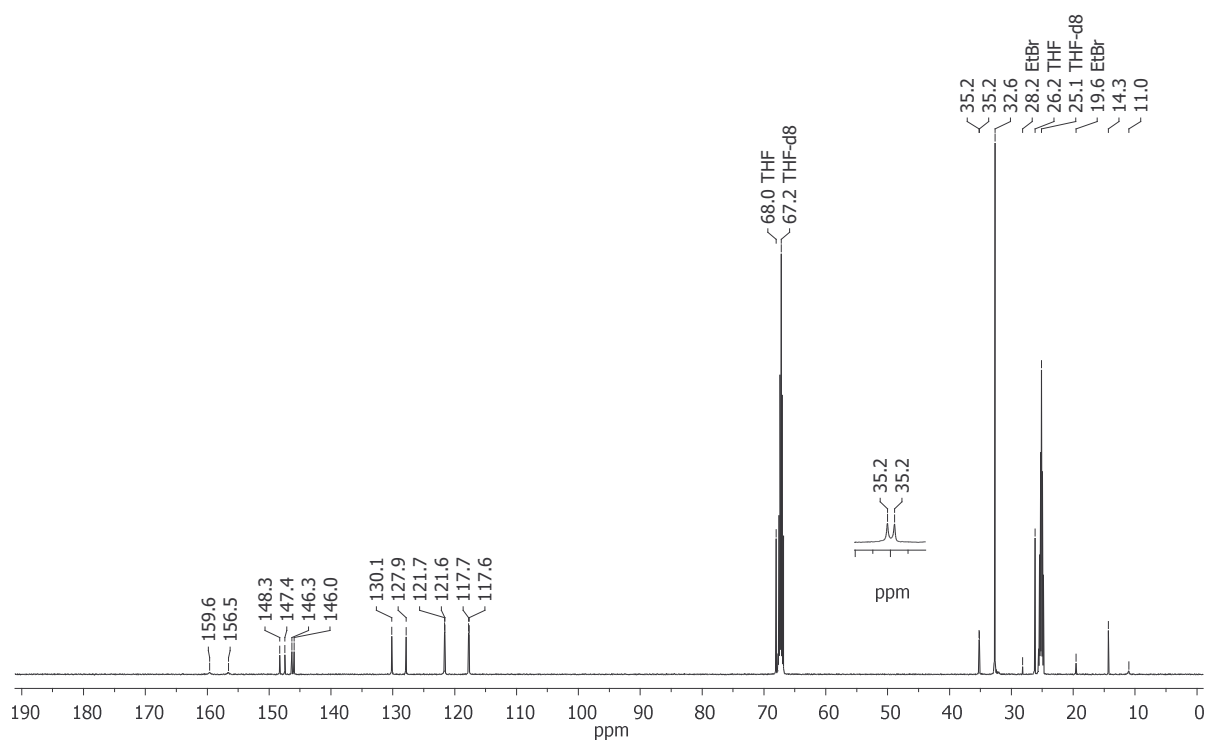


Figure S63: $^{13}\text{C}\{^1\text{H}\}$ NMR spectrum of Li[19] (125.8 MHz, THF- d_8).

3. X-ray

Data for all structures were collected on a STOE IPDS II two-circle diffractometer with a Genix Microfocus tube with mirror optics using MoK α radiation ($\lambda = 0.71073 \text{ \AA}$). The data were scaled using the frame-scaling procedure in the *X-AREA* program system.⁵⁶ The structures were solved by direct methods using the program *SHELXS*⁵⁷ and refined against F^2 with full-matrix least-squares techniques using the program *SHELXL*.⁵⁷

Structure	Internal code	CCDC reference number
[Li(thf) ₄][2]	wa2120	1819687
[Li(thf) ₃][2]	wa2506	1819688
[Li(thf) ₃ (Et ₂ O)][7]	wa2456	1819689
[Li(12-crown-4)(thf)][Li(thf) ₂][11]	wa2374	1819690
[Li(thf) ₄][16]	wa2467	1819691
(14 ^{C2} .thf)·4C ₆ H ₆	wa2473	1819692
14 ^{C3}	wa2461	1819693
14 ^{C4}	wa2477	1819694
[Li(12-crown-4) ₂][15 ^{C5,Cl}]	wa2518	1819695

$[Li(thf)_4][\mathbf{2}]$

Yellow single crystals of $[Li(thf)_4][\mathbf{2}]$ were grown by gas-phase diffusion of hexane into a THF solution of $Li[\mathbf{2}]$ (3 d, room temperature).

The H atom bridging B1 and B2 was isotropically refined; the coordinates of the two H atoms bonded to C1 were also refined. One *t*Bu group is disordered over two positions with a site occupation factor of 0.793(9) for the major occupied site. In two thf ligands, two methylene groups are disordered over two positions with site occupation factors of 0.66(2) and 0.51(2) for the major occupied sites. In one thf ligand, three methylene groups are disordered over two positions, each with a site occupation factor of 0.63(2) for the major occupied site. The lengths of the C–C bonds involving the disordered atoms in the thf ligands were restrained to 1.50(1) Å and the 1–3 distances involving disordered C atoms in the thf ligands were restrained to 2.3(1) Å or 2.3(3) Å. The displacement ellipsoids of all disordered atoms were restrained to an isotropic behavior.

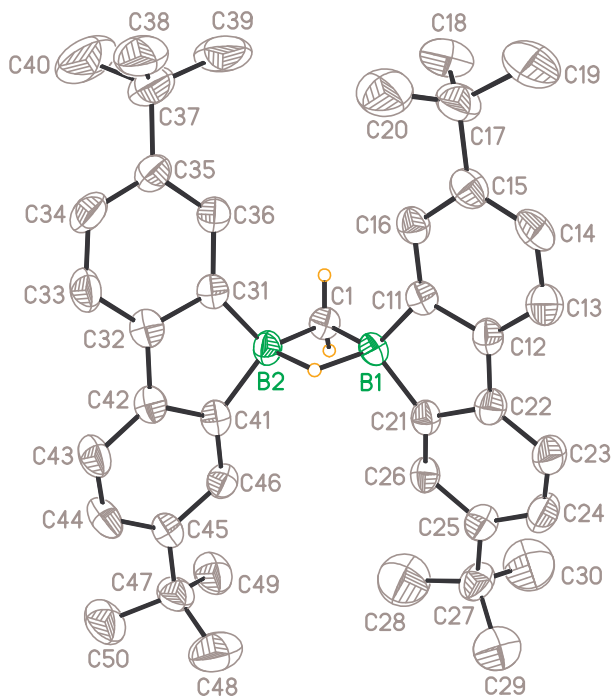


Figure S64: Molecular structure of $[Li(thf)_4][\mathbf{2}]$ in the solid state. The solvent-separated $[Li(thf)_4]^+$ cation and the CH atoms (except on C1) are omitted for clarity. Displacement ellipsoids are drawn at the 50% probability level. Selected atom···atom distance [Å], bond lengths [Å], and bond angles [°]: B(1)···B(2) = 1.974(6); B(1)–C(1) = 1.598(6), B(1)–C(11) = 1.624(5), B(1)–C(21) = 1.615(6), B(2)–C(1) = 1.581(6), B(2)–C(31) = 1.613(6), B(2)–C(41) = 1.629(6); B(1)–C(1)–B(2) = 76.8(3), C(11)–B(1)–C(21) = 100.7(3), C(31)–B(2)–C(41) = 100.2(3).

$[Li(thf)_3][\mathbf{2}]$

Colorless single crystals of $[Li(thf)_3][\mathbf{2}]$ precipitated from a C_6H_6 solution of methyl triflate/ $[Li(thf)_3]_2[\mathbf{1}]$ (1.1:1; 4 d, room temperature).

The asymmetric unit contains two crystallographically independent molecules of $[Li(thf)_3][\mathbf{2}]$. The H atom bridging the boron atoms and the H atoms located on the C atoms bonded to both boron atoms were isotropically refined for both independent molecules. In the asymmetric unit, two *tBu* groups are disordered over two positions with site occupation factors of 0.78(2) and 0.53(4) for the major occupied sites. In two thf ligands, two methylene groups are disordered over two positions with site occupation factors of 0.63(2) and 0.53(1) for the major occupied sites. In one thf ligand, three methylene groups are disordered over two positions, each with a site occupation factor of 0.62(4) for the major occupied site. The displacement ellipsoids of all atoms in the coordinating $[Li(thf)_3]^+$ ion were refined with a rigid bond restraint. The displacement ellipsoids of the disordered atoms were restrained to an isotropic behavior. Due to the absence of anomalous scatterers, the absolute structure could not be determined (Flack-x-parameter 1.5(10)).

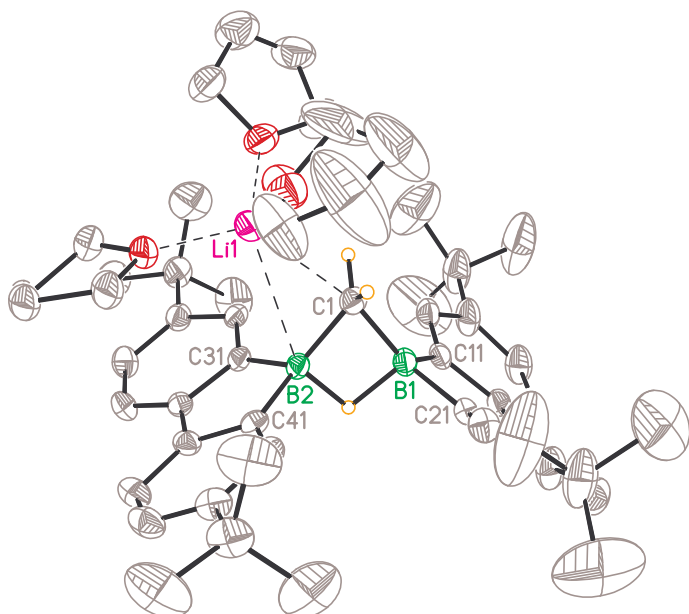


Figure S65: Molecular structure of one of the two crystallographically independent molecules of $[Li(thf)_3][\mathbf{2}]$ in the solid state. The CH atoms (except on C1) are omitted for clarity. Displacement ellipsoids are drawn at the 30% probability level. Selected atom–atom distance [\AA], bond lengths [\AA], and bond angles [$^\circ$] of the two crystallographically independent molecules: $B(1)\cdots B(2)$ = 1.967(9)/1.950(9); $B(1)-C(1)$ = 1.608(8)/1.606(8), $B(1)-C(11)$ = 1.592(9)/1.618(8), $B(1)-C(21)$ = 1.602(9)/1.613(9), $B(2)-C(1)$ = 1.600(9)/1.601(8), $B(2)-C(31)$ = 1.611(9)/1.622(9), $B(2)-C(41)$ = 1.613(9)/1.606(9); $B(1)-C(1)-B(2)$ = 75.7(4)/74.9(4), $C(11)-B(1)-C(21)$ = 101.3(5)/101.1(5), $C(31)-B(2)-C(41)$ = 100.9(5)/100.6(5).

$[Li(thf)_3(Et_2O)][7]$

Colorless single crystals of $[Li(thf)_3(Et_2O)][7]$ precipitated from the THF/Et₂O filtrate of the reaction Li[HBEt₃]/1H₂ (1 d, room temperature).

All the H atoms bonded to B were isotropically refined. Three tBu groups are disordered over two positions with site occupation factors of 0.62(1), 0.59(2), and 0.52(2) for the major occupied sites. In one thf ligand, three methylene groups are disordered over two positions, each with a site occupation factor of 0.62(2) for the major occupied site. The disordered atoms were isotropically refined. Bond lengths and bond angles of one disordered tBu group were restrained to be equal to those of the non-disordered tBu group. Bond lengths and bond angles of the disordered thf ligand were restrained to be equal to those of a non-disordered thf ligand.

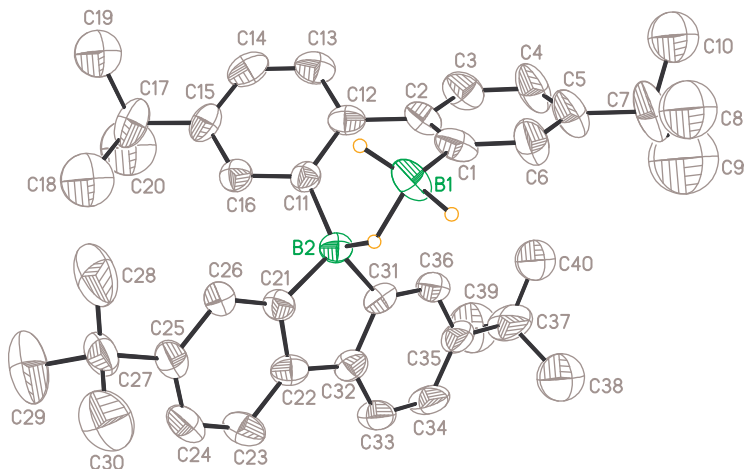


Figure S66: Molecular structure of $[Li(thf)_3(Et_2O)][7]$ in the solid state. The solvent-separated $[Li(thf)_3(Et_2O)]^+$ cation and all CH atoms are omitted for clarity. Displacement ellipsoids are drawn at the 50% probability level. Selected atom···atom distance [\AA], bond lengths [\AA], bond angles [$^\circ$], and torsion angle [$^\circ$]: B(1)···B(2) = 2.382(8); B(1)–C(1) = 1.603(7), B(2)–C(11) = 1.623(7); B(1)–C(1)–C(2) = 122.5(5), B(2)–C(11)–C(12) = 124.6(4), C(21)–B(2)–C(31) = 100.3(3); C(1)–C(2)–C(12)–C(11) = -36.0(7).

[Li(12-crown-4)(thf)][Li(thf)₂][11]

The reaction mixture *t*BuCCLi/Li[1H] in THF was layered with hexane/12-crown-4 and stored at room temperature, whereupon orange single crystals of *[Li(12-crown-4)(thf)][Li(thf)₂][11]* formed.

The H atom bonded to B1 was isotropically refined. Two *t*Bu groups are disordered over two positions with site occupation factors of 0.58(2) and 0.51(2) for the major occupied sites. In one thf ligand, one methylene group is disordered over two positions with a site occupation factor of 0.79(3) for the major occupied site. The displacement ellipsoids of the disordered atoms were restrained to an isotropic behavior.

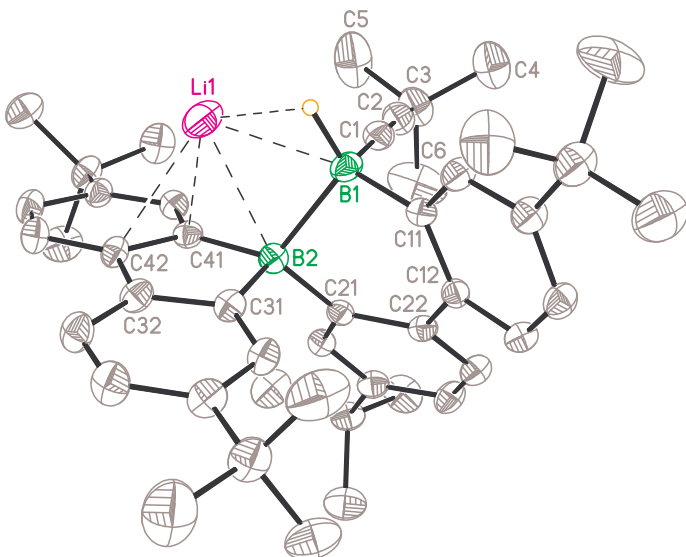


Figure S67: Molecular structure of *[Li(12-crown-4)(thf)][Li(thf)₂][11]* in the solid state. The solvent-separated *[Li(12-crown-4)(thf)]⁺* cation, thf ligands, and all CH atoms are omitted for clarity. Displacement ellipsoids are drawn at the 30% probability level. Selected bond lengths [Å], bond angles [°], and torsion angle [°]: B(1)–B(2) = 1.879(5), B(1)–C(1) = 1.612(6), B(1)–C(11) = 1.617(5), B(2)–C(21) = 1.625(5), B(2)–C(31) = 1.631(5), B(2)–C(41) = 1.630(5), C(1)–C(2) = 1.221(5); B(1)–B(2)–C(21) = 97.5(2), B(1)–C(1)–C(2) = 175.1(3), B(1)–C(11)–C(12) = 120.3(3), B(2)–B(1)–C(1) = 105.9(2), B(2)–B(1)–C(11) = 102.2(2), B(2)–C(21)–C(22) = 121.3(2), C(1)–B(1)–C(11) = 114.4(3); C(11)–C(12)–C(22)–C(21) = -31.8(4).

$[Li(thf)_4][\mathbf{16}]$

Colorless single crystals of $[Li(thf)_4][\mathbf{16}]$ were grown by gas-phase diffusion of hexane into a THF solution of Li[**16**] (3 d, room temperature).

There are two crystallographically independent molecules of $[Li(thf)_4][\mathbf{16}]$ in the asymmetric unit. Boron-bridging H atoms were isotropically refined. In one of the independent molecules three *t*Bu groups are disordered over two positions with site occupation factors of 0.54(1), 0.75(2), and 0.83(2). In the other independent molecule, three *t*Bu groups are disordered over two positions with site occupation factors of 0.52(3), 0.55(1), and 0.57(1). In one thf ligand, the O atom and two methylene groups are disordered over two positions, each with a site occupation factor of 0.69(1) for the major occupied site. In one thf ligand, two methylene groups are disordered over two positions, each with a site occupation factor of 0.51(1) for the major occupied site. The displacement ellipsoids of all disordered atoms and all atoms in the $[Li(thf)_4]^+$ ions were restrained to an isotropic behavior. Bond lengths and angles in the disordered thf ligands were restrained to be equal to those in a non-disordered thf ligand.

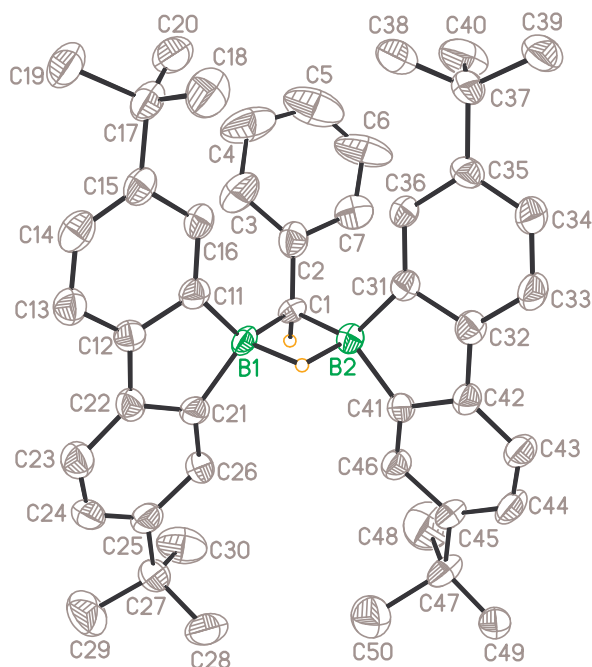


Figure S68: Molecular structure of one of the crystallographically independent molecules of $[Li(thf)_4][\mathbf{16}]$ in the solid state. The solvent-separated $[Li(thf)_4]^+$ cation and the CH atoms (except on C1) are omitted for clarity. Displacement ellipsoids are drawn at the 30% probability level. Selected atom–atom distance [Å], bond lengths [Å], and bond angles [°] of the two crystallographically independent molecules: B(1)–B(2) = 1.974(8)/1.990(8); B(1)–C(1) = 1.597(8)/1.625(7), B(1)–C(11) = 1.624(8)/1.615(8), B(1)–C(21) = 1.618(8)/1.601(8), B(2)–C(1) = 1.605(7)/1.613(9), B(2)–C(31) = 1.633(8)/1.609(8), B(2)–C(41) = 1.630(8)/1.602(9); B(1)–C(1)–B(2) = 76.1(4)/75.8(4), C(11)–B(1)–C(21) = 100.2(4)/102.3(4), C(31)–B(2)–C(41) = 101.0(4)/102.2(5).

(14^{C2}.thf)·4C₆H₆

Yellow single crystals of **(14^{C2}.thf)·4C₆H₆** were grown from the reaction mixture 1,2-dichloroethane/[Li(thf)₃]₂[**1**] in C₆H₆ by slow evaporation of all volatiles at room temperature.

One of the two boron atoms is tetracoordinated by the thf ligand. Two *t*Bu groups are disordered over two positions with site occupation factors of 0.818(6) and 0.61(2) for the major occupied sites. The displacement ellipsoids of the disordered atoms were restrained to an isotropic behavior.

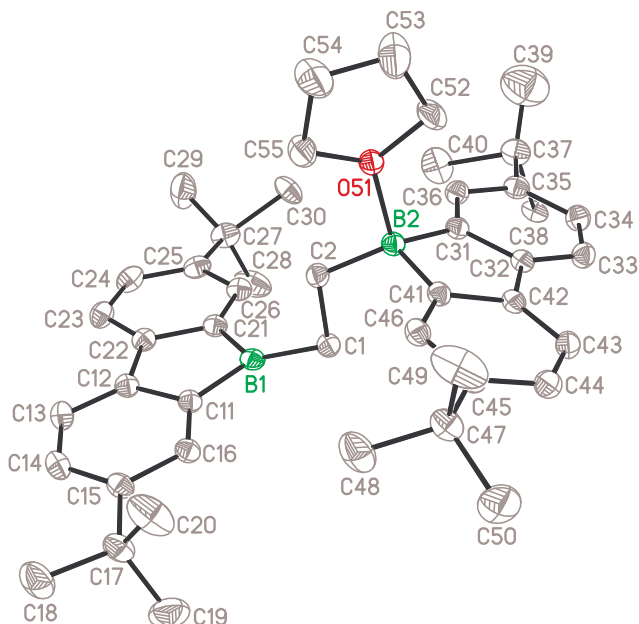


Figure S69: Molecular structure of **(14^{C2}.thf)·4C₆H₆** in the solid state. CH atoms and C₆H₆ molecules are omitted for clarity. Displacement ellipsoids are drawn at the 30% probability level. Selected bond lengths [Å], bond angles [°], and torsion angle [°]: B(1)–C(1) = 1.544(2), B(1)–C(11) = 1.577(2), B(1)–C(21) = 1.577(2), B(2)–C(2) = 1.609(2), B(2)–C(31) = 1.625(2), B(2)–C(41) = 1.620(2), B(2)–O(51) = 1.644(2), C(1)–C(2) = 1.566(2); C(1)–B(1)–C(11) = 128.0(1), C(1)–B(1)–C(21) = 128.3(1), C(11)–B(1)–C(21) = 102.8(1), C(2)–B(2)–C(31) = 118.0(1), C(2)–B(2)–C(41) = 118.1(1), C(31)–B(2)–C(41) = 100.0(1); B(1)–C(1)–C(2)–B(2) = -179.1(1); $\sum(C-B(1)-C) = 359^\circ$; $\sum(C-B(2)-C) = 336^\circ$.

14^{C3}

Yellow plates of **14^{C3}** suitable for X-ray crystallography were grown from the reaction mixture 1,3-dibromopropane/Li₂[1] in THF by slow evaporation of all volatiles at room temperature.

Due to the absence of anomalous scatterers, the absolute structure could not be determined (Flack-x-parameter 1.8(10)).

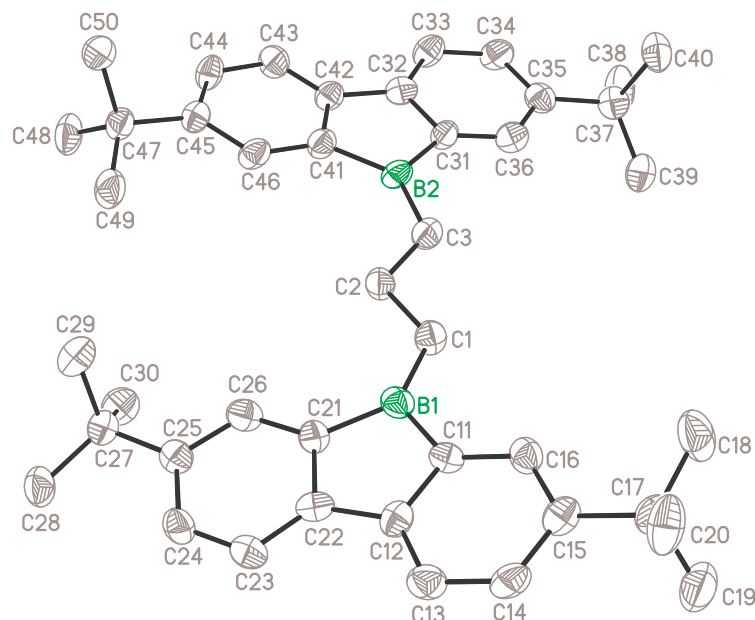


Figure S70: Molecular structure of **14^{C3}** in the solid state. CH atoms are omitted for clarity. Displacement ellipsoids are drawn at the 50% probability level. Selected bond lengths [Å] and bond angles [°]: B(1)–C(1) = 1.563(9), B(1)–C(11) = 1.569(9), B(1)–C(21) = 1.571(9), B(2)–C(3) = 1.577(9), B(2)–C(31) = 1.560(9), B(2)–C(41) = 1.571(10); C(1)–B(1)–C(11) = 125.1(6), C(1)–B(1)–C(21) = 131.8(6), C(11)–B(1)–C(21) = 103.0(5), C(3)–B(2)–C(31) = 121.9(6), C(3)–B(2)–C(41) = 132.6(6), C(31)–B(2)–C(41) = 105.5(5). Angle between the planes of the borol rings [°]: 22.0. $\sum(C-B(1)-C) = 359.9^\circ$; $\sum(C-B(2)-C) = 360.0^\circ$.

14^{C4}

Yellow single crystals of **14^{C4}** were grown from the reaction mixture 1,4-dibromobutane/Li₂[**1**] in THF by slow evaporation of all volatiles at room temperature.

The asymmetric unit contains two half crystallographically independent molecules of **14^{C4}** both located on a crystallographic center of inversion. The crystal was non-merohedrally twinned with a fractional contribution of 0.341(3) of the minor component.

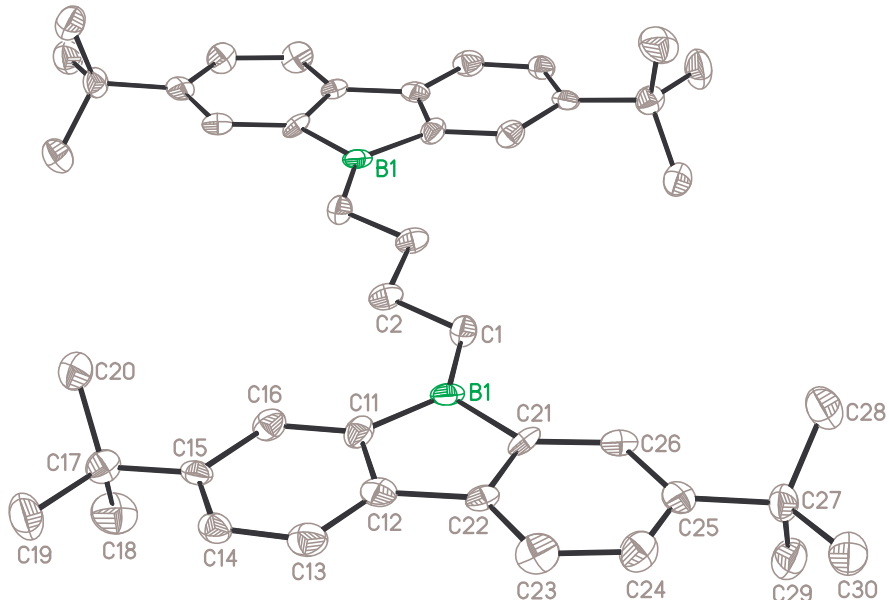


Figure S71: One of the two half crystallographically independent molecules of **14^{C4}** in the solid state. CH atoms are omitted for clarity. Displacement ellipsoids are drawn at the 50% probability level. Selected bond lengths [Å] and bond angles [°] of the two half crystallographically independent molecules: B(1)–C(1) = 1.566(10)/1.577(9), B(1)–C(11) = 1.558(10)/1.595(9), B(1)–C(21) = 1.579(9)/1.558(10); C(1)–B(1)–C(11) = 131.7(6)/125.4(6), C(1)–B(1)–C(21) = 125.1(6)/131.4(5), C(11)–B(1)–C(21) = 103.2(6)/103.1(5). Angle between the planes of the borol rings [°]: 0.0. $\sum(C-B(1)-C)$ = 360.0°/359.9°. Symmetry transformations used to generate equivalent atoms: 1) -x+1, -y+1, -z-1; 2) -x, -y+1, -z-2.

$[Li(12\text{-crown}\text{-}4)]_2[15^{C5,Cl}]$

The reaction mixture 1,5-dichloropentane/Li₂[1] in THF was layered with hexane/12-crown-4 and stored at room temperature, whereupon colorless single crystals of $[Li(12\text{-crown}\text{-}4)]_2[15^{C5,Cl}]$ formed.

The asymmetric unit contains one-half of a molecule of $[Li(12\text{-crown}\text{-}4)]_2[15^{C5,Cl}]$ located on a crystallographic C_2 axis. Three methylene groups and the terminal Cl atom of the pentyl chain are disordered over the C_2 axis with two equally occupied positions. One *tBu* group is disordered over two positions with a site occupation factor of 0.83(3) for the major occupied site. The C–C bond lengths in the pentyl chain were restrained to 1.50(1) Å and 1–3 C–C distances in this chain were restrained to 2.50(1) Å. The C–Cl bond length was restrained to 1.80(1) Å. The displacement ellipsoids of the disordered C atoms were restrained to an isotropic behavior. The Flack-x-parameter refined to –0.2(2). The boron-bridging H atom was isotropically refined.

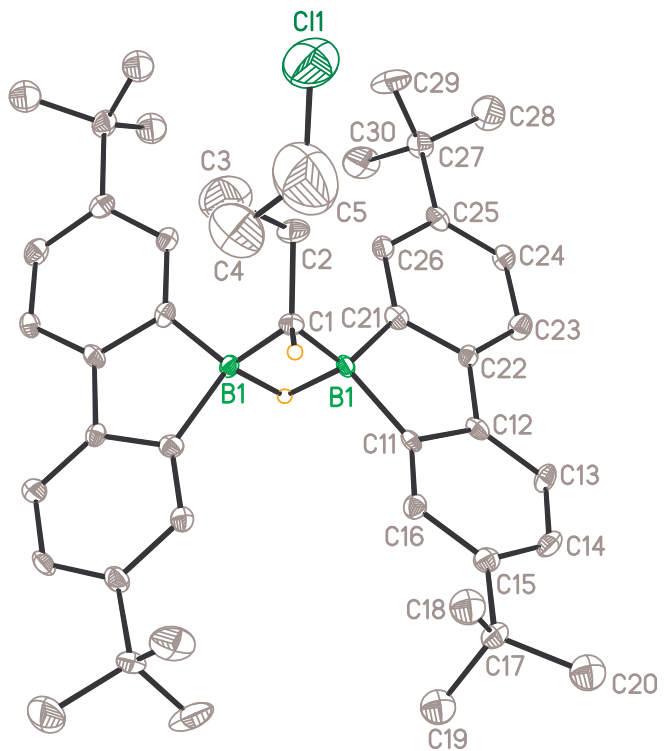


Figure S72: Molecular structure of $[Li(12\text{-crown}\text{-}4)]_2[15^{C5,Cl}]$ in the solid state. The solvent-separated $[Li(12\text{-crown}\text{-}4)]^+$ cation and CH atoms (except on C1) are omitted for clarity. Displacement ellipsoids are drawn at the 30% probability level. Selected atom–atom distance [Å], bond lengths [Å], and bond angles [°]: B(1)…B(1) = 1.93(1); B(1)–C(1) = 1.60(1), B(1)–C(11) = 1.656(9), B(1)–C(21) = 1.643(9); C(1)–B(1)–C(11) = 122.8(5), C(1)–B(1)–C(21) = 124.6(5), C(11)–B(1)–C(21) = 98.6(5). Symmetry transformation used to generate equivalent atoms: $-x+1, -y+1, z$.

Table S2. Selected crystallographic data for [Li(thf)₄][**2**], [Li(thf)₃][**2**], and [Li(thf)₃(Et₂O)][**7**].

	[Li(thf) ₄][2]	[Li(thf) ₃][2]	[Li(thf) ₃ (Et ₂ O)][7]
formula	C ₅₇ H ₈₃ B ₂ LiO ₄	C ₅₃ H ₇₅ B ₂ LiO ₃	C ₅₆ H ₈₅ B ₂ LiO ₄
M _r	860.79	788.69	850.79
color, shape	colorless, needle	colorless, block	colorless, needle
T [K]	173(2)	173(2)	173(2)
radiation, λ [Å]	MoK _α , 0.71073	MoK _α , 0.71073	MoK _α , 0.71073
crystal system	orthorhombic	monoclinic	monoclinic
space group	Pccn	P2 ₁	P2 ₁ /n
a [Å]	21.5605(15)	14.7750(10)	10.7242(12)
b [Å]	26.1802(19)	19.9973(10)	21.4641(16)
c [Å]	19.2608(13)	17.9098(12)	24.027(3)
α [°]	90	90	90
β [°]	90	109.105(5)	97.208(9)
γ [°]	90	90	90
V [Å ³]	10871.9(13)	5000.2(6)	5487.0(10)
Z	8	4	4
D _{calcd} [g cm ⁻³]	1.052	1.048	1.030
μ [mm ⁻¹]	0.063	0.062	0.061
F(000)	3760	1720	1864
crystal size [mm]	0.28 x 0.18 x 0.12	0.24 x 0.22 x 0.17	0.21 x 0.11 x 0.02
rflns collected	42030	44665	66414
independent rflns (R _{int})	9821 (0.1664)	18711 (0.0674)	10391 (0.1431)
data/restraints/parameters	9821 / 190 / 681	18711 / 484 / 1209	10391 / 164 / 572
GOF on F ²	0.946	0.910	1.443
R ₁ , wR ₂ [<i>I</i> > 2σ(<i>I</i>)]	0.0860, 0.1598	0.0712, 0.1404	0.1344, 0.2573
R ₁ , wR ₂ (all data)	0.2038, 0.2033	0.1458, 0.1670	0.2251, 0.2877
largest diff peak and hole [e Å ⁻³]	0.418, -0.233	0.421, -0.211	0.933, -0.296

Table S3. Selected crystallographic data for $[\text{Li}(12\text{-crown-4})(\text{thf})][\text{Li}(\text{thf})_2]$ **[11]**, $[\text{Li}(\text{thf})_4]$ **[16]**, and $(\mathbf{14}^{\text{C}2}\cdot\text{thf})\cdot 4\text{C}_6\text{H}_6$.

	$[\text{Li}(12\text{-crown-4})(\text{thf})][\text{Li}(\text{thf})_2]$ [11]	$[\text{Li}(\text{thf})_4]$ [16]	$(\mathbf{14}^{\text{C}2}\cdot\text{thf})\cdot 4\text{C}_6\text{H}_6$
formula	$\text{C}_{66}\text{H}_{98}\text{B}_2\text{Li}_2\text{O}_7$	$\text{C}_{63}\text{H}_{87}\text{B}_2\text{LiO}_4$	$\text{C}_{70}\text{H}_{84}\text{B}_2\text{O}$
M_r	1038.94	936.88	962.99
color, shape	orange, plate	colorless, plate	yellow, block
T [K]	173(2)	173(2)	173(2)
radiation, λ [\AA]	MoK_α , 0.71073	MoK_α , 0.71073	MoK_α , 0.71073
crystal system	monoclinic	monoclinic	triclinic
space group	$P2_1/c$	$P2_1/c$	$P-1$
a [\AA]	12.9451(8)	19.4970(15)	10.4041(3)
b [\AA]	18.3459(7)	24.7864(18)	11.5484(3)
c [\AA]	27.0962(17)	23.972(2)	25.7360(7)
α [$^\circ$]	90	90	79.323(2)
β [$^\circ$]	101.393(5)	92.463(7)	85.313(2)
γ [$^\circ$]	90	90	81.220(2)
V [\AA^3]	6308.3(6)	11574.0(16)	2998.51(14)
Z	4	8	2
D_{calcd} [g cm^{-3}]	1.094	1.075	1.067
μ [mm^{-1}]	0.068	0.064	0.060
$F(000)$	2264	4080	1044
crystal size [mm]	0.24 x 0.19 x 0.04	0.17 x 0.17 x 0.03	0.24 x 0.19 x 0.14
rflns collected	59630	87491	69450
independent rflns (R_{int})	11144 (0.0915)	21394 (0.1445)	12158 (0.0402)
data/restraints/parameters	11144 / 72 / 764	21394 / 891 / 1484	12158 / 84 / 714
GOF on F^2	1.134	1.302	1.037
R_1 , wR_2 [$I > 2\sigma(I)$]	0.0785, 0.1585	0.1210, 0.2070	0.0673, 0.1755
R_1 , wR_2 (all data)	0.1447, 0.1797	0.2818, 0.2432	0.0782, 0.1838
largest diff peak and hole [e \AA^{-3}]	0.306, -0.212	0.704, -0.334	0.539, -0.424

Table S4. Selected crystallographic data for **14^{C3}**, **14^{C4}**, and [Li(12-crown-4)₂][**15^{C5,Cl}**].

	14^{C3}	14^{C4}	[Li(12-crown-4) ₂][15^{C5,Cl}]
formula	C ₄₃ H ₅₄ B ₂	C ₄₄ H ₅₆ B ₂	C ₆₁ H ₉₀ B ₂ ClLiO ₈
M _r	592.48	606.50	1015.33
color, shape	yellow, plate	yellow, block	colorless, plate
T [K]	173(2)	173(2)	173(2)
radiation, λ [Å]	MoK _α , 0.71073	MoK _α , 0.71073	MoK _α , 0.71073
crystal system	orthorhombic	triclinic	orthorhombic
space group	Pca2 ₁	P-1	Fdd2
a [Å]	41.344(3)	5.9740(9)	12.2698(10)
b [Å]	14.2720(12)	14.639(2)	43.946(3)
c [Å]	6.1349(5)	21.461(3)	21.961(2)
α [°]	90	82.273(12)	90
β [°]	90	89.910(12)	90
γ [°]	90	86.790(12)	90
V [Å ³]	3620.0(5)	1856.9(5)	11841.6(17)
Z	4	2	8
D _{calcd} [g cm ⁻³]	1.087	1.085	1.139
μ [mm ⁻¹]	0.060	0.060	0.116
F(000)	1288	660	4400
crystal size [mm]	0.17 x 0.13 x 0.08	0.14 x 0.09 x 0.04	0.26 x 0.24 x 0.11
rflns collected	24978	16800	29925
independent rflns (<i>R</i> _{int})	6651 (0.1309)	16800	5586 (0.1140)
data/restraints/parameters	6651 / 1 / 406	16800 / 0 / 416	5586 / 63 / 379
GOF on <i>F</i> ²	0.840	1.207	1.121
<i>R</i> ₁ , <i>wR</i> ₂ [<i>I</i> > 2σ(<i>I</i>)]	0.0673, 0.1049	0.0880, 0.1686	0.0854, 0.1603
<i>R</i> ₁ , <i>wR</i> ₂ (all data)	0.1448, 0.1282	0.1850, 0.1839	0.1296, 0.1780
largest diff peak and hole [e Å ⁻³]	0.177, -0.162	0.359, -0.328	0.649, -0.220

4. Computational details

DFT calculations were carried out with the Gaussian program package.^{S8} The PBE0^{S9-12} hybrid functional was used and combined with the D3BJ atom-pairwise dispersion correction with Becke-Johnson damping as devised by Grimme.^{S13, 14} Geometry optimizations and harmonic frequency calculations were computed under gas-phase conditions with the TZVP basis set.^{S15} All stationary points reported were characterized as minima or first order saddle points by eigenvalue analysis of the diagonalized Hessians. Gibbs energies reported correspond to the total energies of single point calculations with the SMD solvation model^{S16} (to account for effects of the THF solvent), corrected by thermal contributions from the gas-phase frequency analyses. Graphical representations of molecular geometries were produced with the *CYLview* software.^{S17}

Minima

[5c]

Total energy = -1013.13778138 Hartree

Thermal correction to Gibbs free energy = 0.315916 Hartree

d(B···B) = 1.690623 Å



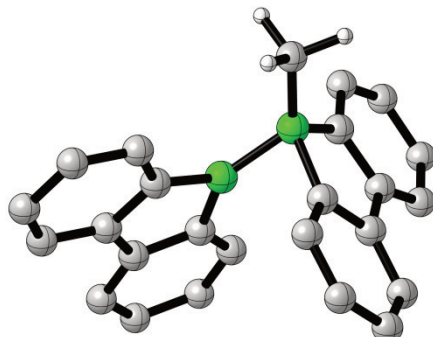
B	-0.441967198	0.464857702	0.127632617	C	2.890633354	2.347533655	-0.658552086
B	0.225700371	-0.679245183	1.178087245	C	1.061197048	3.771214531	-1.248071155
C	-0.571464517	-1.630514359	2.156272199	H	-0.881937078	2.945367287	-0.914556789
C	-1.938766773	0.851279774	0.488876060	C	3.925080647	-0.252221994	0.063459838
C	-2.827741254	-0.138378499	0.005023636	C	3.779272020	-2.202133390	1.454558172
C	-0.711703468	-0.832404114	-0.809277259	H	1.838040302	-2.610152226	2.237639834
C	0.621563346	1.537209407	-0.350327269	H	-3.671719519	-2.469913882	-1.396959802
C	1.790603414	-0.837354507	1.044791777	C	-1.754129712	-3.067852268	-2.157963939
C	-2.481883990	1.890935817	1.244952002	H	-5.765328215	1.008762496	1.245390892
C	-2.100180930	-1.136160851	-0.769401309	H	3.960676850	2.217991538	-0.544309920
C	-4.192188896	-0.093660389	0.284151242	C	2.430670628	3.557561064	-1.145398242
C	0.122999207	-1.678474373	-1.542352293	H	4.525956006	0.373420776	-0.585496480
C	2.015866005	1.321973362	-0.269736172	C	4.521762246	-1.360580706	0.636620842
C	0.188216342	2.775086435	-0.846665187	H	-2.148048827	-3.933502799	-2.681881169
C	2.574236105	0.061804526	0.278656991	H	3.136513462	4.331636258	-1.430343275
C	2.433904652	-1.930841048	1.636349844	H	5.568849148	-1.569562460	0.438157369
C	-3.845293467	1.951460778	1.505035807	H	-4.250553999	2.775549227	2.086047459
H	-1.828623917	2.667125114	1.635910729	H	0.269230697	-3.416972514	-2.794549574
C	-2.608635995	-2.247157632	-1.433386684	H	0.679336625	4.714925827	-1.627555126
H	-4.857533294	-0.870726355	-0.083265376	H	4.237309131	-3.072275506	1.914749260
C	-4.702154460	0.957599006	1.030913842	H	-0.291522991	-1.381184548	3.189353696
C	-0.393309405	-2.776983353	-2.219119525	H	-0.345561851	-2.695052685	2.022475016
H	1.188190946	-1.474342020	-1.587150586	H	-1.653252231	-1.502801358	2.071277747

[6^c-open]⁻

Total energy = -1013.12607437 Hartree

Thermal correction to Gibbs free energy = 0.313661 Hartree

d(B···B) = 1.689778 Å



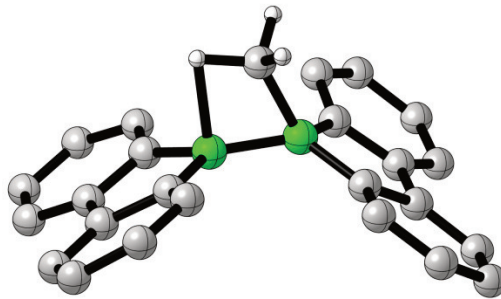
B	0.720147961	-1.135240335	1.206158149	C	-2.207807885	2.932925812	-0.745189863
B	-0.549192749	-0.161076673	0.662901704	H	-3.241465759	3.230229136	-0.898166136
C	0.475381457	-2.271006271	2.337009714	C	-1.176257495	3.810335799	-1.063658056
C	2.107279432	-0.341259185	1.227308617	H	-1.406260279	4.790900996	-1.469774313
C	2.692089520	-0.305127243	-0.060500408	C	0.146015628	3.438696737	-0.853273124
C	3.870833210	0.392946363	-0.311718541	C	0.453118986	2.186457363	-0.325406501
H	4.294454186	0.424204145	-1.312194215	H	1.488416357	1.918887820	-0.149663413
C	4.503498912	1.057829213	0.729161353	C	-2.113139427	-0.497714940	0.666975322
H	5.424616629	1.603347954	0.548017743	C	-2.824831333	0.616940320	0.174036316
C	3.954268169	1.020657011	2.010469389	C	-4.210642339	0.627837411	0.120454105
C	2.770238150	0.333077728	2.251637414	H	-4.747139950	1.493495207	-0.257575647
H	2.350404367	0.330345323	3.254561673	C	-4.915040203	-0.492077329	0.552979444
C	0.726379746	-1.594191318	-0.364092128	H	-6.000082420	-0.497656020	0.511022710
C	1.867049287	-1.042353773	-1.009848143	C	-4.234519413	-1.599715469	1.042115433
C	2.093775785	-1.243672477	-2.365712580	C	-2.841835243	-1.595786719	1.105114934
H	2.969671092	-0.817575202	-2.847409694	H	-2.323323884	-2.460950440	1.503699835
C	1.196648612	-2.002007008	-3.107556384	H	4.455712783	1.540230934	2.822632090
H	1.369674701	-2.161960115	-4.167558667	H	-0.622334772	-3.146285889	-3.081063662
C	0.075619899	-2.555134335	-2.495549713	H	-4.791349294	-2.467709764	1.382026822
C	-0.161591610	-2.340677439	-1.142639316	H	0.945655281	4.131920197	-1.095852287
H	-1.053375709	-2.759990626	-0.687620430	H	1.350242848	-2.926411213	2.437180993
C	-0.557471678	1.282145551	-0.018741001	H	-0.378713997	-2.920819903	2.119088638
C	-1.893869290	1.682435291	-0.233629283	H	0.289276503	-1.831984054	3.324866689

[6^c]

Total energy = -1013.11924082 Hartree

Thermal correction to Gibbs free energy = 0.314099 Hartree

d(B···B) = 1.672597 Å



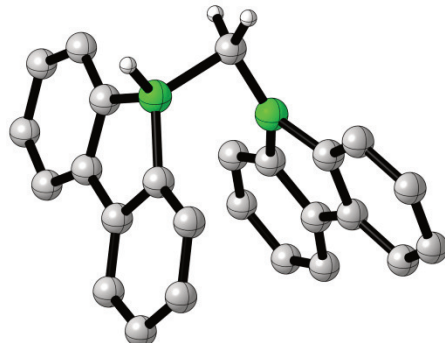
B	0.845333366	-0.123641900	0.772344246	C	-3.658202096	1.875976237	-1.047446566
B	-0.807549224	0.080432464	0.617700224	H	-4.568694722	1.532485257	-1.530240970
C	0.077242733	-0.080809613	2.284120336	C	-3.344734473	3.228556034	-1.038508614
C	1.911146323	1.023933395	0.507228162	H	-4.008159542	3.944255501	-1.514285535
C	2.965688132	0.488105971	-0.269678648	C	-2.177337343	3.663263881	-0.420131263
C	4.031699809	1.274072372	-0.692740603	C	-1.310724712	2.752423546	0.175642605
H	4.825647376	0.847374852	-1.299841548	H	-0.390213579	3.116332854	0.611855638
C	4.097155421	2.607159203	-0.307457188	C	-1.916075530	-1.042969577	0.439254445
H	4.928294139	3.227503641	-0.628810687	C	-3.000807711	-0.470859556	-0.264487730
C	3.109211753	3.135863190	0.517809126	C	-4.100799084	-1.228516824	-0.646247436
C	2.034892629	2.348293737	0.919957177	H	-4.917981915	-0.776780221	-1.201440312
H	1.294911754	2.781270253	1.587981390	C	-4.165863164	-2.568023405	-0.283349670
C	1.624675988	-1.403483736	0.233431984	H	-5.023602837	-3.168223002	-0.570794519
C	2.787725157	-0.953549612	-0.443888906	C	-3.141700557	-3.132204585	0.469551434
C	3.631371688	-1.830950653	-1.115796911	C	-2.029527872	-2.374671576	0.824178305
H	4.508748673	-1.458613278	-1.637883046	H	-1.253878713	-2.835856453	1.425006792
C	3.358714685	-3.192032747	-1.104338715	H	3.180271281	4.167277156	0.851503195
H	4.014996205	-3.885726795	-1.621060199	H	2.031964048	-4.727109934	-0.398058682
C	2.242467680	-3.661485132	-0.419435726	H	-3.209127116	-4.170871442	0.779001807
C	1.388844473	-2.777275987	0.232280537	H	-1.932252485	4.721175128	-0.414856139
H	0.520321620	-3.181839781	0.736922938	H	0.593359029	0.695994150	2.846381238
C	-1.601038313	1.391052471	0.192733423	H	0.163282023	-1.063683775	2.744886097
C	-2.805037684	0.972661461	-0.425635411	H	-1.000733532	0.183912091	2.381245301

[2^c-open]⁻

Total energy = -1013.14164203 Hartree

Thermal correction to Gibbs free energy = 0.314067 Hartree

d(B···B) = 2.343491 Å



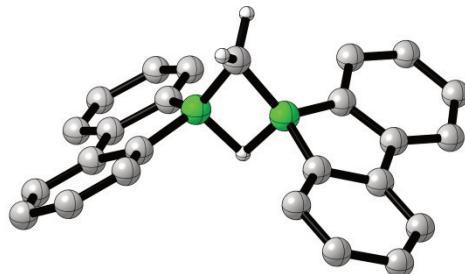
B	-0.656663047	0.008448156	-1.578232600	H	-2.917086865	-1.856388644	-2.246277428
B	0.924016051	-1.684198359	-1.219971128	C	0.299339576	-1.673813670	0.292200336
H	1.017934020	-2.843701814	-1.603452847	C	1.236892488	-1.109852867	1.186128070
C	0.142922501	-0.848116115	-2.517753641	C	0.983672394	-1.019746706	2.551161843
H	0.950937694	-0.390977444	-3.087574191	H	1.714156930	-0.572967603	3.220138618
H	-0.411756896	-1.553356816	-3.137115487	C	-0.212434246	-1.507909808	3.056828161
C	-0.233492773	1.295074225	-0.752204824	H	-0.425250549	-1.434156723	4.119193099
C	-1.340887837	1.716773899	0.012962834	C	-1.136934397	-2.097707252	2.199545892
C	-1.255233840	2.808323648	0.861954730	C	-0.875954245	-2.184478780	0.836902094
H	-2.107465819	3.122025942	1.457702449	H	-1.617641300	-2.638772552	0.188007235
C	-0.048127766	3.496015481	0.956074629	C	2.343752771	-1.002175372	-0.895709477
H	0.035877837	4.347177895	1.625189262	C	2.444713667	-0.689086681	0.475305368
C	1.048614321	3.098790044	0.202820179	C	3.564631525	-0.044741675	0.993175210
C	0.955165254	2.002415374	-0.652640691	H	3.621250258	0.205151715	2.049055912
H	1.823755548	1.688049053	-1.220978677	C	4.607714414	0.298701199	0.143753230
C	-2.177616684	-0.166891663	-1.154964839	H	5.483187427	0.807557430	0.536282149
C	-2.507870706	0.849718191	-0.237806679	C	4.528537121	-0.002973123	-1.213724359
C	-3.782458415	0.942094725	0.299247034	C	3.403305458	-0.645157135	-1.722914767
H	-4.033330375	1.722011839	1.012091689	H	3.350158686	-0.861471597	-2.787930465
C	-4.747091092	0.013802753	-0.083757519	H	1.987562058	3.636064101	0.290855320
H	-5.747503219	0.073508471	0.334205969	H	-5.203239645	-1.700729086	-1.291509528
C	-4.440339331	-0.985733486	-0.998858985	H	5.347471273	0.269255967	-1.874009700
C	-3.156485385	-1.069446907	-1.535964779	H	-2.071790717	-2.482798898	2.596590971

[2^c]

Total energy = -1013.15160474 Hartree

Thermal correction to Gibbs free energy = 0.314029 Hartree

d(B···B) = 1.916075 Å



B	-0.955185592	0.073866560	0.721830180	H	-0.664912282	3.116995251	0.555495530
B	0.955186640	-0.073860255	0.721835402	C	1.810984502	-1.335790407	0.199526715
H	0.000005965	0.000004772	-0.268992240	C	3.028757590	-0.861326347	-0.335320007
C	-0.000002751	0.000006632	1.989491668	C	3.975623742	-1.724762292	-0.875046273
H	-0.106671534	-0.895803478	2.597947110	H	4.906657646	-1.339141390	-1.280893378
H	0.106663546	0.895820250	2.597942444	C	3.724136909	-3.089970727	-0.892694259
C	-1.974809555	-1.127350574	0.403057252	H	4.456065929	-3.773359331	-1.312370606
C	-3.130852473	-0.596042867	-0.204010831	C	2.532335276	-3.578367488	-0.370407143
C	-4.208915011	-1.404252671	-0.548948199	C	1.588411209	-2.707139139	0.166932989
H	-5.092030973	-0.978812030	-1.017207477	H	0.664915124	-3.116987462	0.555537018
C	-4.158561339	-2.763941782	-0.271886902	C	1.974815798	1.127353700	0.403062041
H	-4.993781339	-3.404623202	-0.537894536	C	3.130849380	0.596043324	-0.204021906
C	-3.046019733	-3.299191883	0.367804175	C	4.208911939	1.404249455	-0.548967829
C	-1.971703394	-2.482050495	0.708189535	H	5.092019595	0.978807176	-1.017241312
H	-1.132767190	-2.915041641	1.242199339	C	4.158570454	2.763936496	-0.271894307
C	-1.810986117	1.335794505	0.199518562	H	4.993791129	3.404614873	-0.537907127
C	-3.028765814	0.861326733	-0.335310789	C	3.046042646	3.299187182	0.367820076
C	-3.975639755	1.724758354	-0.875030380	C	1.971725416	2.482049634	0.708211997
H	-4.906678364	1.339133907	-1.280863305	H	1.132802738	2.915039466	1.242243826
C	-3.724153982	3.089966662	-0.892691613	H	-3.019897471	-4.357638630	0.609566433
H	-4.456088851	3.773351994	-1.312363091	H	-2.335130439	4.646270355	-0.383184734
C	-2.532344995	3.578367056	-0.370425063	H	3.019932866	4.357630902	0.609596906
C	-1.588413742	2.707143231	0.166909763	H	2.335121465	-4.646271065	-0.383154341

Transition states

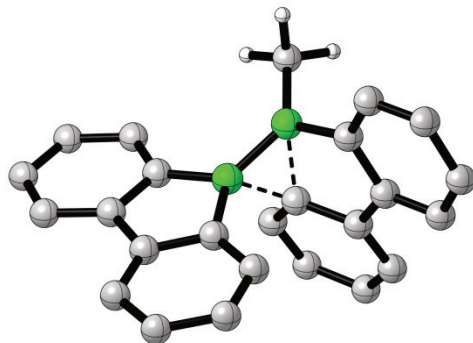
TS1

Total energy = -1013.12056760 Hartree

Thermal correction to Gibbs free energy = 0.314542 Hartree

Imaginary frequency: -241.0656

d(B···B) = 1.634340 Å



B	0.532998293	-0.156226601	0.510418886	C	-2.332863407	-1.646867975	-2.024923581
B	-0.667226025	-0.804368792	1.410663562	C	-0.283071371	-2.874281753	-2.259244957
C	-0.553161829	-2.016399372	2.447619510	H	1.195730954	-2.534373237	-0.754485773
C	2.075325768	-0.549017900	0.589012778	C	-3.855763309	0.422129148	-0.291187441
C	2.839761795	0.557332944	0.147866108	C	-3.923133719	1.346497746	1.926568231
C	0.606033215	1.257543425	-0.225146057	H	-2.283496348	0.857529103	3.218509008
C	-0.555087955	-1.352153855	-0.386554408	H	3.397298331	3.126564701	-0.939987344
C	-2.060188990	-0.065650481	1.290546212	C	1.371994037	3.741356758	-1.309974935
C	2.770341313	-1.664867887	1.050788260	H	5.977400884	-0.600765990	0.690035613
C	1.966145635	1.627744077	-0.341314402	H	-3.339735824	-1.426654581	-2.366297403
C	4.228942299	0.547493095	0.192802324	C	-1.545744857	-2.543821112	-2.731270235
C	-0.349488972	2.166857431	-0.674472294	H	-4.291254811	0.317120145	-1.280895848
C	-1.853824746	-1.056819031	-0.859252152	C	-4.492950802	1.202551230	0.665359924
C	0.198044614	-2.284510732	-1.096112911	H	1.657054071	4.702382717	-1.727767491
C	-2.654246998	-0.202386610	0.023150554	H	-1.926245047	-3.000348311	-3.639972971
C	-2.719186780	0.721078624	2.232430163	H	-5.429262162	1.697915253	0.429073487
C	4.162055769	-1.687808262	1.079834916	H	4.681681833	-2.571176325	1.440108927
H	2.225893913	-2.537211076	1.399095596	H	-0.734154006	4.084823005	-1.559802771
C	2.346801163	2.857790069	-0.866882290	H	0.332935918	-3.586499585	-2.799567244
H	4.798523461	1.410671502	-0.141085003	H	-4.420515301	1.958256784	2.673827754
C	4.892159109	-0.581740612	0.657393965	H	-1.356304931	-2.755008876	2.332318289
C	0.027769940	3.392078610	-1.213751807	H	-0.652129201	-1.606437972	3.461760607
H	-1.403822179	1.927068479	-0.596142088	H	0.401573558	-2.545644205	2.416149554

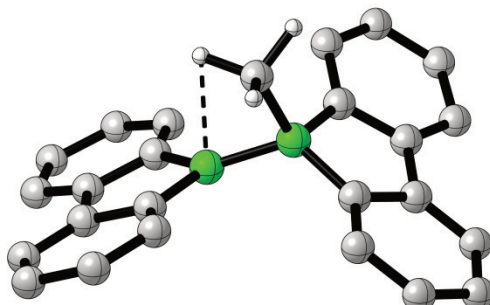
TS2

Total energy = -1013.11549001 Hartree

Thermal correction to Gibbs free energy = 0.314249 Hartree

Imaginary frequency: -116.0814

d(B···B) = 1.674970 Å



B	0.823342668	-0.244773625	0.748845532	C	-3.779222362	1.949358951	-0.897073309
B	-0.775530180	-0.002793182	0.312296136	H	-4.800587335	1.680584218	-1.151034249
C	0.245781499	-0.433839904	2.320737283	C	-3.338032719	3.256957505	-1.077488521
C	1.874189686	0.960366612	0.609823352	H	-4.020655805	4.008994398	-1.461679977
C	2.995656592	0.531612607	-0.135256788	C	-2.024979546	3.598944777	-0.781508326
C	4.055729049	1.387612102	-0.418270504	C	-1.138372247	2.637280085	-0.298905615
H	4.904705461	1.042874316	-1.003023866	H	-0.106819922	2.904551694	-0.104636474
C	4.038994652	2.685408280	0.076717677	C	-1.980782722	-1.057811375	0.324343146
H	4.863940888	3.359636418	-0.133492584	C	-3.152637991	-0.422763904	-0.139125228
C	2.973484474	3.110774366	0.865420652	C	-4.348592200	-1.109833636	-0.279895649
C	1.909017113	2.253020758	1.128641237	H	-5.239788918	-0.608804377	-0.646750542
H	1.092765711	2.603198925	1.756740905	C	-4.402588526	-2.454489610	0.074878891
C	1.689406367	-1.432904928	0.097334668	H	-5.333744045	-3.003742831	-0.025225322
C	2.877654996	-0.892209126	-0.454537476	C	-3.270766734	-3.091522179	0.565774472
C	3.786627753	-1.678485902	-1.155458175	C	-2.069571675	-2.394824505	0.686813471
H	4.686343358	-1.237177189	-1.576624653	H	-1.199905856	-2.906526757	1.081501589
C	3.546826044	-3.037545486	-1.306384032	H	2.976986258	4.116013743	1.278263332
H	4.252715968	-3.660653302	-1.847411436	H	2.212191950	-4.662077715	-0.863685225
C	2.398562045	-3.597091645	-0.754517562	H	-3.322354235	-4.137045622	0.853546030
C	1.484831065	-2.801044498	-0.070361347	H	-1.684300195	4.617519972	-0.939902567
H	0.593059152	-3.271048158	0.330681157	H	1.030426183	-0.074730649	2.995503314
C	-1.560958050	1.332784367	-0.078880860	H	0.034362507	-1.483476412	2.535623845
C	-2.896216991	1.004016523	-0.398310750	H	-0.662640982	0.127121936	2.588834136

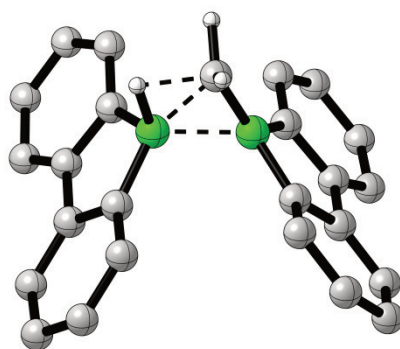
TS3

Total energy = -1013.11106266 Hartree

Thermal correction to Gibbs free energy = 0.312907 Hartree

Imaginary frequencies: -686.9080

d(B···B) = 1.870943 Å



B	-0.826974644	-0.379670080	1.228647026	C	3.784888128	-0.226617992	-1.003987811
B	0.869216144	0.409290660	1.258752301	H	4.230023499	0.333176114	-1.821752333
C	-0.157148429	-0.114867485	2.582327985	C	4.328632723	-1.445853137	-0.622780608
C	-0.965290065	-1.731926439	0.417308576	H	5.188900221	-1.846492265	-1.149976942
C	-2.042357505	-1.581665417	-0.491538883	C	3.779169040	-2.146749362	0.447696255
C	-2.404303002	-2.599518136	-1.365977238	C	2.669867318	-1.646951036	1.119489784
H	-3.229868750	-2.462057888	-2.058960260	H	2.266831381	-2.207054618	1.959087211
C	-1.709414607	-3.801646399	-1.344806247	C	0.988181579	1.756957228	0.448424374
H	-1.983469228	-4.602010106	-2.025389659	C	2.029657571	1.574882938	-0.498024387
C	-0.663071697	-3.977452349	-0.444706536	C	2.362267196	2.574069487	-1.406538286
C	-0.299580413	-2.954788057	0.424598038	H	3.155354505	2.412855843	-2.131468501
H	0.526696546	-3.120090963	1.105019723	C	1.685920133	3.785148543	-1.376667328
C	-2.055296851	0.463478017	0.699342430	H	1.939119479	4.569248437	-2.083455039
C	-2.695691655	-0.281274328	-0.317942572	C	0.683037596	3.991357564	-0.433094901
C	-3.827604294	0.200651032	-0.964542422	C	0.341034825	2.990101931	0.467032040
H	-4.305769951	-0.380983037	-1.747854321	H	-0.452893211	3.178158639	1.178980811
C	-4.358244028	1.429677874	-0.592313467	H	-0.123188921	-4.919745480	-0.423527273
H	-5.240791589	1.815294005	-1.093564320	H	-4.199025727	3.106225121	0.741663578
C	-3.768061689	2.156902526	0.436830782	H	0.158448108	4.941896192	-0.403778321
C	-2.632045577	1.671539225	1.076458578	H	4.220118393	-3.089863168	0.757103700
H	-2.203706275	2.248228426	1.891928144	H	0.296781094	-0.930817938	3.140689487
C	2.083264133	-0.444663988	0.736224173	H	-0.591123166	0.647772130	3.226706021
C	2.681965907	0.277821850	-0.323149301	H	1.097698094	0.646473120	2.483573491

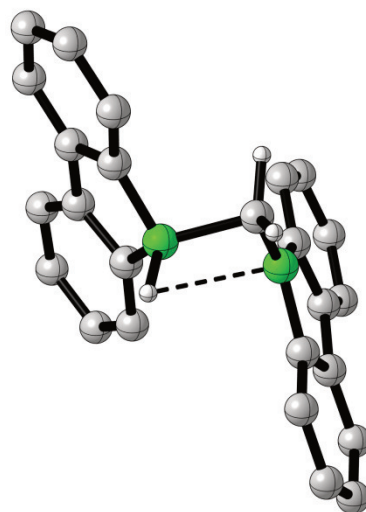
TS4

Total energy = -1013.13848805 Hartree

Thermal correction to Gibbs free energy = 0.315252 Hartree

Imaginary frequency: -13.9254

d(B···B) = 2.377687 Å



B	0.811745936	-0.902545467	0.987350017	H	1.752775470	-3.451981186	-0.289694671
B	-1.175652854	-1.486649396	-0.179897039	C	-0.894963353	-0.145091789	-1.068926462
H	-0.937211902	-2.502153968	-0.815830502	C	-2.053751109	0.662679474	-1.082973719
C	-0.410181361	-1.670897840	1.380829332	C	-2.098699005	1.867963672	-1.777571049
H	-1.055042801	-1.217090611	2.132823160	H	-2.999488833	2.476136726	-1.770903230
H	-0.331423330	-2.746245234	1.533257822	C	-0.986840807	2.283674829	-2.496277481
C	1.157455929	0.621601403	1.247840684	H	-1.008191727	3.225106830	-3.037196131
C	2.485494082	0.854878243	0.839306890	C	0.150162813	1.482753068	-2.532913327
C	3.068593330	2.105406949	0.974083752	C	0.186994053	0.280071254	-1.836200957
H	4.092336409	2.283603244	0.657703740	H	1.087305719	-0.324700729	-1.880691217
C	2.315247058	3.145887621	1.510538589	C	-2.731563697	-1.230527411	0.155223898
H	2.755962254	4.132914626	1.612344618	C	-3.143019630	0.023731439	-0.339680715
C	0.999829979	2.933394019	1.904957168	C	-4.434162160	0.499566134	-0.126427526
C	0.424581090	1.670902040	1.777855699	H	-4.737371648	1.470341330	-0.509632822
H	-0.608412237	1.511909884	2.072434416	C	-5.339895141	-0.278768574	0.582599412
C	2.127009825	-1.419594897	0.269059125	H	-6.350014946	0.082025329	0.752875120
C	3.068579816	-0.369587367	0.255784729	C	-4.952087768	-1.521712797	1.076797720
C	4.333600167	-0.550836033	-0.282208628	C	-3.655921752	-1.984513827	0.870238403
H	5.058431097	0.257929703	-0.291859563	H	-3.361865082	-2.949753323	1.276012881
C	4.665836687	-1.789282057	-0.826134479	H	0.418887732	3.757922045	2.306110419
H	5.651197604	-1.940691531	-1.256401703	H	4.014270556	-3.785812373	-1.266419789
C	3.744534959	-2.829392296	-0.829330474	H	-5.666057558	-2.127725990	1.627985865
C	2.477676547	-2.643507099	-0.277250374	H	1.016384518	1.801450589	-3.105504564

5. References

- S1 A. Hübner, M. Diefenbach, M. Bolte, H.-W. Lerner, M. C. Holthausen and M. Wagner, *Angew. Chem. Int. Ed.*, 2012, **51**, 12514-12518.
- S2 T. Kaese, H. Budy, M. Bolte, H.-W. Lerner and M. Wagner, *Angew. Chem. Int. Ed.*, 2017, **56**, 7546-7550.
- S3 A. Hübner, M. Bolte, H.-W. Lerner and M. Wagner, *Angew. Chem. Int. Ed.*, 2014, **53**, 10408-10411.
- S4 G. R. Fulmer, A. J. M. Miller, N. H. Sherden, H. E. Gottlieb, A. Nudelman, B. M. Stoltz, J. E. Bercaw and K. I. Goldberg, *Organometallics*, 2010, **29**, 2176-2179.
- S5 T. Kaese, A. Hübner, M. Bolte, H.-W. Lerner and M. Wagner, *J. Am. Chem. Soc.*, 2016, **138**, 6224-6233.
- S6 X-AREA: *Diffractometer Control Program System*, Stoe & Cie, Darmstadt, Germany, 2002.
- S7 G. M. Sheldrick, *Acta Crystallogr., Sect. A: Found. Crystallogr.*, 2008, **64**, 112-122.
- S8 M. J. Frisch, G. W. Trucks, H. B. Schlegel, G. E. Scuseria, M. A. Robb, J. R. Cheeseman, G. Scalmani, V. Barone, B. Mennucci, G. A. Petersson, H. Nakatsuji, M. Caricato, X. Li, H. P. Hratchian, A. F. Izmaylov, J. Bloino, G. Zheng, J. L. Sonnenberg, M. Hada, M. Ehara, K. Toyota, R. Fukuda, J. Hasegawa, M. Ishida, T. Nakajima, Y. Honda, O. Kitao, H. Nakai, T. Vreven, J. A. Montgomery, Jr., J. E. Peralta, F. Ogliaro, M. Bearpark, J. J. Heyd, E. Brothers, K. N. Kudin, V. Staroverov, R. Kobayashi, J. Normand, K. Raghavachari, A. Rendell, J. C. Burant, S. S. Iyengar, J. Tomasi, M. Cossi, N. Rega, J. M. Millam, M. Klene, J. E. Knox, J. B. Cross, V. Bakken, C. Adamo, J. Jaramillo, R. Gomperts, R. E. Stratmann, O. Yazyev, A. J. Austin, R. Cammi, C. Pomelli, J. W. Ochterski, R. L. Martin, K. Morokuma, V. G. Zakrzewski, G. A. Voth, P. Salvador, J. J. Dannenberg, S. Dapprich, A. D. Daniels, Ö. Farkas, J. B. Foresman, J. V. Ortiz, J. Cioslowski and D. J. Fox, *Gaussian 09*, Revision D.01, Gaussian, Inc., Wallingford, CT, 2013;
<http://www.gaussian.com>.
- S9 J. P. Perdew, K. Burke and M. Ernzerhof, *Phys. Rev. Lett.*, 1996, **77**, 3865-3868.
- S10 J. P. Perdew, K. Burke and M. Ernzerhof, *Phys. Rev. Lett.*, 1997, **78**, 1396-1396.
- S11 J. P. Perdew, M. Ernzerhof and K. Burke, *J. Chem. Phys.*, 1996, **105**, 9982-9985.
- S12 C. Adamo and V. Barone, *J. Chem. Phys.*, 1999, **110**, 6158-6170.
- S13 L. Goerigk and S. Grimme, *J. Chem. Theory Comput.*, 2011, **7**, 291-309.
- S14 S. Grimme, S. Ehrlich and L. Goerigk, *J. Comput. Chem.*, 2011, **32**, 1456-1465.
- S15 A. Schäfer, C. Huber and R. Ahlrichs, *J. Chem. Phys.*, 1994, **100**, 5829-5835.
- S16 A. V. Marenich, C. J. Cramer and D. G. Truhlar, *J. Phys. Chem. B*, 2009, **113**, 6378-6396.
- S17 C. Y. Legault, *CYLview*, 1.0b; Université de Sherbrooke, Canada, 2009;
<http://www.cylview.org>.